Role of RALA and its Ser194 phosphorylation in tumorigenesis in RAS-independent and RAS-dependent cancers

विद्या वाचस्पति की
उपाधि की अपेक्षाओं की आंशिक पूर्ति में प्रस्तुत
शोध प्रबंध

A thesis submitted in partial fulfilment of the requirements of the degree of Doctor of Philosophy

मयूरेश विश्वास कोंडे द्वारा
BY MAYURESH VISHWAS KONDE
पंजीकरण सं. - २०१७३५१६
Registration No. - 20173516

शोध प्रबंध पर्यवेक्षक : डॉ. नागराज बालसुब्रमण्यम
Thesis Supervisor: Dr. Nagaraj Balasubramanian

भारतीय विज्ञान शिक्षा एवं अनुसंधान संस्थान पुणे
INDIAN INSTITUTE OF SCIENCE EDUCATION AND RESEARCH PUNE

2024

CERTIFICATE

Certified that the work incorporated in the thesis entitled **Role of RalA and its Ser194 phosphorylation in tumorigenesis In Ras-independent and Ras-dependent cancers** Submitted by **Mr. Mayuresh Vishwas Konde** was carried out by the candidate, under my supervision. The work presented here or any part of it has not been included in any other thesis submitted previously for the award of any degree or diploma from any other University or institution.

Dr. Nagaraj Balasubramanian

Date:

Declaration by Student

Name of Student: Mr. Mayuresh Vishwas Konde

Reg. No.: 20173516

Thesis Supervisor(s): Dr. Nagaraj Balasubramanian

Department: Biology

Date of joining program: 01/08/2017

Date of Pre-Synopsis Seminar : 11/12/2024

Title of Thesis : **Role of RalA and its Ser194 phosphorylation in tumorigenesis In Ras-independent and Ras-dependent cancers**

I declare that this written submission represents my idea in my own words and where others' ideas have been included; I have adequately cited and referenced the original sources. I declare that I have acknowledged collaborative work and discussions wherever such work has been included. I also declare that I have adhered to all principles of academic honesty and integrity and have not misrepresented or fabricated or falsified any idea/data/fact/source in my submission. I understand that violation of the above will be cause for disciplinary action by the Institute and can also evoke penal action from the sources which have thus not been properly cited or from whom proper permission has not been taken when needed.

The work reported in this thesis is the original work done by me under the guidance of

Dr./Prof. Dr. Nagaraj Balasubramnian

Date: 21/12/2024

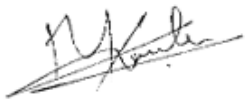

Signature of the student

Acknowledgments

The work presented in this thesis would not have been possible without my close association with many people. I take this opportunity to extend my sincere gratitude and appreciation to all those who made this Ph.D. thesis possible.

First of all, I would like to express my sincere gratitude to my advisor Dr. Nagaraj Balasubramanian for not only giving me the opportunity to pursue my Ph.D. in his laboratory but also believing me when no one else did. In addition to providing freedom to design projects and experiments, Nagaraj has been a constant pillar of support for me, helping me through many difficult times in my journey of past 6 years. His skills in experiment design and presentation is something that I will carry with me for long time.

My special word of thanks also goes to Prof Manickam Jayakannan Mishika, and Mehek for collaborating with our lab and providing us with V_{MLN} and NP-MLN. I would like to thank the rest of my thesis committee: Dr. Mayurika Lahiri, Dr. Girish Ratnaparkhi, and Dr. Deepa Subramanyam, for their insightful comments, encouragement, and for the question which motivated me to widen my research from various perspectives.

I thank the Bio-office staff, academic office staff management and authorities at IISER Pune for providing excellent Infrastructure and the necessary equipment and resources and Wellcome-DBT India Alliance and Indian Council for Medical Research, for funding the research in the lab, UGC for providing Ph.D. scholarship and ICMR for providing JRF fellowship. I would like to thanks INFOSYS foundation for providing travel grant.

I acknowledge microscopy facility at IISER for providing a smooth access and technical help with the confocal microscopes and Saurabh Vaishnav from FACS facility with his help in cell sorting. I would especially like to thank Suraj Ingle, Anubha and Dr. Krishnaveni for training and helping me out with mice experiments. I thank my colleagues from Dr. Anjan lab, Dr. Sanjeev lab, Dr. Nishad Matange and other faculty members for providing me with their insights during troubleshooting and allowing me to borrow resources for my work.

I thank my fellow lab mates in Cell adhesion group Natasha, Siddhi, Keerthi, Omkar, Vishakha, Prachi, Rajeshwari, Debasmita, Radhika, Shaunak, Arnav, Antara, Tushar, Kajal and Sonam who contributed immensely at my personal and professional time at IISER. The group has been a source of support and a great help in troubleshooting experiments and discussion during lab meetings. I have met some very great and interesting people at IISER who have made my time here enjoyable and fun and who have helped me grow not only as a researcher but also as a good human being. Few of these humans are Sanket, Soumen, Shalaka, Ayantika, Ajay and Maithilee. Special thanks to my batchmate (Prachi,Lokesh, Rajeshwari, Ravi, Shruti, Firdousi, Sandra) and my volleyball group for making my time at IISER Pune memorable.

I dedicate this thesis to my parents (Mr. Vishwas Konde and Mrs. Suchitra Konde), this journey would have been impossible without their unconditional support, love and blessings. Special thanks to my sisters for supporting me and taking care of everything while I was away from home.

Finally, I owe a great deal of thanks to my wife Prachi Joshi who happens to be my lab mate and batchmate. I was a blessed to have her accompany me in most important journey of my life till now. I would also like to thank my in-laws for being equally supportive and accommodating.

Mayuresh Konde

August 2024

INDEX

Commonly used Abbreviations

µM	micromolar
µg	microgram
µL	microliter
ECM	Extra cellular matrix
FN	Fibronectin
SA	Stable adherent
SUS	Suspension
GTPase	Guanosine triphosphatases
Ral GTPase	RAS-like GTPase
AURKA	Aurora Kinase A
AURKB	Aurora Kinase B
AURKC	Aurora Kinase C
AIG	Anchorage-independent growth
LOF	Loss of function
GEF	Guanine nucleotide exchange factor
GAP	GTPase activating protein
CON	Control
V_{MLN}	Dextran polysaccharide encapsulated MLN8237
V_{MLN}+RhB	Encapsulated MLN8237 and Rhodamine-B
RhB	Rhodamine-B
DEX	Empty dextran polysaccharide scaffold
RBD	Ral-Binding domain
Ras	Ras (Rat sarcoma) protein
RAS	RAS(Rat sarcoma) gene
RalA	RalA (Ras-related protein Ral-A) protein
RALA	RalA (Ras-related protein Ral-A) gene

Inhibitors used in the study

MLN8237 Aurora Kinase inhibitor

ABSTRACT

RALA (RAS Like Proto-Oncogene A) is a RAS family small GTPase that regulates vital cellular processes like cell spreading, migration and proliferation. Downstream of RAS, activation of RALA is critical for cancer cell tumorigenesis, mediated through RALGEFs. In recent years, the phosphorylation of RALA at S194 has emerged as a novel regulatory player, though its role in RALA activation and tumor progression remains ambiguous. To better understand this, we made stable CRISPR-Cas9-based RALA knockout (RALA KO) in RAS-dependent (MiaPaCa2, T24, UMUC3) and RAS-independent (MCF7, SKVO3) cancer cells. Detection of RALA S194 phosphorylation in these RALA KO cells when probed using the commercial anti-phospho-RALA antibody in western blot lacks specificity in RAS-dependent cancers. Despite the loss of RALA, the pS194RALA band stays detectable in these cell lines, making it difficult to evaluate its regulation or role. AURKA inhibitor MLN8237 delivered in a nanovesicle (V_{MLN}) developed earlier in the lab specifically inhibits AURKA but did not affect the pS194RALA band detected in RAS-dependent cancers. RALA KO MiaPaCa2 (Ras-dependent) and MCF7 (Ras-independent) cells were stably reconstituted with WT-RALA, S194A-RALA, and S194D-RALA mutants and were used to test the role of this phosphorylation. They showed no difference in RALA activation status, detected by Sec5 RBD pulldown. Tumor growth disrupted by the loss of RALA was restored partly by WT-RALA, but not by S194A-RALA or S194D-RALA. These phosphomutants significantly affected tumor formation in both RAS-independent and RAS-dependent cancer cell lines. This supports a role for RALA S194 phosphorylation, independent of its activation in regulating RALA-dependent tumorigenesis, regulated by its localization or effector interaction. Finally, our studies also suggest the possible role the AURKA-RALGEF-RALA (AURKA-RGL1-RALA in the case of WTMEFs) pathway could have in AURKA-mediated regulation of RALA activation, independent of its S194 phosphorylation.

SYNOPSIS

Introduction

Downstream of RAS, RALA is a major regulator of RAS-mediated oncogenesis and anchorage independence (AIG). Multiple studies have shown that RALA activation is regulated by oncogenic RAS and cell-matrix adhesion (by integrins) (Lim *et al.*, 2005; Pawar *et al.*, 2016). In recent years, AURKA has emerged as a novel regulator of RALA (Lim, Donita C. Brady, *et al.*, 2010). AURKA is a well-known mitotic kinase involved in centrosome maturation (Nikonova *et al.*, 2013) and is overexpressed in RAS (HRASV12 and KRASV12) driven carcinogenesis (Vader and Lens, 2008).

RALA is a small GTPase; its function depends on its activation and localization. AURKA-mediated phosphorylation of RALA at S194 regulates RALA localization to cell membranes in HEK TtH cells (Lim, Donita C Brady, *et al.*, 2010). The role of this crosstalk in regulating RALA activation is still unclear. The expression of kinase-dead AURKA caused a reduction in RALA activation (NIH3T3 and MDCK cells) (Wu et al., 2005), and WT AURKA expression was seen to increase RALA activation (HEK293 cells) (Lim, Donita C. Brady, *et al.*, 2010). However, overexpression of kinase-active AURKA^{Thr288} (HEK293 cells) that increases RALA S194 phosphorylation does not increase the RALA activation (Lim, Donita C. Brady, *et al.*, 2010). Similarly, in HEK-TER cells, RALA S194 mutants showed a drop in RALA activation (Sablina et al., 2007), but no such drop in RALA activation was observed in NIH293T cells with the same mutant (Lim, Donita C. Brady, *et al.*, 2010). Despite this variation, studies in non-transformed HEK293 and MDCK cells expressing constitutively active RALAV23 and phosphodeficient S194A-RALAV23 mutants show AURKA-RALA crosstalk to be vital for RALA-dependent anchorage-independent growth (AIG) (Wu *et al.*, 2005; Lim, Donita C. Brady, *et al.*, 2010).

Similarly, in pancreatic cancer cells, the knockdown of RALA and reconstitution with WT RALA vs S194A RALA mutants further support this claim in AIG studies (Lim, Donita C Brady, *et al.*, 2010). However, in another study, AURKA inhibitor (MLN8237) treatment in these pancreatic cancer cells affected the AIG. They did not see any inhibition of RALA S194 phosphorylation, questioning the requirement of these

crosstalk (Neel *et al.*, 2014) (Inchanalkar *et al.*, 2018a). The role of RALA S194 phosphorylation in tumor formation was evaluated in pancreatic cancer cells using WT-RALA vs S194A-RALA mutant, and it revealed that this phosphorylation has a variable effect on tumor growth and it could be cell type-specific (Lim, Donita C. Brady, *et al.*, 2010).

Our study aims to address these uncertainties in AURKA-RALA crosstalk, especially in cancer cells, where it could also be an attractive target for inhibition. While evaluating the role of this crosstalk in regulating RALA activation, we also aim to test any interaction between AURKA and RALGEFs. Knowing the importance of cell-matrix adhesion in AIG, we also strive to evaluate the role of this crosstalk in early adhesion events.

The following are hence the objectives of this thesis:

1. Evaluate the AURKA-RALA crosstalk in cancer cells
2. Test whether RALA phosphorylation at S194 can regulate RALA activation
3. Evaluate the role of RALA and RALA S194 phosphorylation in tumorigenesis
4. Test whether AURKA-RALA crosstalk is different in cancer cells with and without oncogenic RAS

We made a CRSPR-CAS9 RALA KO in RAS-independent cancer cells (MCF7 and SKOV3) and RAS-dependent cancer cells (T24, UMUC3 and MiaPaCa2) to achieve the above objectives. We confirmed the RALA KO by western blot and genotyping in all except SKOV3 cells. In SKOV3 cells, western blotting showed the absence of RALA, but genotyping PCR did not show any amplification of RALA exon to confirm the physical cut. We further confirmed the specificity of RALA KO by confirming the expression and activation of a panel of proteins associated with RALA and of interest for this study (RALB, AURKA, AURKB, ERK, AKT) not to be altered. While confirming RALA KO, we also tested the pS194 RALA phosphorylation using anti-phospho-RALA Antibody (Ser194) (Merck-Millipore, Cat no- 07-2119), which is the only commercially available antibody that detects this phosphorylation. This band detected by the anti-phospho-RALA Antibody (Ser194) in RAS-independent MCF7 and SKVO3 cells was

missing, as expected on RALA KO. However, in RAS-dependent T24, UMUC3 and MiaPaCa2 cells, despite the confirmed RALA KO, a distinct band at the expected size was detected. We further confirmed this observation with siRNA-mediated RALA KD in MiaPaCa2 cells. This also caused no change in the expected band detected by the pS194 RALA antibody despite a ~80% drop in total RALA levels. Overall, this suggested that pS194 RALA detection in RAS-dependent cancer cell lines may be non-specific and limiting the use of this antibody to RAS-independent cancer cell lines.

I. Evaluate the AURKA-RALA crosstalk in cancer cells

To evaluate AURKA-RALA crosstalk in cancer cells, we used nano-vesicle encapsulated MLN8237 (V_{MLN}), previously developed and tested in our lab, for better and specific inhibition of AURKA (Inchanalkar et al., 2018). AURKA inhibition study showed that pS194 RALA phosphorylation drops in RAS-independent cancer cell lines, where the antibody detection was specific. However, it only affected the RALA activation and AIG in SKOV3 cells but not in MCF7 cells, suggesting that although this crosstalk exists in cancer cells, its role in cancer cells could be cell-type specific.

Since the detection of pS194 RALA in T24, UMUC3, and MiaPaCa2 cells was likely to be non-specific (based on earlier data from this study). AURKA inhibition also showed no change in RALA phosphorylation detected by the pS194 RALA antibody. GST-Sec5 pulldown assay also showed no change in RALA activation upon AURKA inhibition in these cancer cell lines, making it difficult to comment on AURKA-RALA crosstalk. AURKA inhibition only affected AIG in MiaPaCa2 cells, not T24 or UMUC3 cells. This suggest that its role and regulation are indeed cell-type specific. It is also likely that if the AURKA-RALA crosstalk is lacking in RAS-dependent cancers, this effect on AIG could be AURKA-dependent and independent of RALA.

II. Test whether RALA phosphorylation at S194 can regulate RALA activation and localization

Limitations in the pS194RALA antibody detection and resulting evaluation and differences in V_{MLN}-mediated AURKA inhibition reflecting dependence or lack thereof on RALA made it difficult to comment conclusively on the role of this phosphorylation.

The best way to hence test the role of RALA S194 phosphorylation in regulating RALA activation, localization and function would be to use RALA S194 mutants (S194A/D). We hence made stable reconstitutions of RALA KO MCF7 and MiaPaCa2 cells with WT-RALA, phosphodeficient (S194A)-RALA or phosphomimetic (S194D)-RALA. These S194 mutants also ensure all RALA expressed in these cells either have (S194D) or lack (S194A) phosphorylation at Ser194, ensuring the effects seen are more complete than if only part of the RALA is phosphorylated in cells, as is likely in physiological conditions.

GST-Sec5 pulldown assays in stable RALA S194 phosphomutant expressing MCF7 and MiaPaCa2 cells showed both the phosphodeficient and phosphomimetic mutants to have no detectable effect on RALA activation. A similar result has been reported previously in NIH293T cells with RALA S194A mutant by Lim et al. (Lim et al., 2010). In HEK-TER cells, the RALA S194A mutant showed a drop in RALA activation (Sablina *et al.*, 2007). In cancer cells, this might be the first time the role of RALA S194 phosphorylation in regulating RALA activation has been examined. Our previous observations with V_{MLN}-mediated AURKA inhibition in MCF7 and MiaPaC2 (limited by the detection of pS194 RALA phosphorylation) also suggest no effect on RALA activation. This shows that RALA S194 phosphorylation does not regulate RALA activation in cancer cells.

Since we don't see an effect of S194A mutation on RALA activation in MCF7 and MiaPaC2 cells but see a significant inhibition of tumor growth, we can speculate the role this phosphorylation could have in tumor formation may stem from its effect on RALA localization. Earlier study in HEKTtH RALA knockdown cells reconstituted with WT-RALA vs S194-RALA mutant suggests a change in their localization to internal membranes, as seen in fractionation studies (Lim, Donita C. Brady, *et al.*, 2010). This study also indicates that S194 phosphorylation can influence the interaction of RALA with downstream effector molecules such as RALBP1, which could affect its role in tumorigenesis. An independent study observed that RALA and RALBP1 localize to the mitochondria, which is dependent on RALA S194 phosphorylation (Kashatus *et al.*, 2011). We found that in MCF7 cells, S194-RALA mutant indeed showed distinctly different localization than WT-RALA. How this localization can regulate tumor growth without affecting RALA activation is an open question. One possibility is that this

change in RALA localization may change how RALA interacts with its downstream effectors, which could affect its functional outcome in tumors.

While this may not happen through the S194 phosphorylation, AURKA can still affect RALA activation in cancer cells. AURKA inhibition in WTMEF cells in early adhesion events affects RalGEF RGL1 localization, and our in-silico analysis reveal potential AURKA phosphorylation sites on RGL1 suggests a possibility of an AURKA-RGL1-RALA pathway to regulate RALA function, that remains to be tested.

III. Evaluate the role of RALA and RALA S194 phosphorylation in tumorigenesis

To evaluate the role of RALA and its S194 phosphorylation in tumorigenesis, we decided to test the tumorigenic potential of RALA KO MCF7 and MiaPaCa2 cells reconstituted with WT RALA or RALA S194 mutants. Both MCF7 and MiaPaCa2 RALA KO cells made significantly smaller tumors, confirming the well-established role of RALA in tumorigenesis. RALA S194A mutant showed that in both MCF7 and MiaPaCa2 cells, this phosphorylation is required for tumor formation. The tumor size in RALA S194A mutant did vary marginally (be it non-significantly) in MCF7 (slightly bigger than RALA KO) and MiaPaCa2 (comparable to RALA KO) cells. This suggests the role of pS194RALA might be marginally different in different cancer types.

Also, the role of RALA S194 phosphorylation in tumorigenesis could be independent of RALA activation since it was not altered in RALA S194 mutants. Since most of RALA functions are associated with its activation, this observation could suggest an activation-independent role for RALA S194 phosphorylation in tumorigenesis. This could have a prominent role for the S194-mediated localization of RALA in tumorigenesis.

IV. Test whether AURKA-RALA crosstalk is different in cancer cells with and without oncogenic RAS

To test the influence of oncogenic RAS on AURKA-RALA crosstalk, we tested the role of AURKA inhibition and RALA mutants in RAS-independent cancer cells (MCF7 and SKOV3) and RAS-dependent cancer cells (T24, UMUC3 and MiaPaCa2). V_{MLN}-

mediated inhibition of AURKA in both cell types was comparable. However, the detection of pS194 RALA in these cancers was variable, with the detection being non-specific in RAS-dependent cancers. This made evaluating the phosphorylation of RALA using this antibody a challenge in RAS-dependent cancer cells. Further, RALA activation remained unaffected in RAS-dependent cancer cells upon AURKA inhibition, suggesting AURKA-RALA crosstalk may be missing or not affect RALA activation in these cells. AURKA inhibition in RAS-independent cancer cell lines showed the presence of AURKA-RALA crosstalk that regulates RALA S194 phosphorylation but showed variable regulation of RALA activation and AIG, in SKVO3 cells but not MCF7 cells.

When evaluated using RALA mutants (S194A), the RALA S194 phosphorylation did not affect RALA activation but was required for tumorigenesis in both MCF7 and MiaPacA2 cells. RALA KO expectedly affected tumor formation comparably in both cancer cell types. This suggests that RALA and its phosphorylation at S194 support tumorigenesis in both cancer types and are not majorly influenced by the presence of oncogenic RAS. This crosstalk could be very cell-type specific and will need careful evaluation in individual cancer cell types to understand if there are any common themes of regulation conserved across cancers.

Summary

Work done in this thesis helps us answer many unanswered questions about the AURKA-RALA crosstalk in cancer cells. For the first time, we discovered there are limitations to how the anti-phospho-RALA Antibody (Ser194) (Merck-Millipore, Cat no-07-2119) detects pS194 RALA in RAS-dependent cancer cells. This lack of specificity could also explain some of the observed variation in AURKA-RALA crosstalk in literature. AURKA inhibition using a specific inhibitor MLN8237 loaded in nanovesicle (V_{MLN}) in cancer cells causes a drop in RALA S194 phosphorylation in MCF7 and SKOV3 cells. Still, it affects RALA activation and AIG only in SKOV3 cells, confirming that the AURKA-RALA crosstalk is variable between cancer cell types. A working pS194RALA antibody in these cells makes this evaluation possible. In RAS-dependent T24, UMUC3 and MiaPaCa2 cancer cells, AURKA inhibition does not affect RALA activation but affects AIG in MiaPaCa2 cells. This study shows the role for RALA S194

phosphorylation, independent of its activation in regulating RALA-dependent tumorigenesis, regulated by its localization or effector interaction. The use of RALA S194 mutants to reconstitute RALA KO cells suggests that RALA and its phosphorylation are both needed for tumor growth although some cell type specific variation may exist. Our studies also suggest the possible role AURKA-RalGEF-RALA (AURKA-RGL1-RALA in the case of WTMEFs) crosstalk could also have a role in AURKA-mediated regulation of RALA, independent of its S194 phosphorylation. These studies clarify some aspects of the AURKA-RALA crosstalk in cancers but also suggest there is more to this regulation than we currently understand. The S194RALA phosphorylation, being vital for RALA-dependent tumors, suggests it could also be an attractive target for disrupting cancer growth.

REFERENCES:

1. Inchanalkar, S. *et al.* (2018a) ‘Polymer Nanovesicle-Mediated Delivery of MLN8237 Preferentially Inhibits Aurora Kinase A To Target RalA and Anchorage-Independent Growth in Breast Cancer Cells.’, *Molecular Pharmaceutics*, 15(8), pp. 3046–3059. Available at: https://doi.org/10.1021/acs.molpharmaceut.8b00163.
2. Kashatus, D.F. *et al.* (2011) ‘RALA and RALBP1 regulate mitochondrial fission at mitosis’, *Nature Cell Biology*, 13(9). Available at: https://doi.org/10.1038/ncb2310.
3. Lim, K.-H. *et al.* (2005) ‘Activation of RalA is critical for Ras-induced tumorigenesis of human cells.’, *Cancer Cell*, 7(6), pp. 533–545. Available at: https://doi.org/10.1016/j.ccr.2005.04.030.
4. Lim, K.-H., Brady, Donita C., *et al.* (2010) ‘Aurora-A Phosphorylates, Activates, and Relocalizes the Small GTPase RalA’, *Molecular and Cellular Biology*, 30(2), pp. 508–523. Available at: https://doi.org/10.1128/mcb.00916-08.
5. Lim, K.-H., Brady, Donita C, *et al.* (2010) ‘Aurora-A phosphorylates, activates, and relocalizes the small GTPase RalA.’, *Molecular and Cellular Biology*, 30(2), pp. 508–523. Available at: https://doi.org/10.1128/MCB.00916-08.
6. Neel, N.F. *et al.* (2014) ‘Response to MLN8237 in pancreatic cancer is not dependent on RalA phosphorylation.’, *Molecular Cancer Therapeutics*, 13(1), pp. 122–133. Available at: https://doi.org/10.1158/1535-7163.MCT-12-1232.
7. Nikonova, A.S. *et al.* (2013) ‘Aurora A kinase (AURKA) in normal and pathological cell division.’, *Cellular and Molecular Life Sciences*, 70(4), pp. 661–687. Available at: https://doi.org/10.1007/s00018-012-1073-7.
8. Pawar, A. *et al.* (2016) ‘Ral-Arf6 crosstalk regulates Ral dependent exocyst trafficking and anchorage independent growth signalling.’, *Cellular Signalling*, 28(9), pp. 1225–1236. Available at: https://doi.org/10.1016/j.cellsig.2016.05.023.
9. Sablina, A.A. *et al.* (2007) ‘The Tumor Suppressor PP2A Aβ Regulates the RalA GTPase’, *Cell*, 129(5), pp. 969–982. Available at: https://doi.org/10.1016/j.cell.2007.03.047.
10. Vader, G. and Lens, S.M.A. (2008) ‘The Aurora kinase family in cell division and cancer’, *Biochimica et Biophysica Acta - Reviews on Cancer*. Available at: https://doi.org/10.1016/j.bbcan.2008.07.003.

11. Wu, J.C. *et al.* (2005) ‘Identification of V23RalA-Ser194 as a critical mediator for Aurora-A-induced cellular motility and transformation by small pool expression screening’, *Journal of Biological Chemistry*, 280(10), pp. 9013–9022. Available at: https://doi.org/10.1074/jbc.M411068200.

Chapter 1

Introduction and Literature Review

1.1 Introduction to Cancer

1.1.1 History of cancer

Cancer has a long history spanning centuries across the globe. The earliest evidence of cancer dates back to 3000 BC in an ancient Egyptian civilization and Greek civilization (Kardinal and Yarbro, 1979). The earliest description of cancer (when the term cancer was not coined) comes from records of 8 medical cases describing breast tumors or ulcers in ancient Egyptian civilization (Gallucci, 1985). Greek physician Hippocrates, also known as the 'father of medicine' used the term *carcinos* and *carcinoma* to describe non-ulcer-forming and ulcer-forming tumors. Roman physician Celsus later translated this Greek term into *cancer,* the Latin word describing tumor (Hajdu, 2011). Later, this became a common term used to describe malignant tumors.

In the 18th and 19th century, many theories were developed to explain cancer. The first and short-lived one was the 'lymph theory' based on discovering the lymphatic system that links cancer to environmental clues. The next one, which is still relevant to date and makes a foundation of today's oncology, is 'cell theory', which proposes that cancer originates from abnormal cell growth (Hoda and Hoda, 2020). In the 20th century, oncology saw exponential growth in understanding and treating cancer.

From the 15th century onwards, as our understanding of the human body increased, our knowledge of cancer also increased. In the 18th century, Scottish surgeon John Hunter, for the first time in history, suggested that cancer might be cured by surgery, and a century later, the development of anesthesia allowed for cancer surgeries (Hajdu, 2012). In the 19th century, the advancement of microscopy and other techniques gave birth to the field of oncology. Autopsy, linked with microscopic observation of cancer tissues, leads to the advancement of cancer surgery to remove cancer efficiently. In the 20th century, the rise of molecular biology, the discovery of X-rays and a better understanding of the human body led to the development of multiple therapeutic approaches like radiation therapy, chemotherapy and immunotherapy. Despite tremendous growth in the field of oncology, the fight against cancer is far from over and continuous research and investment in prevention, cause and treatment is required.

1.1.2 Biology of cancer

Decades of research and discoveries have allowed us to understand cancer as a disease better. According to the World Health Organization (WHO), cancer is defined as follows: ‘Cancer is a large group of diseases that can start in almost any organ or tissue of the body when abnormal cells grow uncontrollably, go beyond their usual boundaries to invade adjoining parts of the body and/or spread to other organs’. In general terms, cancer is the uncontrolled growth of cells or tissue with the potential for invasion. This uncontrolled growth of cells harms the body and its functioning. Cancer disrupts the normal functioning of the cell and tissue of origin and the neighboring tissue (Schwartz *et al.*, 2023). The uncontrolled cell growth is accompanied by increased demand for nutrients and hijacks resources like nutrients and oxygen. This ultimately leads to metabolic reprogramming of the body (Faubert, Solmonson and DeBerardinis, 2020).

Carcinogenesis, which is the start of cancer, begins with a single normal cell turning into an abnormal cell. Dysregulation of the cell cycle by a combination of genetic and environmental factors leads to cell transformation. Most of the time, the body’s immune system gets rid of these transformed cells, but occasionally, few cells survive, forming progenitor cells. This cell grows and forms primary tumor mass. At this point, the tumor is still benign (non-malignant) and confined to its original location. During this growth, cells accumulate mutations and make heterogenous tumor mass. Eventually, some cancer cells undergo EMT (Epithelial to Mesenchymal) transition which helps cancer cell acquire Anchorage Independent Growth (AIG) property and leave the primary tumor site. At this point, the tumor becomes malignant and begins to spread to other parts of the body, and this process is called ‘cancer metastasis’. Cells from primary tumors get access to either blood vessels or the lymphatic system and migrate to other parts of the body, where they attach and form secondary tumors. This process of carcinogenesis is described in Figure 1.1 and in detail in existing literature (Culp *et al.*, 1998; Diori Karidio and Sanlier, 2021).

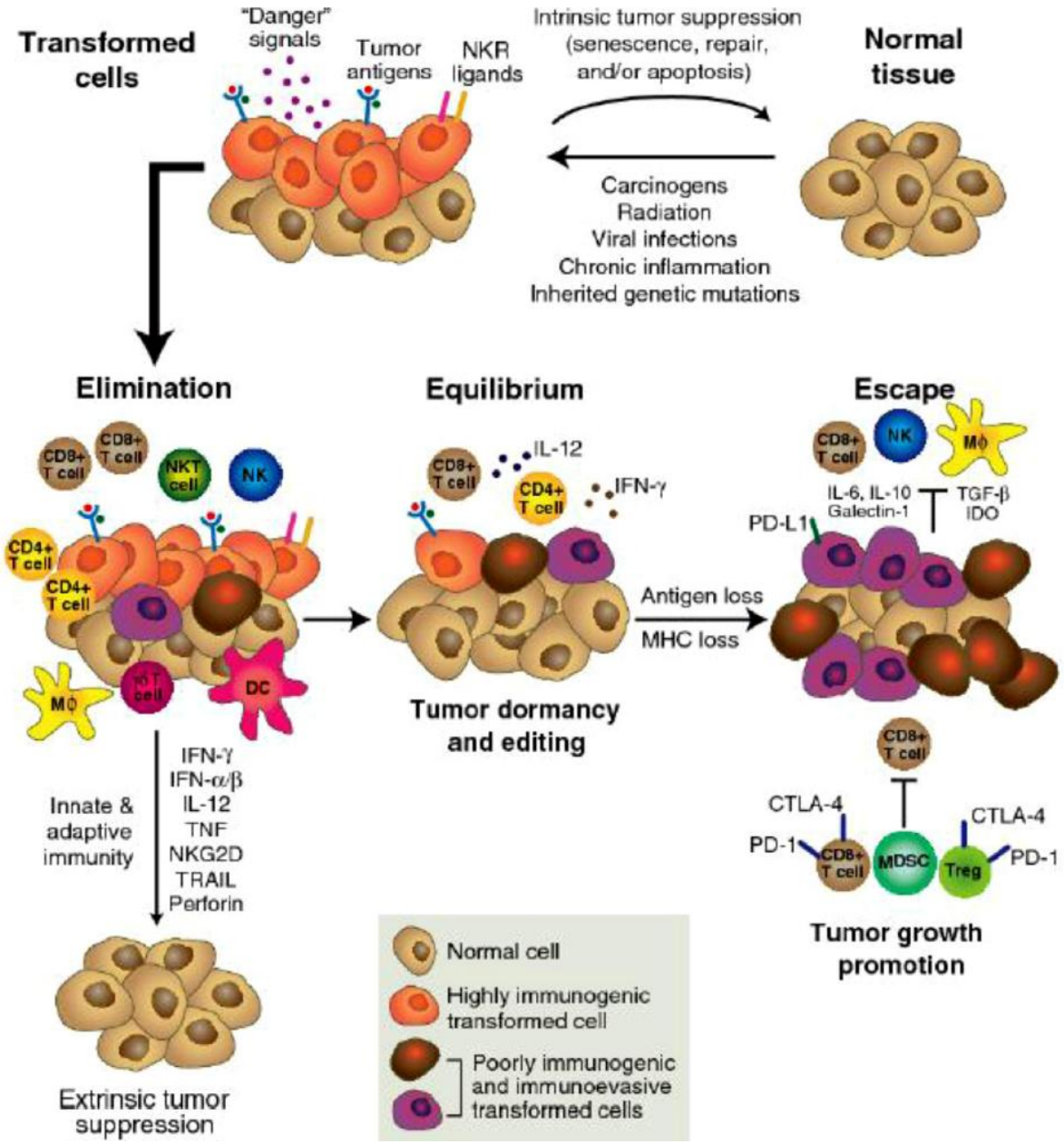

Figure 1.1: Process of carcinogenesis. The figure represents the process of carcinogenesis and factors effecting it. The process involves three phases: Elimination, Equilibrium, and Escape. (Schreiber, Old and Smyth, 2011). (License type: CC-BY)

1.1.3 Tumor grades and cancer stage

Based on the time of diagnosis, cancer and tumors are classified into different categories. Cancer is classified in stages, and tumors are classified in grades (Figure 1.2). Following are the tumor grades and cancer stages according to MD Anderson Cancer Center:

Tumor grades are based on microscopic observation of tissue and how similar or different it is from surrounding normal tissue.

Grade 1: In this tumor, tissue and cells look similar to normal tissues and cells, and these are also known as well-differentiated tumors and considered low grade

Grade 2: In this tumor, tissue and cells are slightly abnormal, and tumors are moderately differentiated and intermediate grade

Grade 3: In this tumor, tissues and cells are very abnormal, and tumors are poorly differentiated and considered high-grade

Grade 4: In this tumor, tissues and cells are most abnormal, tumors are undifferentiated and typically grow and spread faster

Cancers are classified based on the stage on metastasis:

Stage 0: Abnormal cells that haven't spread and are not considered cancer, though they could become cancerous with time. This stage is also called "in-situ.

Stage I – III: Cancers that haven't spread beyond the primary tumor site or have only spread to nearby tissue. The higher the stage number, the larger the tumor and the more it has spread.

Stage IV: Cancer has spread to distant areas of the body.

Apart from this, another standard classification is TNM based on primary tumor type (T), access to the regional lymph nodes (N) and distant metastasis (M).

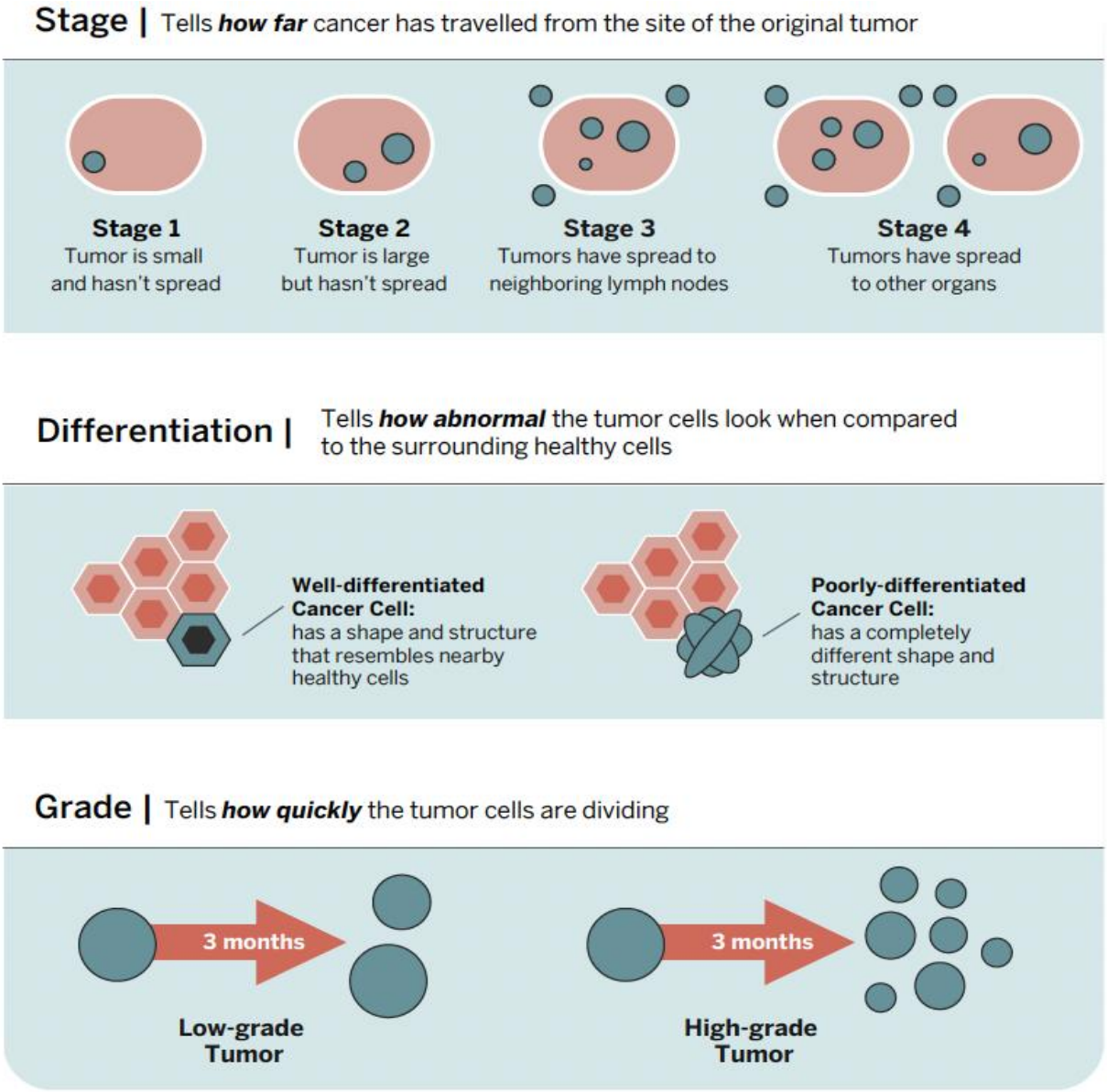

Figure 1.2: Cancer stages and tumor grades in cancer diagnosis. This figure represents the classification of cancer stages (based on spread), differentiation (based on cell appearance) and tumor grade (based on tumor cell growth) used in cancer diagnosis. *(image credit: Neuroendocrine tumor research foundation).* (License type: CC-BY)

1.2 Hallmarks of cancer

Cancer is a very complex and dynamic disease. Centuries of research and technological advancements have allowed us to understand and characterize this disease. Irrespective of the origin of cancer, all cancer cells show certain common traits known as the 'hallmark of cancer', a term first used in 2000 by Hanahan and Weinberg. Hallmarks of cancer have been updated in the last couple of decades, and out of those, the following are the most classical and well-characterized hallmarks or traits observed in cancer (Figure 1.3):

1.2.1 Selective growth advantage

The cell cycle is tightly regulated in normal cells to maintain tissue homeostasis (Malumbres and Barbacid, 2009). However, in cancer cells, one or more regulatory pathways are altered due to the accumulation of mutations over time (Vogelstein *et al.*, 2013). Ligand-receptor interactions carry out this regulation of the cell cycle. Cancer cells often show an increase in autocrine and paracrine secretion of growth-promoting ligands and suppression of growth-inhibitory ligands (Witsch, Sela and Yarden, 2010). Cancer cells also show alteration in receptors such as: 1. Overexpression of receptors by gene amplification to promote signaling, 2. Mutations causing constitutive activation of the receptor, 3. Mutations causing fusion protein production, and 4. Alteration of receptor recycling and degradation (Bache, Slagsvold and Stenmark, 2004; Lemmon and Schlessinger, 2010).

Along with alteration in ligand-receptor interaction, downstream signaling pathways in cancer cells are often altered. The well-known examples of this are RAS and P53 proteins. In 30% of the cancers, RAS has a mutation that keeps it constitutively active and acts as a signaling hub that decouples the ligand-receptor interaction with downstream signaling (Ratner and Miller, 2015) and P53, which is responsible for cell cycle arrest is mutated, which leads to uncontrolled cell proliferation (Kim, Zhang and Lozano, 2015). In cancer, this balance between tumor suppressor genes and tumor-promoting oncogenes is disturbed and discussed later. This selective growth

advantage in cancer cells helps them form tumors in a stressful environment, and this can be tested by doing mice xenograft assays with these cells to form tumors.

1.2.2 Resistance to cell death

During carcinogenesis, cancer cells face multiple challenges and stress, such as DNA damage, limited supply of nutrients and oxygen, loss of cell-matrix adhesion, excessive signaling and targeting by the immune system or anti-cancer therapy, which in case of normal cells leads to programmed cell death known as apoptosis. However, cancer cells show remarkable adaptability to overcome these challenges and avoid cell death. This apoptosis is regulated by extrinsic and intrinsic pathways that ultimately converge to activate caspases and cleavage proteins, leading to cell death (Koff, Ramachandiran and Bernal-Mizrachi, 2015; Lopez and Tait, 2015). To overcome the irreversible DNA damage that leads to apoptosis by DNA damage repair pathways, cancer cells either accumulate the mutation in DNA damage repair pathways or overexpressed the DNA damage repair protein to overcome the DNA damage (Kraemer *et al.*, 1994; Bartkova *et al.*, 2005; Kelley, Logsdon and Fishel, 2014; Srivastava and Raghavan, 2015).

Another important factor involved in apoptosis is loss of cell-matrix adhesion. Cell-matrix adhesion is known to regulate several critical cellular processes, mainly cell survival in the absence of which cell undergoes anoikis, i.e. loss of cell-matrix associated apoptosis (Berrier and Yamada, 2007; Khalili and Ahmad, 2015; Niit *et al.*, 2015). To overcome anoikis, cancer cells utilize multiple mechanisms, the most common of which is constitutive activation of adhesion-dependent signaling by oncogenes, mainly by RAS (Pylayeva-Gupta, Grabocka and Bar-Sagi, 2011; Cox *et al.*, 2014). This hallmark can be tested in an AIG (Anchorage-independent growth) assay or soft agar assay, where cells are forced to grow due to a loss of adhesion.

1.2.3 Vascularization

As mentioned earlier, another stress that leads to apoptosis is the lack of nutrients and oxygen, due to which tumors do not grow beyond 2-3 mm^2 without metastasizing (Sherwood, Parris and Folkman, 1971). To overcome this, tumors form a new vasculature to access nutrients and oxygen. At the beginning of carcinogenesis, microtumors use vascular co-option, a process by which cancer cells hijack the existing blood vessels (Donnem *et al.*, 2013). After reaching a specific size, tumors adapt to angiogenesis, where endothelial cells from existing blood vessels sprout, divide, migrate and assemble themselves to form the new vascular architecture of blood vessels (Carmeliet, 2000). Angiogenesis is mainly utilized during embryogenesis and works at a limited capacity during wound healing, female reproductive cycle and chronic inflammation (Ribatti, Nico and Crivellato, 2015). The process of angiogenesis is regulated by the balance of pro and anti-angiogenic factors (Carmeliet and Jain, 2000). One of the most prominent pro-angiogenic factors is HIF (hypoxia-induced transcription factor), expressed by cancer cells in hypoxic conditions and binds to epithelial cells of blood vessels and tips the balance towards pro-angiogenic signals (Carmeliet and Jain, 2000; Fraisl *et al.*, 2009). Finally, in aggressive tumors, the functional plasticity of the cells allows them to mimic blood vessels (vasculogenic mimicry) by forming a stem-like structure (Kirschmann *et al.*, 2012).

1.2.4 Invasion and metastasis

The ability to invade and metastasize is a defining feature of cancer, and it is responsible for over 90% of cancer-related deaths (Steeg, 2006). This involves three main steps: invasion and survival in the vascular system, extravasation, and metastasis. For invasion, cells undergo the EMT (Epithelial to Mesenchymal) transition, where immobile, rigid epithelial cells become more polar and mobile mesenchymal cells. This is triggered by hypoxia, metabolic and mechanical stress, growth factors and mechanical stress (Craene and Berx, 2013; Lamouille, Xu and Derynck, 2014; Ye and Weinberg, 2015; Rankin and Giaccia, 2016). Following EMT, cells must modify the ECM with the help of MMP (Matrix metalloproteinases) to reach vascular structure (Lamouille, Xu and Derynck, 2014). Once the cancer cell is near the vessel, it enters its lumen through a poorly understood intravasation process

(Reymond, D'Água and Ridley, 2013). Into the lumen, cancer cells face harsh selective conditions such as shear forces and immune clearance till they are trapped in microcapillaries (Valastyan and Weinberg, 2011; Stegner, Dütting and Nieswandt, 2014).

Once trapped in micro capillaries, cancer cells start to extravasate into surrounding tissues, and mechanical barriers and surrounding tissue type limit this process. Metastasis is frequently observed in tissues like the liver and bone, where highly permeable sinusoidal vessels are available for extravasation (Lorusso and Rüegg, 2012). Many times, organ-specific metastasis is observed in specific cancer types, which contradicts the mechanical barrier model of extravasation. This tissue-specific metastasis depends on cooperation between genes regulating organ-specific metastasis and adaptive programs working in surrounding tissue (Lorusso and Rüegg, 2012; Croucher, McDonald and Martin, 2016).

The final stage of 'metastasis' is a limiting step. In this, tumor-derived secreted factors by cancer cells modify surrounding tissue to form a pre-metastatic niche' often observed in bone marrow (Peinado, Lavotshkin and Lyden, 2011; Sceneay, Smyth and Möller, 2013). Till these niches are formed, cancer cells remain dormant and are responsible for late relapse in cancer patients (Giancotti, 2013). What factors affect the dormancy and how cancer cells escape this dormant state is not clear, but colonizing cancer cells must show a remarkable renewable capacity to form secondary tumors (Valastyan and Weinberg, 2011; Giancotti, 2013).

1.2.5 Metabolic reprogramming

Metabolic reprogramming in cancer cells provides cells with unique growth advantages during the initial stage of carcinogenesis. Metabolic reprogramming mainly involves deregulation of nutrient uptake and utilization. To efficiently acquire nutrients, primarily glucose and glutamine, cancer cells overexpress the glucose transporters on the cell surface (Szablewski, 2013). Micropinocytosis is also increased in cancer cells to increase the uptake of glutamine and other essential nutrient (Altman,

Stine and Dang, 2016; X. Wang *et al.*, 2017). This upregulation of transporters and micropinocytosis is linked with hypoxia in the tumor environment and oncogenes like RAS, BRAF and MYC (Altman, Stine and Dang, 2016).

Apart from uptake, even nutrient utilization inside the cell is altered in cancer cells. Cancer cells show the “Warburg effect” in glucose utilization, i.e. they prefer the glycolytic pathway instead of oxidative phosphorylation in the presence of oxygen (Warburg, Wind and Negelein, 1927). This helps cancer cells divert excess glucose to make TCA cycle intermediates, which can make building blocks for macromolecules that can be used to increase lipid production and support cell proliferation (Röhrig and Schulze, 2016). Diverting resources to the TCA cycle also increases ROS production at a lower level, stimulates stress signaling, and increases the mutation burden in cancer cells, which is beneficial to cancer cells (Sabharwal and Schumacker, 2014; De Berardinis and Chandel, 2016). Besides glucose, cancer cells also use glutamine to increase fatty acid production (Altman, Stine and Dang, 2016). Metabolic reprogramming is not a cause of cancer but often plays an active role in cancer progression. Mutations in metabolic enzymes are shown to lead to metabolic reprogramming that promotes cancer progression (Richarson *et al.*, 2016; Gentric, Mieulet and Mechta-Grigoriou, 2017).

1.2.6 Immune system modulation

The host’s innate immunity is one of the most difficult challenges cancer cells face in forming a tumor. Increased susceptibility to cancer in immunodeficient mice models and strong reaction to tumors in transplant studies shows the importance of the immune system in cancer prevention (Burnet, 1957).

Immune surveillance is crucial not only in cancer prevention but also shapes the course of cancer through a process called 'cancer immunoediting'. This process involves three stages, beginning with eliminating cancer cells by the innate immune system. This process is then taken over by an adaptive immune system involving T-lymphocytes. This process lasts till fewer immunogenic cancer cells are enriched in the population. At this point, the system reaches equilibrium, involving the continuous killing of tumor cells, which is replenished by less immunogenic cancer cells (Dunn *et al.*, 2002). This prolonged process ultimately leads to resistant clones that can evade the immune system (Malladi *et al.*, 2016). These resistant clones utilize numerous strategies to escape immune surveillance. These strategies involve a change in surface antigen, lack of recognition of tumor antigen by immune cells, resistance to cell death or secretion of immunosuppressive factors that will suppress the cytotoxic component of the immune system or recruit immunosuppressing inflammatory cells (Malmberg, 2004; Welte *et al.*, 2016). Along with this tumor, derived microsomes and tumor metabolic reprogramming also play an essential role in immune system modulation (Buck *et al.*, 2016; Muller *et al.*, 2016).

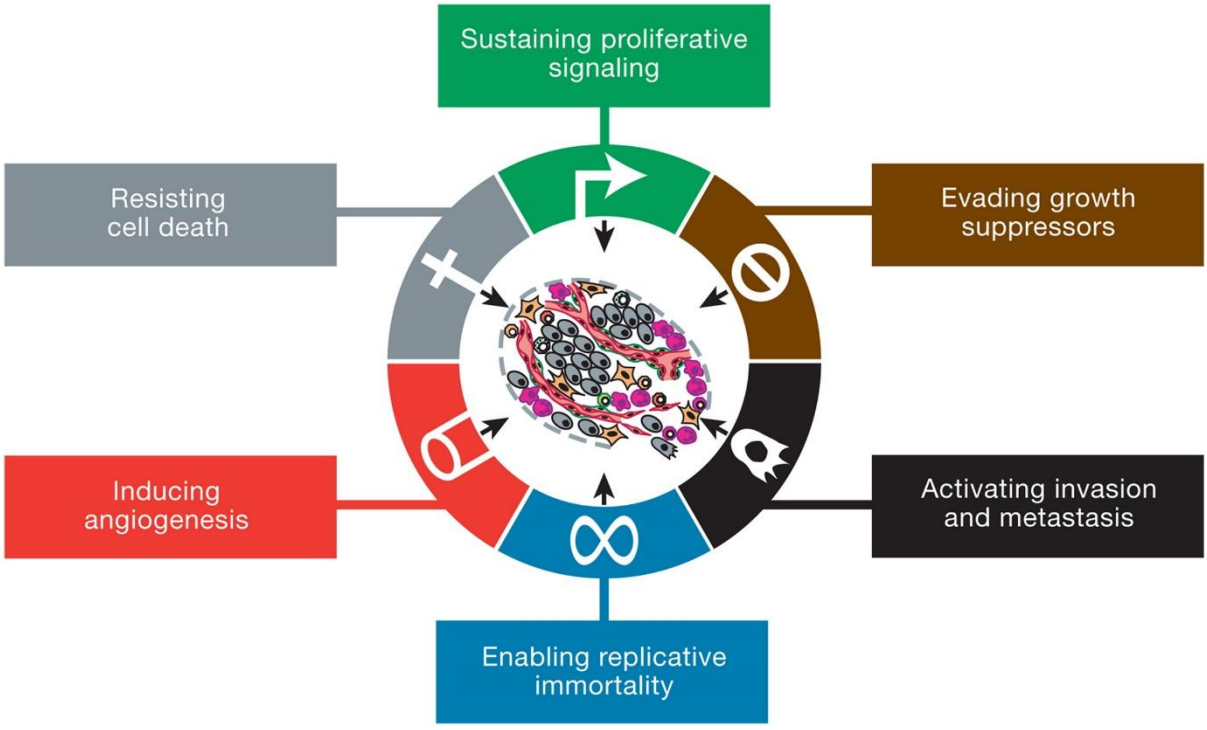

Figure 1.3: Hallmarks of cancer. This figure represents the major hallmarks capabilities of cancer cells that are observed in all cancers. These hallmarks collectively drive the transformation of normal cells into malignant cancer cells, contributing to the complexity and resilience of cancer as a disease. (Hanahan and Weinberg, 2011) (License type: CC-BY)

Apart from these classical hallmarks, recent studies have identified new hallmarks important in cancer progression: the remodeling of tumor microenvironment, phenotypic plasticity, non-mutational epigenetic programming and polymorphic microbiomes (Hanahan and Weinberg, 2011; Fouad and Aanei, 2017; Senga and Grose, 2021; Hanahan, 2022).

1.3 Cancer-causing oncogenes

One of the significant causes of cancer is oncogenes. In simple terms, oncogenes are genes that have the potential to cause cancer. According to the NIH, an oncogene is a mutated gene that has the potential to cause cancer. The critical role of oncogenes in cancer promotion first came into light with the discovery of viral oncogenes in 1970 (Duesberg and Vogt, 1970). Using viral genetics and biochemistry, Peter Duesberg and Peter Vogt identified the Src gene from the Rous Sarcoma virus (RSV) responsible for sarcomas in chickens (Rous, 1911; Duesberg and Vogt, 1970; Martin, 2004). Vogt and Duesberg continued to work with avian acute leukemia viruses MC29 and avian erythroblastosis virus. Further, they discovered two more viral oncogenes, myc and erbB, which were later shown to be derived from cellular genes (Duesberg, Bister and Vogt, 1977; Bister and Duesberg, 1979; Bister and Jansen, 1986; Martin, 2004).

In 1976, further investigation revealed that the src gene in the viral genome (v-src) is picked up from its mammalian counterpart (c-src) by recombination during the retroviral lifecycle (Stehelin *et al.*, 1976). This groundbreaking discovery linking viral oncogenes to cellular genes confirmed the existence of proto-oncogenes, i.e. genes involved in normal cell function that undergo mutation or deregulation, leading to cancer. Although various oncogenes have been identified, the exact mechanism that activates proto-oncogene to oncogenes is still unclear. Proto-oncogenes are typically involved in regulating vital cellular functions such as cell cycle, proliferation and cell death. Their function is tightly regulated at the level of gene expression and function. However, multiple mechanisms have been identified in cancer that lead to the activation of proto-oncogenes to oncogenes, some of which act at the level of gene

regulation, others act at the level of protein function, and often multiple mechanisms are in play.

Following are the mechanisms that are described earlier to work at the level of gene expression (Cooper, 2000; Kontomanolis *et al.*, 2020):

1. **Chromosomal translocation** - In this, gene with low expression moves to a high expressing gene locus (e.g. the chromosomal translocation of the MYC oncogene in human Burkitt's lymphoma, Translocation of *abl* in myelogenous leukemias)

2. **Deregulation of gene expression** - In this, mutation in the promoter region of gene or mutation in transcription factor regulating gene expression leads to a change in proto-oncogene levels

3. **Gene amplification** - In this, defects in mitosis lead to an increase in the copy number of genes which could in turn affect its expression (e.g. c-MYC in neuroblastoma)

4. **Epigenetic alteration** - Epigenetic alterations, which are changes in gene expression without altering the DNA sequence and involves DNA methylation, Histone modification and many more.

Other mechanisms that affect gene function include (Cooper, 2000; Kontomanolis *et al.*, 2020):

1. **Mutation(s)** that occurs in the gene and affect its function. Mutation includes point mutations or deletions that could either decrease or increase protein function (e.g. a point mutation at codon 12 of the RAS oncogene)

2. **Fusion protein(s)** while rarely seen in cancers are caused by translocation events that lead to the generation of a fusion oncogene where a single gene can now code for a fused proteins with distinctly different functions (e.g. Tel/PDGFR oncogene, PML/RARα fusion protein)

In cancer cells, more than one of the above-mentioned mechanisms often activates more than one oncogene; hence, most therapies fail to cure cancer completely.

1.3.1 RAS

Till date, 50 to 60 more oncogenes have been identified using gene transfer assays (such as viral transduction and transfection), most first discovered in human cancer (Lee and Muller, 2010; Weiss, 2020; McCormick, 2022). The first human oncogene identified in the gene transfer assay was a human homolog of the HRAS oncogene of Harvey sarcoma virus (Harvey, 1964; Langbeheim, Shih and Scolnick, 1980). Over a few years, remaining RAS isoforms, i.e. KRAS and NRAS, were also discovered using this method (Marshall, Hall and Weiss, 1982; Shimizu *et al.*, 1983). Characterization studies confirmed the individuality of these three RAS isoforms and showed that they are coded by different genes present on other chromosomes, i.e. chromosome 11 (HRAS), 12 (KRAS) and 1 (NRAS) (Figure 1.4) (McBride *et al.*, 1982; Hall *et al.*, 1983; Sakaguchi *et al.*, 1983).

Figure 1.4: Roadmap of RAS discovery. This figure represents the timeline of important discoveries related to the RAS structure and function (Gasper and Wittinghofer 2020) (License type: CC-BY)

1.3.1.1. Structure and function of RAS

Most information regarding RAS protein structure has been derived from early studies involving HRAS. All three RAS isoforms share a high degree of structural similarity in protein structure (Figure 1.5). RAS protein consists of two domains: a highly conserved G-domain (1-165 amino acids) towards the N-terminal and a hypervariable region (HVR, 166-188/189 amino acid) towards C-terminal (18). G domain contains the effector lobe, which comprises switch I and switch II regions (residue 1 - 86), and it is

conserved perfectly across all RAS isoforms (Buhrman *et al.*, 2011). This region is responsible for the effector binding function of RAS protein and also houses the most common RAS mutation site (G12, G13 and Q61) (Ryan and Corcoran, 2018). Contradictory to the G domain, HVR is significantly less conserved across RAS isoforms and houses the CAAX motif, which is required for post-translational modification and proper functioning of RAS. Cysteine of the CAAX motif undergoes farnesylation, following which RCE1 removes AAX residue, and finally, ICMT attaches the methyl group to the carboxyl group of the now-farnesylated cysteine (Cox, Der and Philips, 2015). Isoform-specific variation has been observed in this process, and observed distinction across RAS isoforms could be attributed to the differences between HVR regions (Berndt, Hamilton and Sebti, 2011). Along with the CAAX

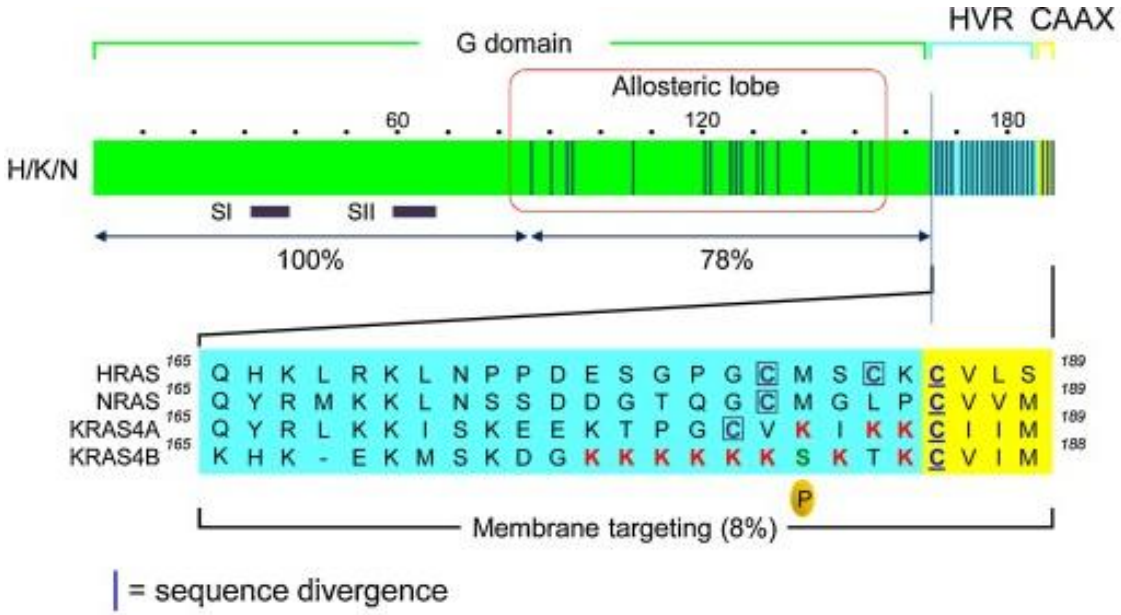

Figure 1.5: RAS structure. This figure represents the structural similarities and differences between different RAS isoforms (Zhou, Der and Cox, 2016) (License type: CC-BY)

domain, another secondary signal domain is believed to be present in all RAS isoforms, which can influence the RAS localization to the plasma membrane. HRAS and NRAS undergo palmitoylation, whereas KRAS has a polybasic stretch of lysine in the HVR region (Hancock, Paterson and Marshall, 1990; Roy *et al.*, 1999).

RAS is known to activate three major downstream pathways (Figure 1.6). The first pathway is the PI3K-AKT pathway, where activation of membrane-bound RAS results in generation of secondary signals (PI3K), ultimately activating AKT in the cytoplasm

(Burgering and Coffer, 1995). The second pathway is the Raf pathway. RAS-Raf interaction activates Raf, which in turn activates MEK, which then activates ERK kinase, and this pathway has been shown to be involved in promoting cell proliferation downstream of RAS (Pagès *et al.*, 1993). The last pathway is the RALGEF pathway, where RAS can interact with RALGEF, activating RALA and RALB GTPases (Yan and Theodorescu, 2018), which are mainly required to promote AIG (Lim, Donita C. Brady, *et al.*, 2010). Along with these three major pathways, RAS is also known to interact with p120RASGAP (RAS inactivator), and this interaction helps RAS to modulate various effector pathways, including RHO, Aurora kinase and AKT (Pamonsinlapatham *et al.*, 2009).

Although all the pathways mentioned above are regulated by all three RAS isoforms (HRAS, KRAS and NRAS), not all three pathways are equally utilized by these RAS isoforms. HRAS activates the PI3K pathway more strongly than the other two isoforms (Suire, Hawkins and Stephens, 2002).

Later, it was shown that this preference for the PI3K pathway by HRAS is not dependent on the membrane localization of HRAS (Prior *et al.*, 2001). KRAS activates the Raf signalling pathway more strongly than other RAS isoforms (Walsh and Bar-Sagi, 2001). Although these differences in preferential signalling pathways are observed, the exact mechanism regulating this is still not precise. Recent studies focus on the allosteric lobe of RAS (87 - 166 aa) isoforms, which has around 80-90% sequence similarity between all isoforms (Buhrman *et al.*, 2011). As the name suggests, this region supports RAS signaling, which involves membrane binding, ligand interactions, and nucleotide binding (Buhrman *et al.*, 2011).

Functionally, RAS is mainly required for cell proliferation and progression of the cell cycle (Mulcahy, Smith and Stacey, 1985), and Raf signaling is needed to promote cell proliferation in fibroblast cells (Pagès *et al.*, 1993). Besides this, RAS is also known to regulate other cellular processes like cell differentiation, cell migration and vesicle trafficking. Oncogenic RAS is shown to cause neuronal differentiation of

pheochromocytoma PC12 cells or differentiation of 3T3L1 fibroblasts into adipocytes (Bar-Sagi and Feramisco, 1985; Benito *et al.*, 1991). RAS can regulate cell migration by expressing cytokine responsible for migration (Nabi *et al.*, 1991) or controlling the RHO/RAC pathway (Yamauchi *et al.*, 2005). RAS can also regulate the RALGEF pathway to promote the export of vesicles to the plasma membrane (Hofer *et al.*, 1994; Lim, Donita C. Brady, *et al.*, 2010).

1.3.1.2 Regulation of RAS

RAS, being a small GTPase, has very low hydrolytic activity. Its activation depends on GTP binding. RAS switches between active (GTP bound) and inactive (GDP bound form), and this switch is regulated by RASGEFs and RASGAPs (Simanshu, Nissley

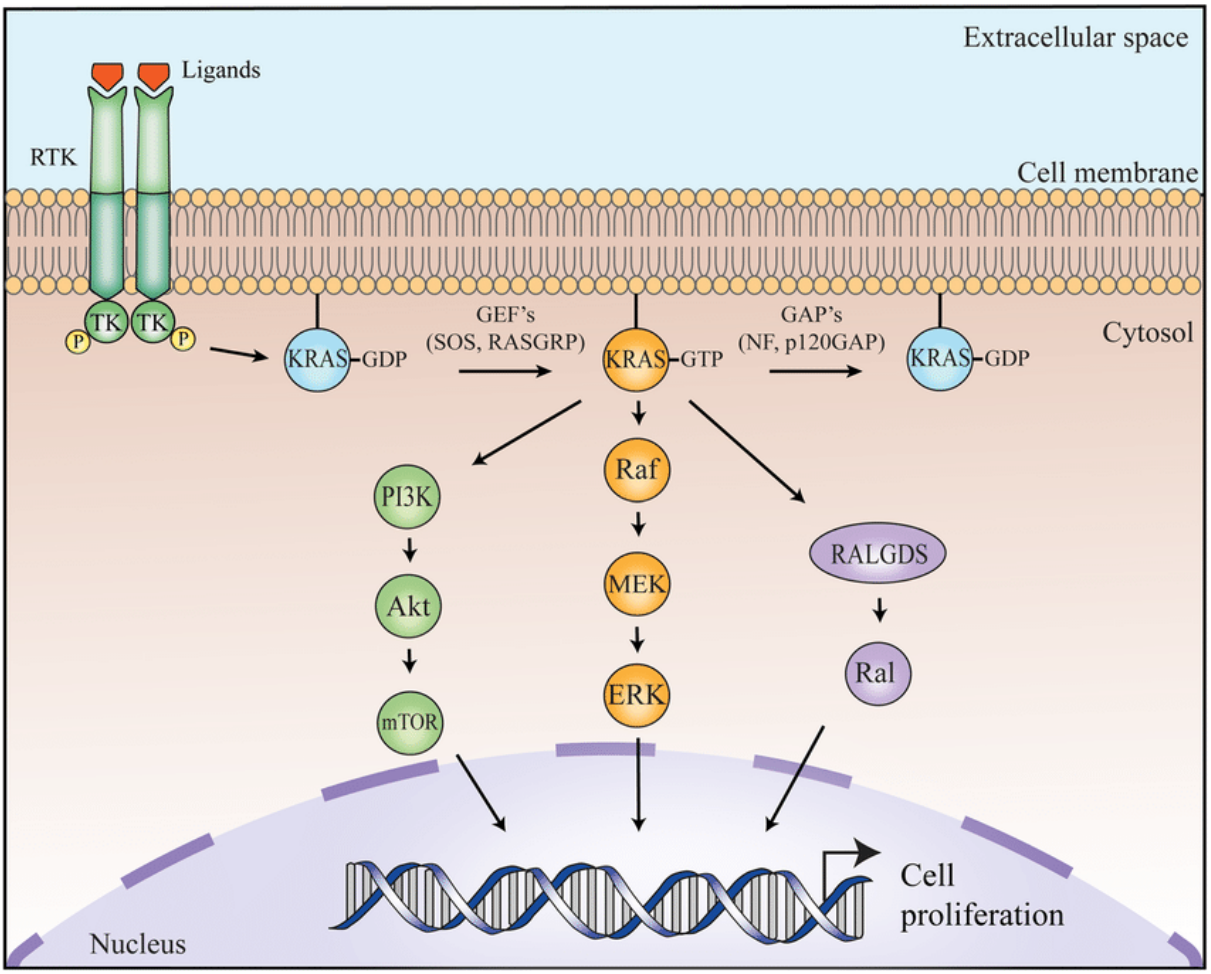

Figure 1.6: RAS signaling in cancer. This figure represents the RAS activation by membrane receptors and major RAS signaling pathways downstream of RAS (Kwan et al. 2022) (License type: CC-BY)

and McCormick, 2017). RASGEFs (such as SOS1, SOS2, GRB2, SHC1-4 RASGRP1-4, RASGEF1-2 and RASGRF1-2) trigger the GEF exchange activity of RAS and result in replacing GDP with GTP to activate RAS while RASGAPs (such as RASA 1-3, RASAL 1-3, DAB2IP, NF1, SPRED 1-3 and SYNGAP 1) which activates GTPase activity of RAS and facilitates hydrolysis of GTP to GDP results in inactivation of RAS (Simanshu, Nissley and McCormick, 2017)

As mentioned earlier, RAS localizes to the plasma membrane, and later, it was discovered that the regulation cited above of RAS activation takes place at the plasma membrane. Membrane receptors, including cell-matrix adhesion and growth factor receptors, can regulate RAS activation (Simanshu, Nissley and McCormick, 2017; Fernández-Medarde, De Las Rivas and Santos, 2021). Dimerization of these receptors at the cell membrane leads to the recruitment and activation of GRB2 and SOS protein, which activates RASGEFs, resulting in RAS activation (Gale *et al.*, 1993). Apart from this, RAS can also be regulated by post-translational modification. As mentioned earlier, RAS undergoes palmitoylation and farnesylation at the HVR region, which governs its plasma membrane localization.

Along with it, HRAS and NRAS, but not KRAS, are known to undergo mono or di-ubiquitination, which targets these two isoforms to endosomes (Jura *et al.*, 2006). Further, this mono-ubiquitination of RAS also decreases the sensitivity of RAS to GAP activation (Baker *et al.*, 2013). Phosphorylation of KRAS by PKC ar S181 can also regulate its localization and downstream signaling (Bivona *et al.*, 2006). These post-translational modifications do not regulate RAS activity directly but regulate its interaction with RASGEFs and RASGAPs to regulate RAS activity.

1.3.2.3 RAS in cancer

As described earlier, RAS is a proto-oncogene that regulates key cellular processes in physiological conditions, and its deregulation leads to oncogenic RAS activation, which promotes cancer. The most common deregulation observed in cancer with oncogenic RAS is a point mutation at G12, G13 or rarely at Q61 (Ryan and Corcoran,

2018)and RAS amplification (Punekar *et al.*, 2022). Although RAS is often mutated in many cancers, the disparity is observed in how oncogenic RAS isoforms are distributed in cancers (Figure 1.7). KRAS mutations make up for more than 60% of all observed RAS mutations, and HRAS is the least mutated isoform (Punekar *et al.*, 2022) In one of the most commonly diagnosed cancers (such as colon cancer, pancreatic cancer, head and neck cancer and squamous cell carcinoma), KRAS mutation is observed in almost 70 - 80% of solid tumors (Prior, Hood and Hartley, 2020), and often these mutations are located at G12 and Q61 (Gallego *et al.*, 1992). On the other hand, NRAS mutations are mainly present in melanoma and many haematological malignancies, while HRAS mutations frequently occur in the bladder, thyroid, cervical, and head and neck cancers (Gallego *et al.*, 1992).

The role of oncogenic RAS and its effector pathways in cancer promotion has been studied over a few decades. Early studies in mouse fibroblasts found Raf but not PI3K or RALGEF-RAL pathways sufficient to mediate RAS-driven tumor formation (Urano et al. 1996). This pathway is mainly responsible for uncontrolled cell growth and tumor formation in cancer (Gallego *et al.*, 1992). RAS also alters cytoskeletal organization in mammary epithelial cells to increase contractility (Panciera *et al.*, 2020). Inhibitor studies showed that this change results from the ERK/MAPK pathway modulating the Rho GTPases activity (Kubiniok *et al.*, 2017). The study in MEFs (Mouse Embryonic Fibroblasts) using specific inhibitors showed that the PI3K-AKT pathway significantly contributes to KRAS and NRAS-mediated cell transformation (Sheffels *et al.*, 2018). PI3K-AKT pathway is one of the major pathways responsible for anti-apoptotic signaling in RAS transformed cells (Qi, Wildey and Howe, 2006). the role of RALGEF-Ral signaling in RAS-driven tumors was initially overlooked. In 2002, the Counter group reported that the RALGEF-RAL pathway, but not Raf or PI3K, was essential for the RAS-mediated transformation of immortalized human cells (Hamad 2002). Apart from this, the role of RAS in promoting cell migration, cell-matrix adhesion and mechano-sensing in cancer cells is also known (Nyga *et al.*, 2023).

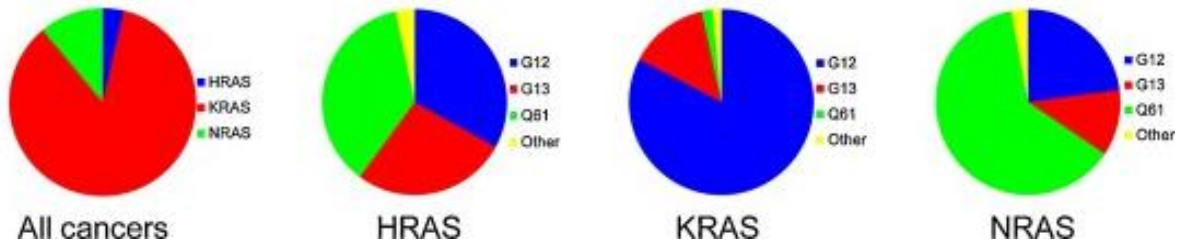

Figure 1.7: RAS in cancer. This figure represents the frequency with which RAS isoforms are mutated in cancer. This also represents the distribution of RAS mutation in each RAS isoform across cancers (Zhou, Der and Cox, 2016) (License type: CC-BY)

1.3.3 Ras superfamily in cancer

After the discovery of RAS in the 1980s, searching for related genes and gene products using antibodies and nucleic acid probes led to the identification of a large

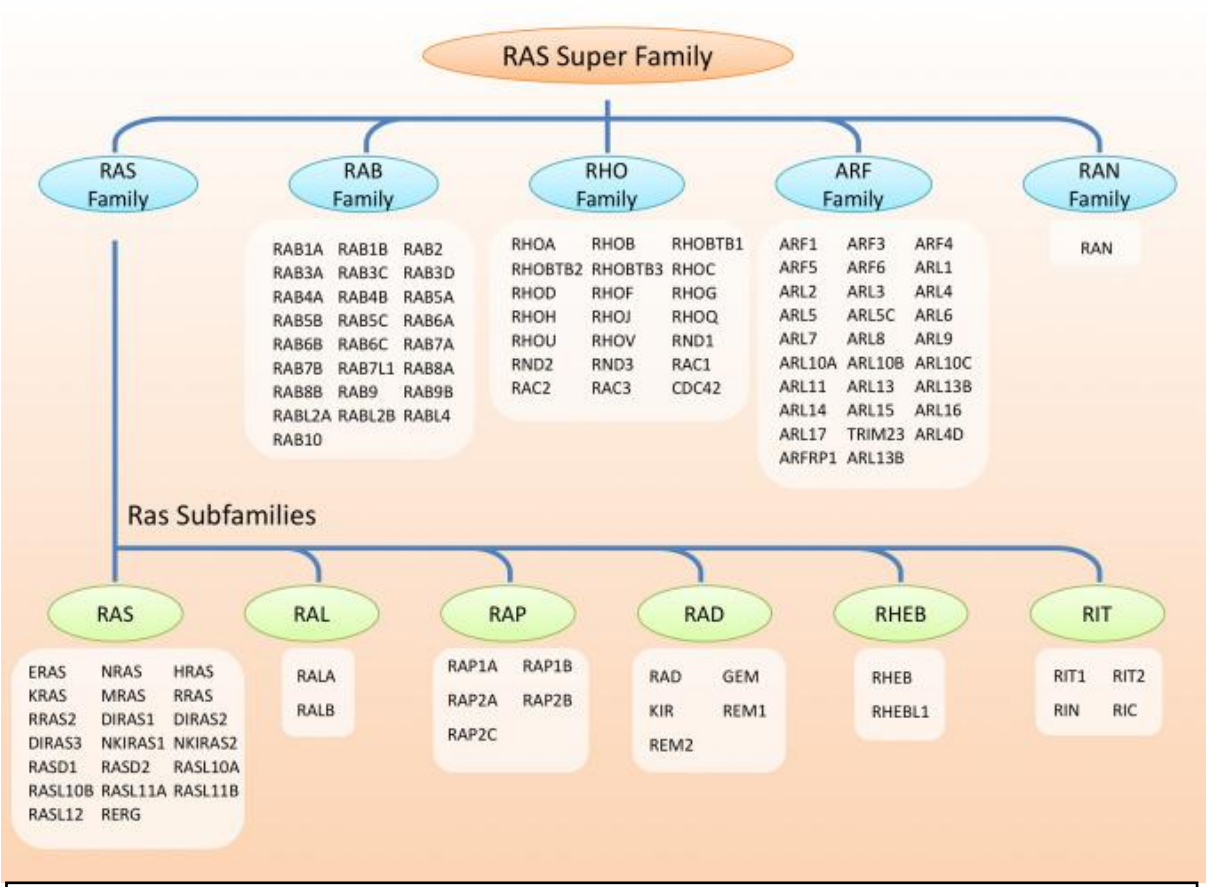

Figure 1.8: Ras superfamily. This figure represents the RAS superfamily which is made up of five major family and six subfamilies (Liu et al. 2018) (License type: CC-BY)

superfamily of small GTPases sharing structure and polygenetic similarities with original H, K and NRAS (Fernández-Medarde, De Las Rivas and Santos, 2021). Most adhesion and growth factor receptors have members of this small GTPases family working downstream of them. Over 150 members of this superfamily (Figure 1.8), similar to RAS, switch between active (GTP bound) and inactive (GDP bound form), which are regulated by GEFs and GAPs and share similar structural features (Yin *et al.*, 2023). Based on their sequence, structural similarity, and functions in the cell, gene in this superfamily can be split into five smaller, evolutionarily conserved subfamilies—RAS, RHO, RAB, ARF, and RAN (Heider *et al.*, 2010).

1.3.3.1 RHO

The RHO family genes regulate various key cellular processes in cells. They hence are associated with tumorigenesis and cardiovascular disease, including lymphomas, Kaposi's sarcoma, prostate cancer, gastric cell carcinoma, breast cancer, non-small cell lung cancer, squamous cell carcinoma, and glioblastoma (Figure 1.9) (Yin *et al.*, 2023). RHO family is a crucial regulator of cell-matrix adhesion and cytoskeleton organization, both of which play an essential role in cell migration and invasion in cancer (Crosas-Molist *et al.*, 2022). cdc42 can interact with RAS and its downstream signaling pathway to promote cell proliferation to induce RAS-mediated transformation (Lamas *et al.*, 2020). In thyroid cancer, cdc42 can encourage cancer cell migration, and at the same time, it can induce polarization of M2 macrophage that inhibits T cells (Huang *et al.*, 2022). Additionally, Rac1 is overexpressed in various cancers, and the inhibition of Rac1 prevents bladder cancer metastasis (Liu *et al.*, 2021). Rho GTPases are proven to be required for coordinated DNA damage response (DDR), which can determine the fate of cancer cells (Fritz and Henninger, 2015).

1.3.3.2 RAB

RAB family consists of 70 members that are known to be involved in regulating vesicular trafficking between plasma membrane and membrane-bound organelles in cells (Tzeng and Wang, 2016). Rab GTPases and their associated factors are essential regulators of transport, adhesion, anchoring, and fusion of vesicles in normal

and cancer cells (Krishnan *et al.*, 2020). RAB proteins (such as Rab25 and Rab31) are overexpressed in many cancers (Figure 1.9), and mutations in them often deregulate the overall trafficking network and result in tumor progression and metastasis (Chua and Tang, 2015; S. Wang *et al.*, 2017; Krishnan *et al.*, 2020). Mutation in the Rab35 gene can activate the PI3K-AKT pathway downstream to RAS and promote tumor progression (Salvatore *et al.*, 2018). Recent studies have shown that few members of this family have tumor suppressive activity, inhibiting angiogenesis and promoting programmed cell death in certain tumor types (Tzeng and Wang, 2016; Krishnan *et al.*, 2020).

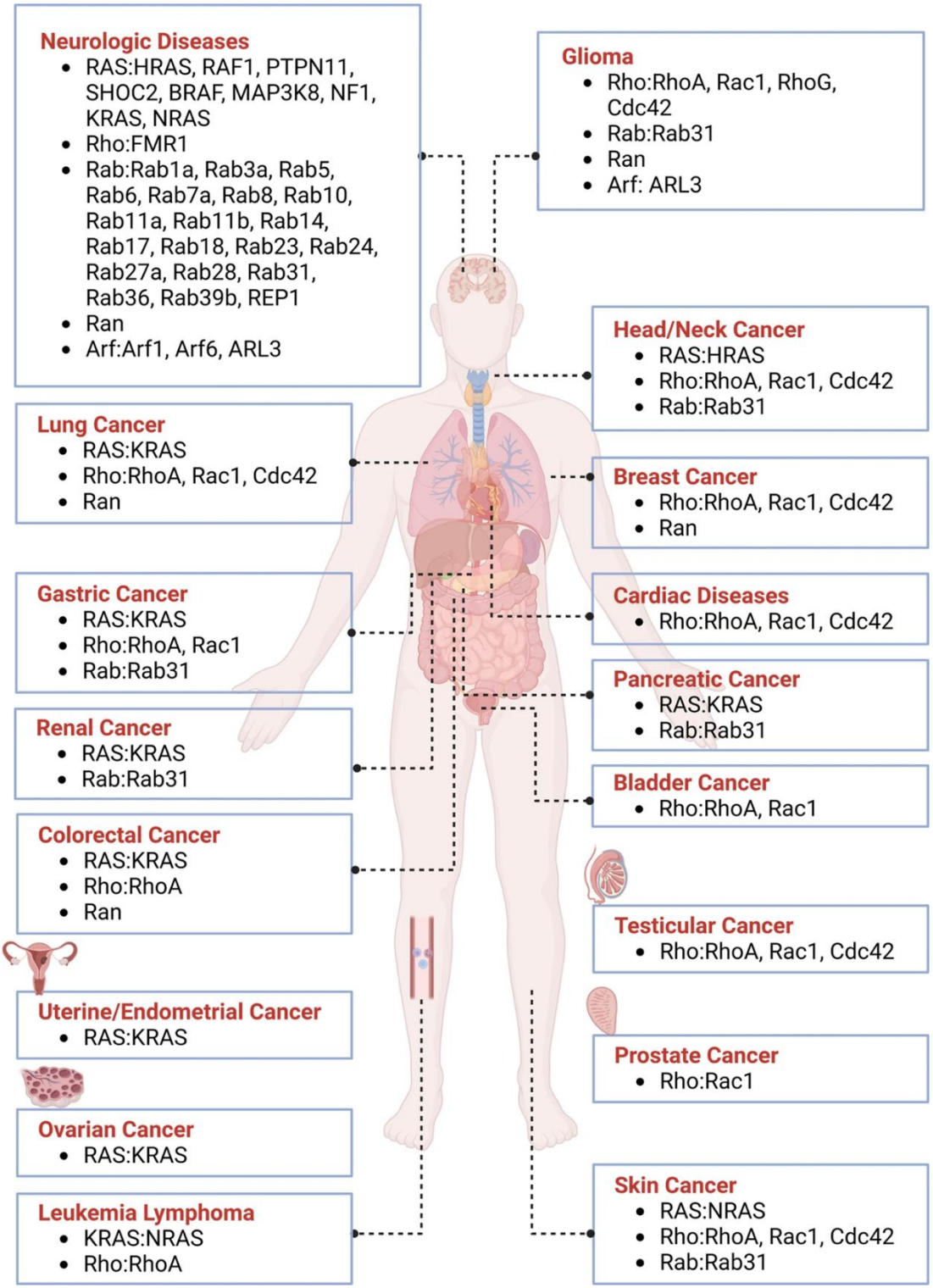

Figure 1.9: Small GTPases in cancer. This figure represents the distribution of mutation and aberrant expression of small GTPases across the cancers. (Yin et al. 2023) (License type: CC-BY)

1.3.3.3 Ran

Ran GTPases are mainly localized at the nuclear membrane, and their activation is essential in nuclear-cytoplasmic export and import (Cekan *et al.*, 2016). Apart from regulating nuclear transport, it is also known to regulate mitotic spindle assembly, thus modulating chromosome spatial organization during cell division (Prieto-Dominguez, Parnell and Teng, 2019). Because of its crucial role in regulating nuclear transport, overexpression of Ran GTPase has recently been associated with increased cancer aggressiveness and the promotion of tumor cell proliferation, progression, and metastasis (Sheng *et al.*, 2018). Ran GTPases are often overexpressed in breast and lung cancers, and knockdown of Ran leads to a reduction of Met receptor expression that contributes to drug resistance of tRAStuzumab and gefitinib (Yuen *et al.*, 2016). Increased levels of Ran and its activation results in nuclear-cytoplasmic transport. This allows cells to evade DNA damage-induced cell cycle arrest and senescence, which is crucial for cancer cell survival (Cekan *et al.*, 2016).

1.3.3.4 Arf

ARF GTPases family regulates multiple cellular processes ranging from organization of the cytoskeleton, sorting vesicle cargo, Golgi organization, recruitment of vesicle coat proteins, and alteration of lipid membrane composition (Prieto-Dominguez, Parnell and Teng, 2019). ARF family members play essential roles in tumor progression and invasion, particularly tumor angiogenesis (Casalou, Ferreira and Barral, 2020). Low expression of ARL3 in gliomas relates to poor prognosis, probably because of its essential role in angiogenesis and immune cell infiltration in the cancer microenvironment (Wang *et al.*, 2019). Dysregulation of ARF isoforms also promotes cancer formation and progression by stimulating tumor cell proliferation by activating RAS-controlled mitogen-activated protein kinases (MAPK) (Davis *et al.*, 2016).

1.4 Role and Regulation of RAL

RAL stands for RAS-like and belongs to one of the subfamilies of RAS (RAS, RAL, RIT, RAP, RHEB, and RAD). RAL was discovered in 1986 during the search of RAS

like genes using a cDNA library (Chardin and Tavitian, 1986). Downstream of RAS, the RALGEF pathway that regulates RALA and RALB is one of the major signaling pathways required for transformation; however, it has been ignored for a long time. Since the last decade or two, many reports have implicated the vital role of RAL downstream of RAS (Lim *et al.*, 2005; Lim, Donita C. Brady, *et al.*, 2010; Martin and Der, 2012; Wang *et al.*, 2013; Richardson *et al.*, 2022). The RAL subfamily is made up of RALA and RALB, both of which have a high degree of sequence similarity with RAS (~50%) (Richardson *et al.*, 2022). They are highly conserved across species, and invertebrates only harbor a single RAL gene.

RALA and RALB share around 82% sequence similarity; the first few amino acids are required for indirect interaction with ARF1 (Luo *et al.*, 1998). Similar to RAS isoforms,

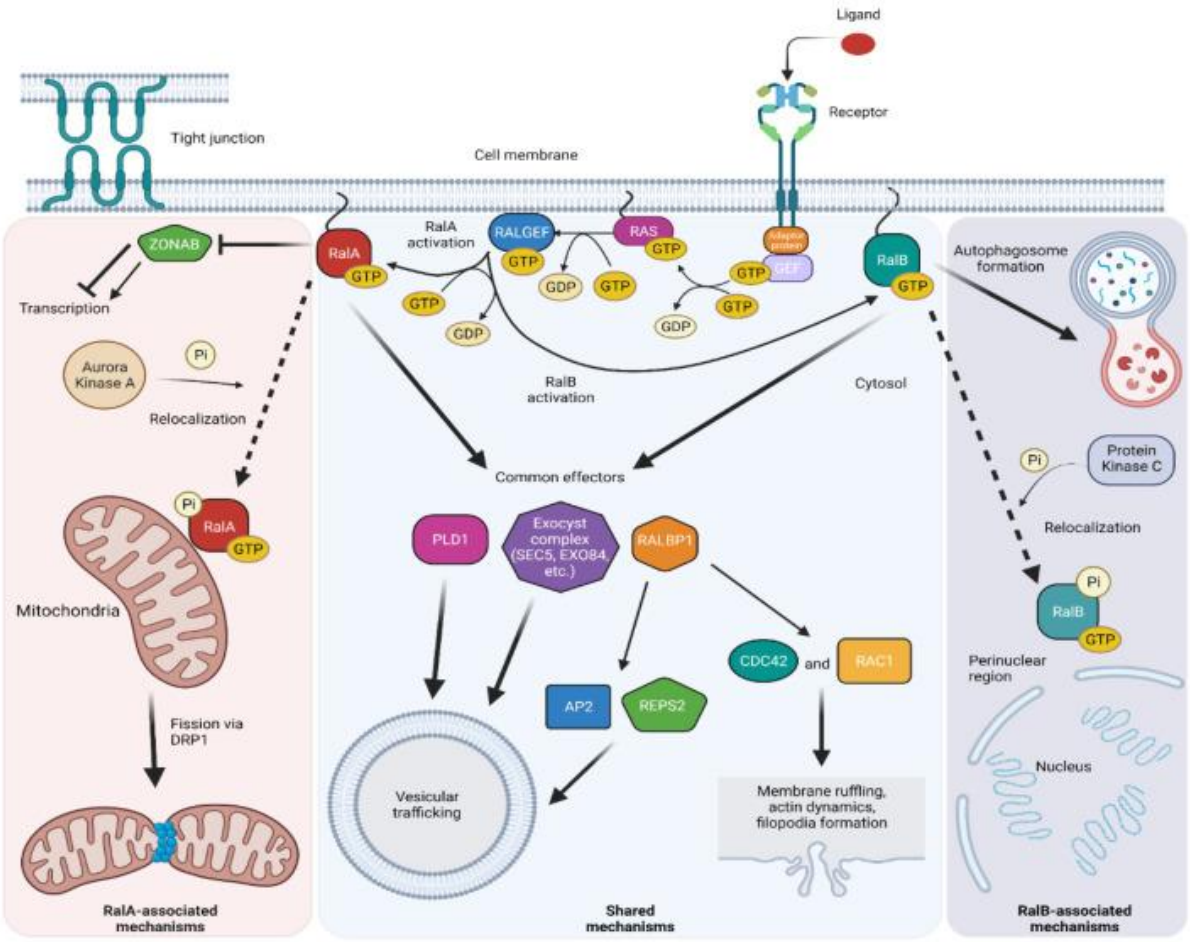

Figure 1.10: RALGEF signaling. This figure represents the RALGEF signaling pathways and their role in regulating cellular function downstream of RAS in normal cells. (Richardson et al. 2022) (License type: CC-BY)

in RALA and RALB, SWITCH regions and GTP binding pockets in G domain are conserved and mutation in this region results in generation of constitutively active (Q72L or G23V mutation locks RAL-GTPases in their GTP-bound, activated conformations) and dominant-negative mutants (G26A or S28N mutants are confined to their inactive, GDP-bound states) (De Leeuw *et al.*, 2001; Papini *et al.*, 2015). The C-terminal HVR region of RALA and RALB harbor most of the differences in amino acid sequence. Like RAS, this region undergoes post-translational modification to regulate and differentially localize RALA and RALB.

Cancer Subtype	RALA Role	RALB Role
Bladder cancer	RALA inhibits migration [97]	Phosphorylation of RALB is required for tumor growth and metastasis [23] and migration [97]
Blood Cancers	Upregulated and supports proliferation in CML [154]	May promote AML colony formation [156], regulates migration in MM [99]
Breast cancer	Involved in tamoxifen resistance [159], required for tumor growth, invasion, and metastasis [22]	Opposes proliferation and tumor growth [22], promotes metastasis [103]
Colorectal cancer	Stable RALA knockdown reduced colony formation via Exo84 [161]	Stable RALB knockdown increased colony formation via SEC5 [161], transient knockdown increased cell death and RALB is upregulated in the CRIS-B subtype [162]
Gastric cancer	Interacts with RCC2 and the MAPK/JNK pathway [163]	Limited data
Hepatic Cancer	Upregulated and activated in cancer tissue [47,66,174], increases migration and stemness [166]	Limited data, does not appear to be upregulated [166]
Pancreatic cancer	Required for tumor establish-ment [176], involved in anchorage-independent growth [84]	Involved in invasion [91]
Lung cancer	Important for tumorigenesis, proliferation, and invasion [167]	Important for invasion [188], cell cycle regulation [56], and migration [169]
Melanoma	Disruption of either RALA or RALB decreases tumor growth [170]	Disruption of either RALA or RALB decreases tumor growth [170]
Nerve sheath tumors	Associated with invasion [171] and apoptosis [172]	Limited data, upstream inhibition of RALB induces apoptosis when NF1 is decreased [172]
Ovarian cancer	GTP-RALA is overexpressed in cancerous cells, important in growth and invasion [173]	Limited data, GTP-RALB is not overexpressed in cancerous cells [173]
Prostate cancer	Central to invasion and migration [93], promotes prostate to bone metastasis [180,181]	Limited data
Renal cancer	Required for invasion [186]	Limited data, not required for invasion [186]

Figure 1.11: Role of RALA and RALB in cancer. This figure represents known role of RALA and RALB in all known cancer. This also summarizes the tested function of RALA and RALB in each cancer. (Richardson et al. 2022)

1.4.1 RAL function in normal and cancer cells

RAL is known to regulate both endocytosis and exocytosis in cells (Figure 1.10). RAL-dependent regulation of endocytosis is mediated by RALBP1 interaction (Awasthi *et al.*, 2001). RALBP1 and REPS2 regulate the binding and internalization of EGFR receptors (Nakashima *et al.*, 1999). RALBP1-AP2 interaction downstream of RAL is also shown to regulate receptor-mediated endocytosis (Jullien-Flores *et al.*, 2000). Along with endocytosis, RAL also regulates exocytosis. Expression of G23V RALA increases insulin secretion by beta cells, but expression of S28N RALA decreases insulin secretion (Lopez *et al.*, 2008). In MDCK cells, RALA but not RALB is involved in the trafficking of EFGR to the basolateral membrane, which is mediated by binding with SEC5 (Shipitsin and Feig, 2004). Apart from this, RALA, but not RALB, is also known to regulate cell spreading in WTMEFs (Balasubramanian *et al.*, 2010). Although RALA and RALB share 82% sequence similarity, they exhibit different functions in cancer, as shown in Figure 1.11.

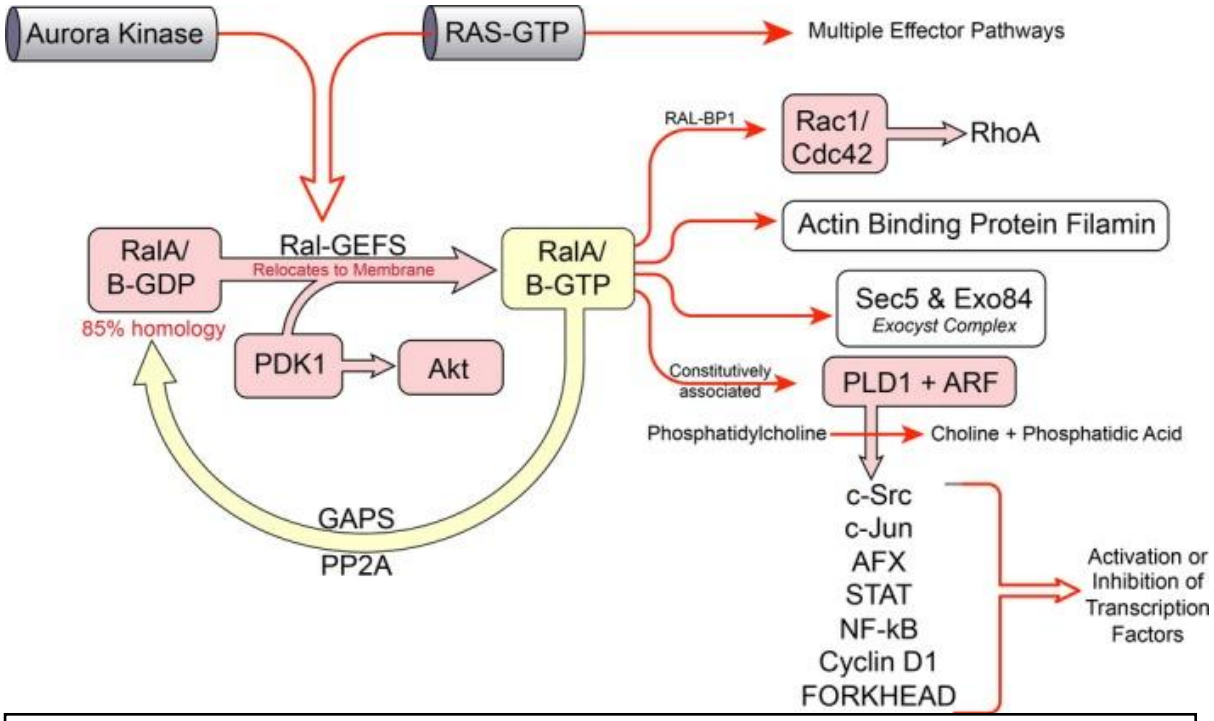

Figure 1.12: Role and regulation of RAL. This figure represents complex pathways involved in RAL activation and its downstream signaling. (Moghadam et al. 2017) (License type: CC-BY)

1.4.2 Regulation of RAL GTPases

These observed differences in RALA and RALB function are primarily attributed to their differential regulation. Similar to RAS, RAL are regulated by GEFs and GAPs (Figure 1.12). RALGEFs trigger the nucleotide exchange to activate RAL, and seven RALGEFs now identified are RGL1-3. RALGDS, RALGPS1-2, RCC2 (Richardson *et al.*, 2022). RALGDS and RGL1-3 have RA (RAS association) domains for binding RAS and are RAS effectors (Rebhun, Chen and Quilliam, 2000). In many cancers, RALGEF levels are elevated, and it is often linked with metastasis and inhibition of RALGEFs releases RALA and RALB activation and resulting metastasis in both *in-vitro* and *in-vivo* (González-García *et al.*, 2005; Zago *et al.*, 2018; Guo *et al.*, 2021). Out of all known RALGEFs, only RCC2 is known to differentiate between RALA and RALB. It activates only RALA but not RALB in HeLa and U2OS cells (Papini *et al.*, 2015). RALGAPs trigger the RAL GTPase function to hydrolyze GTP to GDP, resulting in RAL inactivation. RALGAPs are heterodimeric proteins; until now, two RALGAPs, i.e. RALGAP1-2, have been identified (Shirakawa and Horiuchi, 2015). Decreasing RALGAP expression is correlated with metastasis, and overexpression of RALGAPs inhibits the metastasis (Uegaki *et al.*, 2019; Yoshimachi *et al.*, 2021).

RAS-mediated activation of RAL has been very well studied, and it is known to work downstream of EGF, PDGF, LPA, and insulin signaling (Wolthuis *et al.*, 1998; Zwartkruis *et al.*, 1998; Gildea *et al.*, 2002). However, whether this signaling can differentially activate RALA and RALB is still unclear. An RAS-independent mechanism involving Ca2+/calmodulin binding in platelets activates RALA and RALB (Park, 2001). The yeast dihybrid cross revealed that calmodulin binds more strongly to RALA than RALB and is independent of the HVR region (Clough, Sidhu and Bhullar, 2002). Apart from this, adhesion receptors and cell-matrix signaling can regulate RALA activation but not RALB, and this activation is required for cell spreading in WTMEFs (Balasubramanian *et al.*, 2010).

Similar to RAS, RALA also undergoes farnesylation or geranylgeranylation at CAAX residue, and this modification is essential for membrane association and cellular localization (Falsetti *et al.*, 2007; Xu *et al.*, 2015). RALA and RALB are known to undergo

ubiquitination at lysine residue, which changes their localization. RALB ubiquitination at K47 is crucial for interaction with EXO84 and SEC5 (Simicek *et al.*, 2013). Whether or not this post-translational modification regulates RAL activation is still an open question. Apart from this, RALA and RALB both undergo phosphorylation at the HVR region. RALB is phosphorylated at S192 and S198 by PKCa, and S198 phosphorylation is required for RALB perinuclear localization and cell migration in UMUC3 cells (Wang *et al.*, 2010). RALA also undergoes phosphorylation at S183 and S194. S194 phosphorylation is carried out by PKA and AURKA (Neel *et al.*, 2014)(Wu *et al.*, 2005). However, the role of mediated regulatory crosstalk in cells remains untested. AURKA-RALA crosstalk has been tested for its role in RALA regulation and its implication in cancer, and it is discussed in the next section, along with the independent role of AURKA in cancer.

1.4.3 Aurora Kinase A (AURKA)

Aurora kinases are mitotic kinases that belong to the serine/threonine protein kinase family, discovered in *Drosophila melanogaster* mutants with defects in centrosome separation and spindle formation during mitosis (Glover et al. 1995). This kinase family comprises three members: Aurora Kinase A (AURKA), Aurora Kinase B (AURKB) and Aurora Kinase C (AURKC). Aurora kinases have three structural domains: the N-terminal domain, the protein kinase domain in the middle and the C-terminal domain (Figure 1.13). While the C-terminal domain is conserved, the N-terminal domain differs

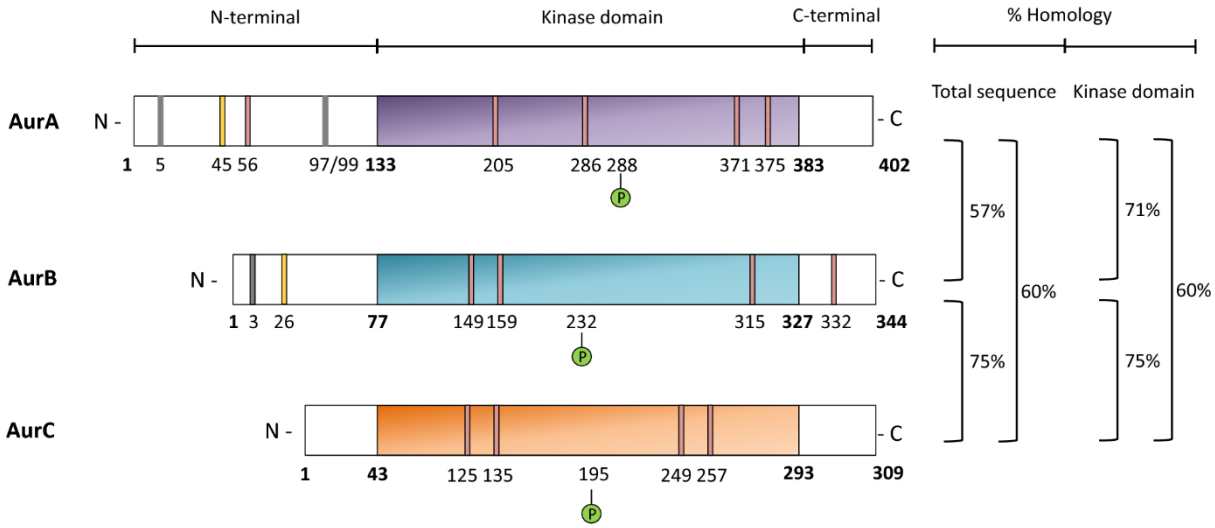

Figure 1.13: Structure of Aurora kinase. This figure represents the structural domains and similarity in aurora kinase isoforms. (Willems et al. 2018) (License type: CC-BY)

in all isoforms and plays a vital role in differential localization and substrate interaction (S. Li et al. 2015). The middle kinase domain contains an activation loop and has an auto-phosphorylation site required for a positive feedback loop, as well as a D box (degradation box) for protein degradation. The location and sequence of the D box varies in all Aurora kinase isoforms, getting differential regulation of three isoforms (Crane et al. 2004).

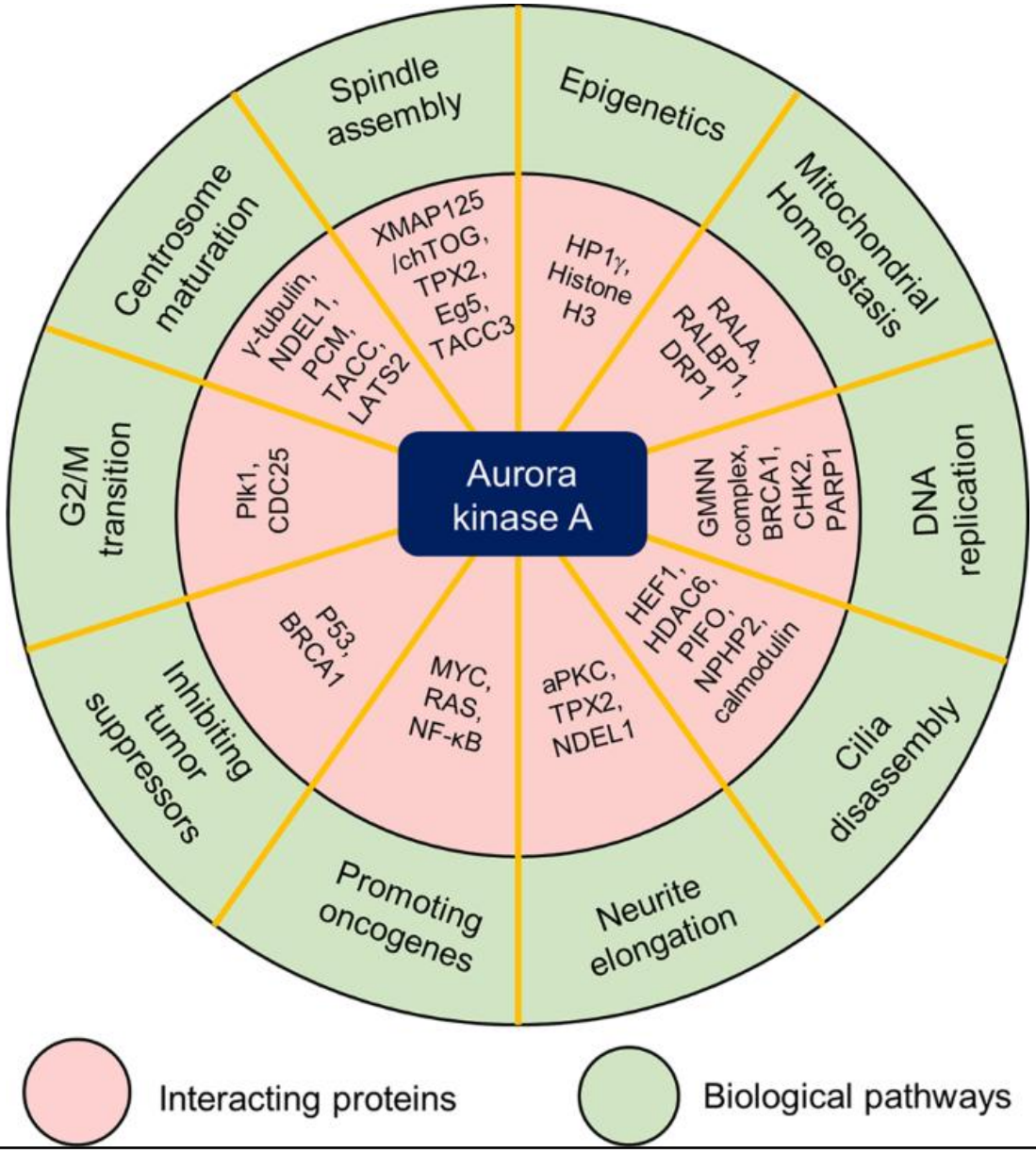

Figure 1.14: Role of AURKA. This figure represents the AURKA function and its interacting partners in downstream signaling (Mou et al. 2021) (License type: CC-BY)

1.4.3.1 Aurora kinase A function and regulation

Since Aurora kinases are mitosis kinases, their expression is regulated in a cell cycle-dependent manner. This is regulated at the level of transcription. Aurora kinases promoter region houses regulatory sequences CDE (cell cycle-dependent element) and CHR (cell cycle gene homology region) and serve as binding site for Cyclin-A, CDC25C, CDK1, PLK and AURKA (Tanaka et al. 2002; Vader & Lens 2008; Crosio et al. 2002) and E2F-1, E2F-4, DP-2 and FoxM1 transcription factor in case of ARUKB (Kimura et al. 1999).

Apart from this, Aurora kinases are regulated by post-translational modification. As mentioned earlier, Aurora kinase has a T loop harboring auto-phosphorylation site that activates these kinases (Beenstock et al. 2016; Adams 2002). This autophosphorylation of Aurora kinase requires Ajuba, TPX2, Bora and TACC3 as co-factors (Hirota et al. 2003) (Kufer et al. 2002; Zorba et al. 2014). AURKA is kept in inactive form by binding with protein phosphatase 1 γ (PP1), and during mitosis, TPX2 released from chromosomes compete with PP1 to bind AURKA and activates AURKA by promoting auto-phosphorylation at Thr288 (Kufer et al. 2002; Carmena & Earnshaw 2003b). AURKA auto-phosphorylation at Ser51, Ser53/54, Ser66/67, and Ser98 residues could also be induced by Ca2+/Calmodulin (CaM) (Plotnikova et al. 2010; Plotnikova et al. 2012). Other kinases, including PKA and PAK-1, can activate or inhibit AURKA by phosphorylating it at Thr288 or Ser342 residue, respectively (Zhao et al. 2005)(Willems et al. 2018; Dodson & Bayliss 2012). Further, acetylation of AURKA at residues K75/K125 by ARD1 has been shown to help maintain its activity (Vo et al. 2017). Nevertheless, Thr288 auto-phosphorylation seems crucial for activating AURKA over any other modification (Zorba et al. 2014). AURKA degradation is initiated by the Cdh1 protein that recognizes the D box sequence on AURKA (Littlepage and Ruderman 2002). Cdh1 activates APC/C, which then ubiquitinates AURKA, leading to its proteasomal degradation. This process begins at the end of mitosis and is completed in the G1 phase of the cell cycle.

AURKA is primarily involved in centrosome growth and maturation (Figure 1.14). Cdk11 and Src signaling recruits and activates AURKA and PLK1 (polo-like kinase 1) at centrosomes (Barretta et al. 2016). AURKA then recruits centrosomic (Terada et al. 2003) and g-TuRC (g-tubulin ring complex) (Sen et al. 2008) for nucleation and

elongation of microtubules and phosphorylates NDEL1, TACC, LATS2 and BRCA1 to the MTOC (Giet et al. 2002; Ouchi et al. 2004). AURKA also helps stabilize the microtubule's minus end at centrosomes (Barros et al. 2005; LeRoy et al. 2007). AURKA-mediated phosphorylation of cyclin B1-Cdk1 is essential for the cell cycle's G2 phase to M phase transition (Gavet & Pines 2010; Jackman et al. 2003). Once centrosomes are matured, they move to the opposite end during mitosis. URKA inhibition causes monopolar spindle assembly, suggesting a further role in centrosome separation (Glover et al. 1995). During centrosome separation, AURKA regulates microtubule assembly and disassembly and phosphorylates kinesin Eg5, which is involved in regulating the anti-parallel forces of the spindle MT (Asteriti et al. 2011; van Heesbeen et al. 2013) (C.-Y. Jang et al. 2009).

Apart from regulating mitosis, it also has vital functions in cell interphase. In the G0/G1 phase, it localizes in the proximity of cilia, and when the cell leaves a quiescent state

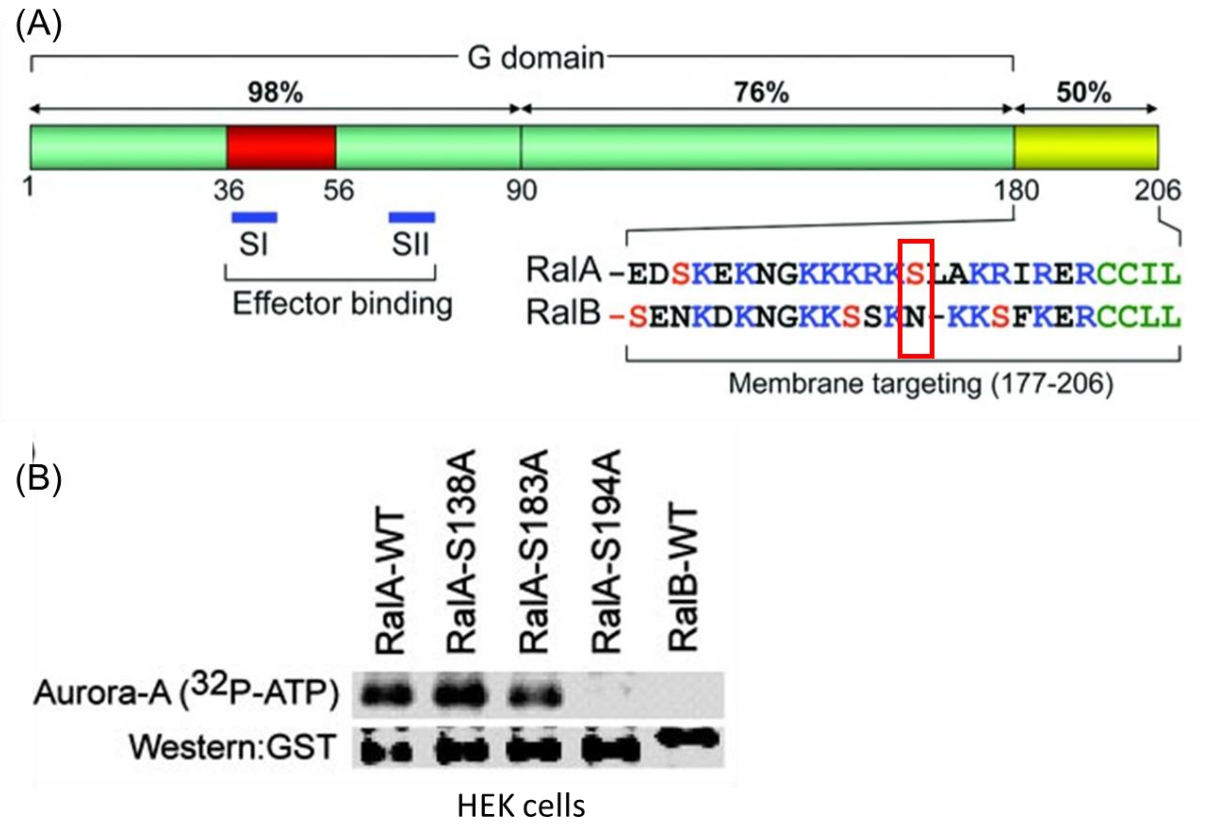

Figure 1.15: AURKA mediated phosphorylation of RALA. (A) Figure showing differences in HVR region of RALA and RALB (Bodemann and White 2008). (B) *In-vitro* assay data to identify AURKA phosphorylation site on RALA (serine 194 residue). This also shows that AURKA does not phosphorylate RALB (Wu et al. 2005).

and re-enters the cell cycle, AURKA activation is required for cilia disassembly (Pugacheva et al. 2007). During neuronal growth, AURKA stabilizes MTOC in neuronal cells, which is essential in cargo transport (D. Mori et al. 2009). In COS7 cells, PLD2-AURKA-SRC-FAK is essential for maintaining cell migration (Mahankali et al. 2015).

1.4.3.2 AURKA in cancer

Of the three Aurora isoforms, AURKA is most frequently involved in cancer and tumorigenesis. AURKA overexpression and amplification have been reported in various cancers, including breast (Hole, Pedersen, Lykkesfeldt & Yde 2015b), colorectal (Bischoff et al. 1998), gastric (X. Liu et al. 2016), bladder (N. Zhou et al. 2013) and prostate cancers (Das et al. 2010). Further, AURKA expression is linked with poor prognosis of colorectal, breast, nasopharyngeal, bladder and gastric tumors (J. Xu et al. 2014; Nadler et al. 2008).

Overexpression, AURKA, or aberrant AURKA activity both leads to aneuploidy, which is known to drive cancer progression (Meraldi et al. 2002)(Carmena & Earnshaw 2003). AURKA overexpression is responsible for overcoming the spindle assembly checkpoint in cancer (Anand & Penrhyn 2003). AURKA is known to phosphorylate tumor suppressor genes like p53, BRCA1 which often leads to their inactivation or degradation (Meraldi et al. 2002) (Ouchi et al. 2004) and overexpression of AURKA in cancer cells, eventually leading to inhibition of these tumor suppressor genes. AURKA also promotes other oncogenic signaling pathways such as RAS/Raf/ERK/MAP (Furukawa et al. 2006). Similarly, AURKA is often overexpressed with oncogenic RAS, complementing the RAS transformation in NIH3T3 cells (Furukawa et al. 2006).

1.4.4 AURKA-RALA crosstalk in cancer

The non-canonical role of AURKA, which interacts with the RALGEF pathway downstream of RAS, has been established in the last decade. *In-vitro* kinase assay studies showed AURKA phosphorylates RALA at Serine 194 residue (S194) but did not affect RALB (Figure 1.15) (3). AURKA-mediated phosphorylation of RALA at S194 regulates RALA localization to cell membranes (4). RALA is a small GTPase; its function is dependent on its activity. However, it remains unestablished as to whether AURKA-mediated RALA phosphorylation at S194 can regulate RALA activation.

Studies in non-transformed HEK293 and MDCK cells expressing constitutively active RALAV23 and phosphodeficient S194A-RALAV23 mutants show this phosphorylation to be vital for RALA-dependent anchorage-independent growth (AIG) (1, 3). In pancreatic cancer cells (ASPC1, HPAC, HPAF-II, PANC-1, SW1990, CAPAN-1, CFPac-1, MiaPaCa2, T3M4) knockdown of RALA and reconstitution with WT RALA vs S194A RALA mutant further supports this claim in AIG studies (4). AURKA inhibitor (MLN8237) treatment of pancreatic cancer cells like (ASPC1, HPAC, PANC-1, SW1990, CAPAN-2, CFPac-1, MiaPaCa2, T3M4, PANC10.05, HuPT3) is also seen to affect their AIG (5,6).

The only known tumor formation study in RALA knockdown pancreatic cancer cells (CFPac-1, HPAC, Capan1) reconstituted with WT-RALA vs S194A-RALA phosphodeficient mutant showed loss of RALA to affect tumor formation that is restored by WT-RALA reconstitution. S194A-RALA mutants, however, had variable effects, comparable to WT-RALA in CFPac-1, comparable to RALA KD in Capan-1, and better than RALA KD but not equivalent to WT-RALA in HPAC tumors (1). Targeting AURKA activation using known inhibitors like MLN8237 (Alisertib) in pancreatic cancers (PancT4 cell line and Primary cells from tumors) is seen to suppress tumor formation (5). However, this study showed no change in S194A-RALA phosphorylation, suggesting the effects seen might be independent of RALA.

1.5 Hypothesis and objective

Based on the literature, it is evident that AURKA-RALA crosstalk is poorly understood. Since it was first discovered using *in-vitro* assay and initial studies were carried out in immortalized non-transformed cell lines, its relevance in cancer remains unclear. Only two known studies have used RALA S194A mutant to evaluate the role of this crosstalk in cancer cells. However, their results are ambiguous, especially regarding the role AURKA-RALA crosstalk has in tumorigenesis. Also, the only known AURKA inhibition study in cancer cells did not affect the RALA S194 phosphorylation. This also raises questions about the presence of this crosstalk and possibly its detection with the pS194 RALA antibody in cancer cell lines. Whether RALA S194 phosphorylation by AURKA can regulate RALA activation remains an open question in cancer cells. Also, suppose AURKA can activate RALA signaling to promote AIG and tumorigenesis. It is still unclear how much of this effect can also come through AURKA regulating RALA-independent pathways. Apart from this, both AURKA and RALA work along with RAS in cancer progression, and it is helpful to know whether oncogenic RAS can influence this crosstalk to promote RAS-dependent transformation. This leads us to ask the following questions:

1. Is AURKA-RALA crosstalk present and detectable in cancer cells?
2. Does AURKA-mediated RALA phosphorylation at S194 regulate RALA activation?
3. Does RALA S194 phosphorylation regulate tumorigenesis in cancer cells?
4. If AURKA can regulate the RALA pathway to promote AIG and tumorigenesis, what is the relative contribution of AURKA and RALA, respectively?
5. Does AURKA-RALA crosstalk change in the presence of oncogenic RAS in cancer cells?

This thesis tests and establishes the AURKA-RALA crosstalk in cancer cell lines using a novel nanovesicle drug delivery system to deliver MLN8237 and specifically inhibit AURKA in cancer cells. It also evaluates the effect AURKA-mediated RALA phosphorylation at S194 has on RALA activation. Further, it tests the impact of RALA and its phosphorylation on tumorigenesis using CRISPR-Cas9 mediated RALA KO

and reconstitution with S194 mutants. Finally, we also address whether AURKA-RALA crosstalk differs in the presence of oncogenic RAS in cancer cells.

Objectives of this study:

1. Evaluate the AURKA-RALA crosstalk in cancer cells
2. Test whether RALA phosphorylation at S194 can regulate RALA activation
3. Evaluate the role of RALA and RALA S194 phosphorylation in tumorigenesis
4. Test whether AURKA-RALA crosstalk is different in cancer cells with and without oncogenic RAS

Chapter 2

Materials and Methods

2.1 Reagents

Human plasma fibronectin (Cat#F2006), nocodazole (Cat # M1404), DMSO (Cat # D2438), DAPI (Cat# D9542), Propidium iodide (Cat# P4170), Cesium chloride (Cat# C3032), sodium orthovanadate (Cat# S6508), sparfloxacin (Cat# 56968) and thiazolyl blue tetrazolium bromide (MTT, Cat# M2128) were purchased from Sigma, and Phalloidin-Alexa-488 (Cat# A12379), Phalloidin-Alexa-633 (Cat # A22284) was from Molecular Probes (Invitrogen). Fluoromount-G was used to mount cells for imaging and was obtained from Southern Biotech (Cat# 0100-01). Glutathione sepharose beads used for the RAL activity assay were from GE (Cat# 17075601). Crystal violet was used for staining colonies in the AIG assay from Amresco (Cat# 0528). Collagen for doing 3D uptake studies was purchased from Corning (Cat# 354236). Dextran (6000 Mw), dicyclohexylcarbodiimide (DCC), dimethylamino pyridine (DMAP), ethylchloroacetate, polyethylene glycol (PEG) (4600 Mw) were purchased from Sigma- Aldrich. Horse liver esteRASe was purchased from Sigma (Cat# 46069) and used as such.

Alisertib (MLN8237) was purchased from Selleckchem (Cat# S1133). BQU57 (Ral inhibitor Cat# SML-1268) and AZD1152 (AURKB inhibitor Cat# SML0268) were purchased from Sigma. N, N dimethyl formamide (DMF) and all of the necessary solvents were purchased from Spectrochem Laboratories. Carboxylic acid-substituted 3-pentadecylphenol (PDP-acid) was synthesized following our earlier report(Pramod et al. 2012). The BCA protein estimation kit (Cat# 23227) was purchased from Thermo Scientific. Nonidet P40 Substitute (Cat# 68387-90-6) and RNAase-A (Cat# 9001-99-4) were purchased from USB corporation. Trizol (Cat# 15596018) was purchased from Ambion. Immobilon western blot substrate (Cat# WBKLS0500) was purchased from Millipore.

2.2 Antibodies

Antibodies used for western blotting include anti-phospho-aurora A (Thr288)/aurora B (Thr232)/ aurora C (Thr198) (Cat #2914), anti-AURKB (Cat #3094), anti-phospho AKTSer473 (Cat# 9271) (1:2000 dilution), anti-phospho-FAK-Tyr397 (Cat# 3283), anti-phosphop44/p42 ERK1/2 (Thr202/Tyr204) (Cat# 4370) (1:2000 dilution), anti-p44/p42 ERK1/2 (Cat#4695) (1:2000 dilution), anti-FAK (Cat#3285), anti-AKT (Cat#

4691) antibodies were purchased from Cell Signaling Technologies and used at 1:1000 dilution unless mentioned otherwise. Anti-AURKA (Cat #610939) and anti-RALA (Cat# 610221, clone 8) were purchased from BD Transduction Laboratories and used at 1:1000 dilution. anti-Phospho-RALA (Ser194) (Cat# 07-2119) was purchased from Millipore, and Anti-RALB was purchased from R&D Laboratories (Cat# AF3204), both used at 1:1000 dilution. Anti-beta actin (Cat# Ab3280) antibody was purchased from Abcam and used at 1:2000 dilution. Secondary antibodies conjugated with HRP were purchased from Jackson Immunoresearch and were used at a dilution of 1:10000.

Antibodies used for immunofluorescence include Anti-myc (Cat# sc-789) obtained from Dr Sanjeev Galande's Lab (IISER, Pune) used at a dilution of 1:200 and anti-phospho-p44/p42 ERK1/2 (Thr202/Tyr204) (Cat# 4370) from Cell signalling technologies used at 1:200 dilution. Secondary antibodies with Alexa conjugate (488 or 594) were purchased from Invitrogen Molecular Probes (Cat. No. # A12379 and A12381) and were used at a dilution of 1:1000.

2.3 Plasmids and primers

Plasmids:

pMIG: Cat no – 12282, (Addgene)

pSpCas9(BB)-2A-Puro (PX459): Cat no – 48139 (Addgene)

Genotyping primers for RALA exons

sgRNA Primer	Target exon	sequence	Amplicon size
hRALA exon2 gFP1	2	ACTGAGCATTACTTATTCTTTCATTC	194
hRALA exon2 gRP1	2	TAGCACTTACCTCATCGTACA	
hRALA exon2 gFP2	2	TCCTTTGGTGAAAACTGAGACAC	155
hRALA exon2 gRP2	2	AAAATTAGCACTTACCTCATCGT	

hRALA exon4 gFP1	4	TCTTATCCAGGGAGCAGATT	199
hRALA exon4 gRP1	4	GAGTCACGTGTTACCTTGTC	
hRALA exon4 gFP2	4	TTTCATTTTCTCTTATCCAGGGAGC	150
hRALA exon4 gRP2	4	AACATTCCACTGCTCAGCTCT	

siRNA for RALA Knockdown

siRNA	**Sequence from paper**
RGL1 (Smartpool)	GAGCCAGAGUCAUCGAGAA, GAUCAACAUUGCUCACGAA, CCUGGACAGCAGCGUGAAA, ACGCAUAUCGUGUGUGUAU
RGL1-KB	GCAUCAGUGUAGAAGACAA
RALA	AAGGCAGGTTTCTGTAGAA
RALA-NB	AAGGCAGGTTTCTGTAGAA
RalB	GGTGGTTCTCGACGGAGAA

RT-PCR primers

Primers	**Sequence of primes from datasheet**	***In-silico* amplicon**
mRGL1-B	CAGCAGAATTCACGAACTTC, TATCCCGCTGAGACCAAATA	123
mRALA-N	CTGACCAGTGGAACGTTAAC, CTTTCTGGCTCGTATTTCCC	101
mRalB-A	CCATCCGTGACAACTACTTC, AACTTTTCTTGCTCTTGCCTG	366
mActin-N	CTCCTAGCACCATGAAGATC, GACTCATCGTACTCCTGCTT	133

2.4 METHODS

2.4.1 Cell culture

Wild-type Mouse embryonic fibroblasts (WT-MEFs) were obtained from Dr Richard Anderson (University of Texas Health Sciences Centre, Dallas TX), MCF-7 cells obtained from Dr. Amit Dutt (ACTREC, Mumbai), T24, UMUC3, HT1080, A549, Calu1, SKOV3, CFPAC-1, MDAMB- 231 and U87MG obtained from ATCC or ECACC were cultured in DMEM (Cat# 11995-065) supplemented either with 5% (v/v) fetal bovine serum (FBS) (for SKOV3, HEK293T, UMUC3 and T24) or with 10% (v/v) fetal bovine serum (FBS) (MCF7 and MiaPaCa2) (Cat# 26140-079) and 1% (v/v) penicillin-streptomycin (Cat# 15140-122) (all from Invitrogen) at 37°C under 5% CO2 humidified atmosphere. MIA-PaCa-2 and DLD1 were cultured in RPMI1640 and SW620 in L15 media supplemented with 5% FBS and 1% PS at 37°C. Cells were treated regularly with an anti-mycoplasma agent, sparfloxacin from Sigma (Cat# 56968) and, when needed, with mycozap from Lonza (Cat# VZA-2011) to keep them mycoplasma-free. Cells were detached using 0.05% trypsin (Cat# 25300-062) and seeded in 60 mm dishes (Eppendorf) for all transfection and inhibition assays and in 6-well plates (Eppendorf) for uptake studies unless mentioned otherwise.

2.4.2 Preparation of MLN8237-Loaded Polysaccharide Vesicles (V_{MLN})

Amphiphilic dextran (DEX-PDP) was synthesized as reported earlier (Pramod et al. 2012) by chemically conjugating the hydrophobic unit of carboxylic acid-substituted 3-pentadecylphenol (PDP) on the hydrophilic dextran backbone (Mw= 6,000) by an enzyme-responsive aliphatic ester chemical linkage. The degree of substitution of PDP in dextran was kept at 5%. To encapsulate MLN8237 in the polysaccharide (dextran) vesicles, 20 mg of DEXPDP and 0.2 mg of MLN8237 were dissolved in 2 mL of DMSO, and then 2 mL of Milli-Q water was added. The solution was stirred for 12 hours in the dark and dialyzed (MWCO = 3500) against Milli-Q water for 48 hours to remove any unencapsulated drug. The resulting solution was filtered, lyophilized, and stored at 4°C. This powder was reconstituted for use as needed. The drug loading content (DLC) and drug loading efficiencies (DLE) were determined by dissolving a known amount of a lyophilized drug-loaded sample in methanol and estimating its drug content by absorption spectroscopy. For this purpose, the molar extinction coefficient

of MLN8237 was determined as 76500 L mol−1 cm−1 in methanol. The DLC and DLE were determined as 0.40% and 56%, respectively.

2.4.3 Cellular Uptake of Encapsulated MLN8237 (VMLN) by Confocal Microscopy.

Cells were seeded at a density of 1 × 10^5 cells on coverslips coated with 2 µg/mL of fibronectin in 6-well plates containing DMEM or RPMI 1640 with 5% or 10% FBS (depending on cell line) and incubated at 37°C for 18 hours. Cells were then incubated with the required concentration of the DEX nanovesicles loaded with MLN8237 and Rh-B (VMLN+RhB) for 48hours, with or without nocodazole at a concentration of 10 ng/mL (to activate Aurora kinases). After 48 hours, the drug-containing medium was removed, cells were washed twice with PBS (1 mL per wash) and fixed with 3.5% paraformaldehyde solution in PBS for 15 min at room temperature. They were then washed with PBS and stained with phalloidin conjugated to Alexa 488 (Invitrogen) diluted 1:400 in 5% BSA solution in PBS for 45 min dark. Excess dye was washed from the cells, coverslips were incubated with DAPI (0.05 mg/mL) for 2 min to stain the nucleus, and finally, they were mounted using Fluoromount-G mounting medium (Southern Biotech). Slides were then dried overnight at room temperature in the dark and imaged using an LSM780 multiphoton microscope with the λ 405 nm (blue channel), λ 568 (red channel), and λ 488 (green channel) lasers.

2.4.4 Treatment of cells using MLN8237 and dextran encapsulated MLN8237 (V_{MLN}) for AURKA inhibition

Cells (0.5 ×10^5 cells) were seeded in 6 well plates and allowed to attach for 24 hours, followed by treatment with 0.02 µM MLN8237 as a free drug or in the nanovesicle (V_{MLN}) for 48 hours. In all inhibition experiments, DMSO (CON) and empty dextran scaffold (DEX) were used as solvent controls for MLN8237 (MLN) and encapsulated MLN8237 (V_{MLN}), respectively. At the end of 48 hrs, cells were lysed in 150ul of laemmli buffer and western blotting was performed to check pAURKA and pRALA inhibition.

2.4.5 RAL activity assay

To determine Ral activity post MLN8237/BQU57 treatment, 2.5 X 10^5 cells were seeded in a 10cm dish and treated with 0.02 µM of free inhibitor (MLN) or nanovesicle-encapsulated inhibitor (V_{MLN}) or BQU57 (5 µM) for 48 h. Following the above treatments, cells were frozen at -80°C (not more than 24 hours). The frozen dishes were thawed together on the ice and then lysed with RAL activity assay buffer (50mM Tris pH 7.4, 150mM NaCl, 10mM MgCl2, 0.1% NP-40, 1mM NaF, 0.1mM Na-orthovanadate and 1X PIC). A cell scrapper was used to scrap and lyse the cells in 1ml RAL activity assay buffer. 180 µl of lysate was added to 45 µl of 5X laemmli buffer to make whole cell lysate (WCL). 400 µl of lysate were incubated with 60 µg GST-Sec5-RBD bound to Glutathione Sepharose beads for 35 minutes at 4°C on a rotary mixer. These beads were washed twice with lysis buffer before use. Post-incubation with lysate beads were washed thrice with activity assay buffer at 4°C and eluted with 20 µl of 2X laemmli buffer to make pulled-down lysate (Sec5-PD). 30 µl of WCL and all of the Sec5-PD lysate were resolved by 12.5% SDS-PAGE and transferred to the PVDF membrane (Millipore). Blots were blocked with 5% milk in 0.1% Tween-20 containing Tris-buffered saline (TBST) for 1 hour at room temperature and incubated with anti-RALA or anti-RALB antibody diluted in 5% BSA or 2.5% milk respectively at 4°C overnight. Blots were then washed thrice with TBST and incubated with anti-mouse HRP and anti-goat HRP for RALA and RalB, respectively, for an hour, followed by detection of RALA and RALB using chemiluminescent substrates from Pierce and Millipore. LAS4000 (Fujufilm-GE) was used to image the blots, and densitrometric band analysis was performed using Image-J software (NIH).
Percentage of active RALA and RALB, was calculated using:

Percentage RAL activity

= Pulldown Band Intensity x 100/(Corresponding WCL Band Intensity **x** Dilution factor)

The dilution factor was calculated as the ratio of the amount of total cell lysate used for the pulldown (400 µl) and the amount of this lysate resolved by SDS PAGE as the whole cell lysate (WCL) (24 µl WCL + 6 µL 5X Lamelli buffer). The dilution factor was hence 400 ÷ 24 = 16.66. This was constant in all experiments.

2.4.6 Anchorage-Independent growth (AIG) assay

Cells treated with 0.02 μM of free inhibitor (MLN) or dextran-encapsulated inhibitor (V_{MLN}) were trypsinized after 24 hours, and 5000 cells were mixed with 0.3% agar containing DMEM and layered on top of 0.5% agar base per well in 6-well plates. Each of the control and inhibitor-treated cells were plated in duplicates. The agar was allowed to solidify, and 1.5 mL of DMEM containing 5% FBS and 0.02 μM MLN8237 (as free drug or nanovesicle-encapsulated inhibitor V_{MLN}) was added. These dishes were maintained in the incubator for 15 days, and their medium was changed every three days. Freshly reconstituted free drug or V_{MLN} at the same used concentration were added to the medium during this change. A similar protocol was followed to study the AIG of MCF7 and MiaPaCa2 cells treated with 20 μM BQU57 (RAL inhibitor). To study the effect of RALA KO and S194 phosphorylation, AIG was performed with RALA KO and mutant cells without any drug treatment. The colonies formed in agar at the end of the 15-day incubation were stained with 0.05% crystal violet dissolved in 20% ethanol for 1 hour at room temperature and de-stained by repeated washing with distilled water until stained colonies were visible. The colonies were then imaged on an Olympus MVXC10 microscope at 1X zoom with 1X objective in the HDR mode and counted using the particle analysis tool of Image J software.

2.4.7 Making of CRISPR-Cas9 mediated RALA KO in cancer cell lines

We designed three sgRNAs against RALA, two were targeted against exon 2, flanking the TSS (Translation start site) and one against exon 4. CHOP-CHOP and CRISPR KO online tools were used to design sgRNAs with high efficiency and low off-target binding. Low off-target binding was confirmed with the CCTOP online tool. sgRNAs were cloned into the pSpCas9-Puro vector, as mentioned by Ran et al. 2013. sgRNAs were cloned into the pSpBBCas9-puro vector using a restriction-based cloning method (Ran *et al.*, 2013). Insertion of sgRNAs at the desired site was confirmed by DNA sequencing.

To make CRISPR-Cas9 KO, 1 X 10^5 cells were seeded in a 6 cm dish for 24 hrs. After 24 hrs, cells were transfected with 1ug of empty pSpCas9-GFP vector and 1ug of

sgRNAs cloned in pSpCas9-Puro vector. After 48 hours of transfection, we sorted the cells using GFP as single or double cells in 96 well plates using BD FACSAria cell sorter. Cells were allowed to grow in 10% media till they formed colonies. Colonies were split and cultured in 48 well plates as duplicates. They were screened by lysis and western blotting for RALA and Actin. Positive clones were expanded to 6cm dishes, and genotyping confirmed knockout.

2.4.8 Genotyping of RALA KO cells

For genotyping, cells from a confluent well of a 48 well plate were lysed in 200ul of tail-lysis buffer. 2ul of 20mg/ml proteinase K and 2ul of 10mg/ml RNAse A were added to the lysate and incubated overnight at 55ºC in a water bath. Proteinase K and RNAse A were denatured by heating at 95ºC for 20 min. An equal amount of PCI (Phenol: Chloroform: Isopropanol) was added to this vortex for 1 min and spun at 16000g/4ºC/30min. The supernatant was collected in a fresh tube, and an equal amount of Isopropanol was added. The mix was kept at -20ºC overnight, spun at 16000g/4ºC/30min and supernatant discarded. The DNA pellet was then washed with 100ul of ethanol twice at 7500g/4ºC/30min and air dried. The DNA was resuspended in TE buffer or NFW. 0.5ug of DNA was used for genomic PCR in standard conditions and DNA resolved on 2% agarose gel and imaged using Olympus MVX microscope.

2.4.9 Reconstitution of RALA (WT/S194A/S194D) in RALA KO cells

To reconstitute RALA Knockout (KO) cells with RALA (WT/S194A/S194D) mutants, 10 X 10^5 HEK293T cells were seeded in a 10 cm dish for 24 hrs and transfected with 2ug of pGagPol, 3ug of pVSVG, 7.5ug of pBABE puro (control) or pBABE puro with RALA (WT/S194A/S194D) or empty pBABE GFP and 37.5ul of lipofectamine 2000. 48 hrs after transfection, 2ml of fresh media was added to the dish. 60 hrs after transfection, all media (virus titer) was collected and passed through a 0.4-micron filter. 1 X 10^5 RALA KO cells were seeded in 6 well plate 36 hrs after transfection of HEK293T cells. 3ml virus titer, 1ml fresh media and 4ul of polybrene (10mg/ml) were added to the RALA KO cells 24 hrs after seeding. Cells were allowed to grow for 48-60 hrs (till we

saw detectable transduction with the pBABE GFP vector). Transduced cells were treated with 1ug/ml puromycin for 48 – 72 hrs till all cells in the control plate (transduced with empty pBABE GFP) were dead. Cells left unaffected and hence selected for in the WT or mutant RALA transduced dishes were allowed to recover for 24 hrs with a change in medium. After this, cells were transferred to 24 well plate, grown, lysed, and western blotting was performed to check the expression of RALA in the knockout background.

2.4.10 siRNA mediated knockdown

For siRNA-mediated knockdowns, WT-MEFs seeded in 60 mm dishes were transfected using the RNAiMax transfection reagent (Invitrogen) with 25pmoles siRNA smart pool oligo (Dharmacon) or 100pmols individual siRNA oligo (Sigma). These transfections were repeated after 24 hours, and cells were used 48 hours after the second transfection.

For cancer cells, 3 X 10^5 cells per well were seeded in 6 well plate for 24hrs. After 24 hrs, cells were transfected with 50pmol of RALA siRNA and 3ul of Lipofectamine RNAimax. The media was changed 24 hours after the first transfection, and a repeat transfection was done. 48 hrs after the second transfection, part of the cells were lysed for western blotting to confirm the KD.

2.4.11 Immunofluorescence assay

1 x 10^5 cells were seeded on glass coverslip. 48 hrs after seeding, cells were fixed with 3.5% paraformaldehyde for 15minutes. Cells were permeabilized with PBS containing 5% BSA and 0.05% Triton-X-100 for 15 minutes and blocked with 5% BSA for 1 hour at room temperature followed by incubation with 1:500 mouse anti-RalA (BD Transduction laboratories) antibodies in 5% BSA at 4 degrees for overnight. Cells were finally stained with 1:1000 diluted secondary antibodies (anti-mouse Alexa-488) or 1:500 diluted phalloidin-Alexa 594 for 1 hour at room temperature. All incubations were done in a humidified chamber. Washes were done with 1X PBS at room temperature.

Stained and washed coverslips were mounted with Fluoromount-G (Southern Biotech) and imaged using a Zeiss LSM780 multiphoton microscope with a 63x objective.

All image processing was done using FIJI ImageJ software. Initially, brightness and contrast of all images were adjusted to have a comparable signal intensity. Following this, image thresholding was done to look at the localization RALA in cells.

2.4.12 Quantitative RT-PCR to determine Knockdown efficiency

Total RNA was isolated from cells using Trizol reagent followed by cDNA preparation using Reverse Transcriptase and oligo-dT primers (BioRad iScript Kit). Quantitative Real-time PCR reactions were set up using SYBR FAST qPCR master mix reagent from Kapa Biosystems (Catalog No KK4601) using the BioRad CFX96 Real-Time System. The list of specific primers used for measuring transcript levels in qPCR is mentioned above in section 2.1.3. Their optimal Tm was determined using a gradient PCR. Actin was used as a reference gene to determine the percentage of knockdown of the target gene in siRNA-treated cells (Target KD) relative to treatment control (CON) cells.

ΔΔCt was calculated as follows:

$$\Delta Ct\ (CON) = Ct\ Target\ of\ CON - Ct\ Actin\ of\ CON$$

$$\Delta Ct\ (TARGET\ KD) = Ct\ Target\ of\ Target\ KD - Ct\ Actin\ of\ Target\ KD$$

$$\Delta\Delta Ct = \Delta Ct\ (TARGET\ KD) - \Delta Ct\ (CON)$$

Fold change was determined by calculating 2 (-ΔΔCt). Fold change was then converted to percentage knockdown as follows: Percentage knockdown = 100 - (100 × fold change).

2.4.13 Tumorigenesis assay in NOD-SCID mice

To study the role of RALA and its S194 phosphorylation in tumor formation, we did xenograft assay in an equal number of male and female NOD-SCID mice. 1 x 10^6 cells of WT, Cas9 control, RALA KO, and RALA KO reconstituted with WT/S194A/S194D

RALA were injected subcutaneously in 5-6 week-old mice. Mice were observed over 4-5 weeks, and mice weight and tumor size were measured weekly.

2.4.14 Kinase prediction

Kinase prediction was performed using KinasePhos 2.0 and PhosphoNET to identify potential AURKA phosphorylation sites on RGL1. We tested their ability to correctly predict the AURKA-specific phosphorylation site using known old and recently discovered AURKA targets. Following this, we developed a pipeline to integrate these two tools as shown in (Figure 7.6) to identify the potential AURKA phosphorylation site on RGL1. Throughout the analysis, protein sequence or ID number for target proteins was obtained from UniProt.

2.4.15 Statistical analysis

All analyses were done using Prism GraphPad analysis software. Statistical data analysis was done using the two-tailed unpaired Student's T-test or two-tailed paired T-test. When normalized to respective controls, they were compared using the two-tailed single-sample T-test. Mice tumor data was analyzed using two-way annova (comparing columns within each row).

Chapter 3

Making of RALA KO cell lines in RAS-independent and RAS-dependent cancer cells using CRISPR-Cas9

3.1: Rationale

AURKA and RALA's role in normal cells is significantly altered in cancer cells. A lot of variation in AURKA-RALA crosstalk is also observed in these cells. This variation ranges from how AURKA effects RALA S194 phosphorylation to its role in tumorigenesis. This variation could be partly mediated by other regulatory influencers, such as oncogenic RAS. Oncogenic RAS-mediated regulation of the RAL GTPases pathway is vital for RAS-mediated transformation and is seen to drive AIG downstream of RAS (Lim, Donita C. Brady, *et al.*, 2010). RAS-dependent regulation of RAL is known to be mediated by RAS-dependent RAL GEFs (Neel *et al.*, 2011). Constitutively active RAS is also seen to promote AURKA expression in cancer cells (dos Santos *et al.*, 2016). RAS is known to interact with AURKA (Umstead *et al.*, 2017) and joint expression of both is further seen to promote AIG (Tatsuka *et al.*, 2005). RAS-independent (MCF7 and SKOV3) and RAS-dependent (T24, UMUC3 and MiaPaCa2) cell lines were chosen for study based on their known AURKA and RALA expression and activation status determined previously in the lab. We decided to use CRISPR-Cas9 over the siRNA approach, given that RNAi has much more significant off-target effects than CRISPR-Cas9 (Smith *et al.*, 2017). Also, since CRISPR works on the DNA level, it allows us to test for the effect complete loss of Function (LOF) or null phenotype of RALA has on these cells. Knowing the phosphorylation of RALA in S194 residue is regulated by AURKA, we made stable RALA S194 phosphomutants (deficient and mimetic) reconstitutions of RALA KO in RAS-independent and RAS-dependent cancer cell lines to evaluate their role in these cancers comprehensively. In this chapter, I discuss the making of RALA KO cell lines in RAS-independent and RAS-dependent cancer cell lines and the evaluation of how this affects the expression and activation of RalB, AURKA, AURKB and other proteins, including AKT, AMPK and ERK.

3.2 Results

3.2.1 Selection of exons to target using sgRNAs

To make the RALA knockout (KO) in cancer cells, we began by designing the sgRNAs for RALA. We also designed the sgRNAs for RALB for future use. As a first step, we

narrowed down the exons to target using sgRNAs. We used the following criteria for this selection:

1. DNAse 1 sensitivity
2. Common exons in transcript variants
3. Alternate transcription start site and
4. Exons coding for functional protein

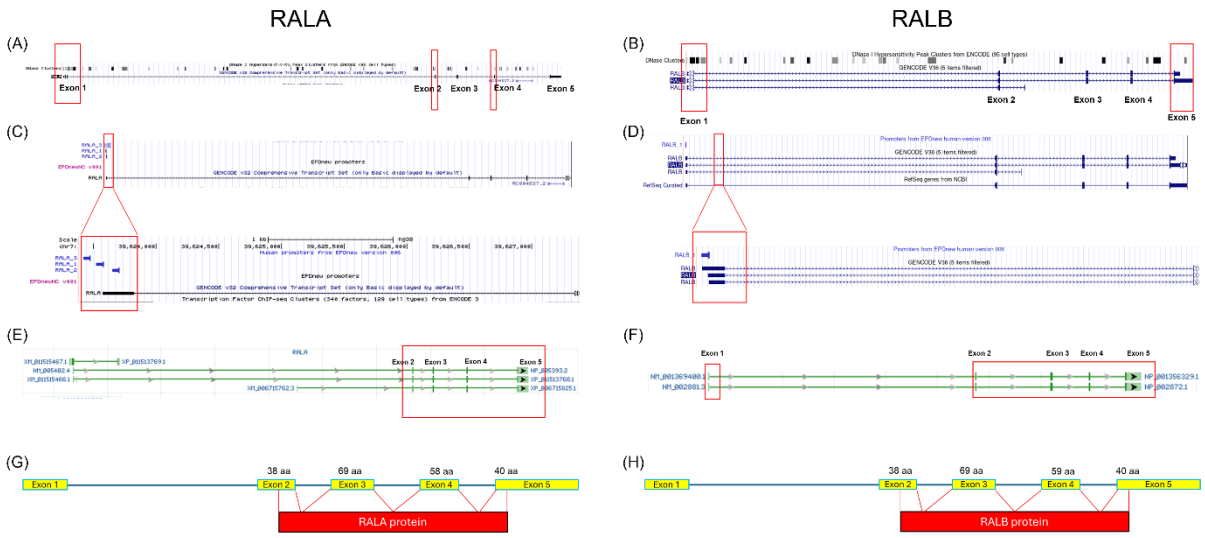

Figure 3.1: identifying optimal region to target RALA and RALB using CRISP-Cas9. Image representing the steps involved in identify optimal region on DNA to target RalA and RalB using CRISPR-Cas9, In-silico analysis results from UCSC genome browser showing open chromatin (red boxes) structure using DNAse 1 sensitivity (A,B), alternate transcription start site (red boxes) (C,D), common exons (red boxes) (E,F) and protein coding region (G,H) for RalA and RalB respectively.

We used the UCSC genome browser to check the above parameters for RALA and RALB. DNAse 1 sensitivity represents the open chromatin structure in DNA. High DNAse1 sensitivity means more open chromatin and easy access to sgRNA and Cas9. RALA showed high DNAse 1 sensitivity at exons 1, 2 and 4, while RALB showed high DNAse 1 sensitivity at exons 1 and 5 (Figure 3.1 A and B). Both RALA and RALB have

alternate transcription start sites located in exon 1 (Figure 3.1 C and D), excluding it from being a suitable exon for sgRNA designing.

Table 1: Comparison and identification of target exon to design sgRNA for RALA

Criteria	Exon 1	Exon 2	Exon 3	Exon 4	Exon 5
TSS site	+	-	-	-	-
DNase 1 sensitivity	+	+	-	+	_
Protein coding region	-	+	+	+	+
Presence in isoforms coding for functional protein	-	+	+	+	+

Table 2: Comparison and identification of target exon to design sgRNA for RALB

Criteria	Exon 1	Exon 2	Exon 3	Exon 4	Exon 5
TSS site	+	-	-	-	-
DNase 1 sensitivity	+	-	-	-	+
Protein coding region	-	+	+	+	+
Presence in isoforms coding for functional protein	+	+	+	+	+

We later checked for all transcript variants for RALA and RALB. RALA had no known transcript variants but had 2 predicted variants, while RALB had 1 known transcript variant, and both RALA and RALB share 4 exons (Exon 2, 3, 4 and 5) (Figure 3.1 E and F). Exons 2, 3, 4 and 5 (partially) code for functional RALA and RALB proteins (Figure 3.1 G and H). Overall, RALA exons 2 and 4 fit all criteria for an open chromatin structure, no alternate transcription start site, common exons in all transcripts and codes for functional RALA protein (Table 1). In the case of RALB, only exon 5 fit all criteria (Tabel 2); however, most of it codes for 3'-UTR and hence was not considered further. We selected exon 2 and exon 4 for both RALA and RALB to target using sgRNAs.

3.2.2 Designing of RALA and RALB sgRNAs

To target exon 2 and exon 4 in RALA and RALB, we designed a pair of sgRNAs against each exon in both RALA and RALB (Figure 3.2). The idea was that the pair of sgRNAs designed against each exon would work together, preferably to make a deletion instead of a frameshift mutation. Also, there was a slight chance we could completely delete exon 3.

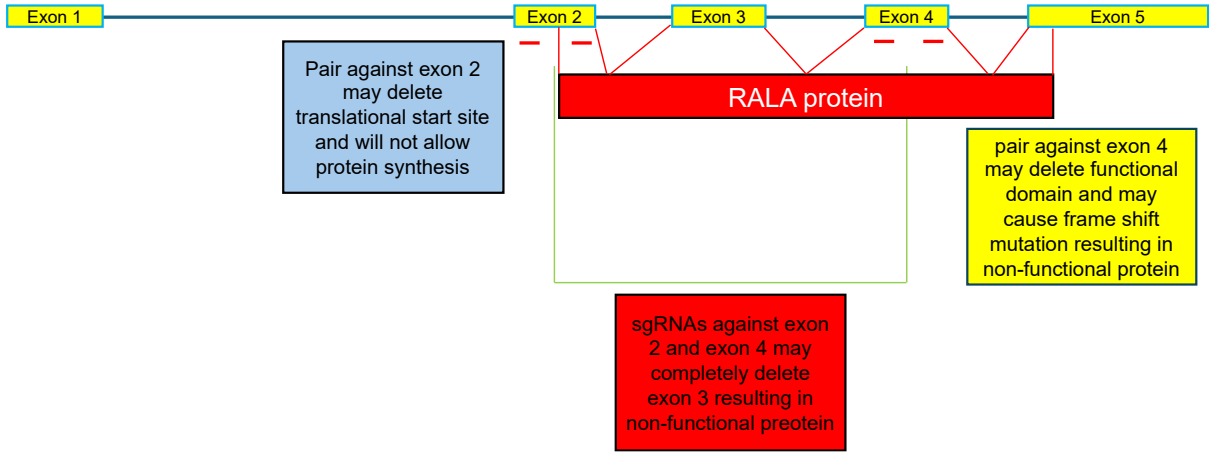

Figure 3.2: Strategy to designing sgRNAs to target RALA and RALB. Schematic representing the location of sgRNAs (red lines) on exon two and four to increase the probability of having small deletion in RalA or RalB genes to make CRISPR-Cas9 mediated KO.

We used free online tools (CHOP-CHOP and CRISPR Ko) to design sgRNAs suitable with *S. Pyogenes* Cas9. Individual exon sequence was used in these tools to get exon 2 and exon 4 specific primers. We only selected the sgRNAs predicted by both tools to have very high on-target efficiency and predicted low off-target. With this parameter, only three sgRNAs were designed for RALA, and two were targeted at exon 2 close to the translation start site and one in exon 4. Similar to RALA, only three sgRNAs fit our parameters of design for RALB, one against exon 2 and two against exon 4 (Table 3, 4, 5 and 6).

For sgRNAs to transcribe correctly into the cells, they should start with guanine (G) nucleotide to promote transcription by U6 RNA polymerase. To ensure the proper functioning of sgRNAs, we added additional G in sgRNA sequence of 2nd sgRNA

designed for exon 2 of RALA (RALA sgRNA 2.2), first sgRNA designed for exon 4 and exon 2 of RALB. We also designed genotyping primers for exons 2 and 4 of RALA to check the physical cut on exons for evaluating the RALA knockout clones.

Table 3: Efficiency of RALA sgRNAs

Target sequence	Target exon	On target efficiency		Strand
		CHO-CHOP	CRISPRko	
GGCTTTACACAAAGTCATCATGG	2	56	56	Sense
ATGGCTGCAAATAAGCCCAAGGG	2	65	65	Sense
GCAGTGGAATGTTAACTACGTGG	4	76.5	76.5	Sense

Table 4: RALA sgRNAs off-target prediction

Target sequence	Target exon	CHOP-CHOP			CRISPRko		
		MM1	MM2	MM3	MM1	MM2	MM3
GGCTTTACACAAAGTCATCATGG	2	1	2	2	1	2	6
ATGGCTGCAAATAAGCCCAAGGG	2	1	1	13	1	1	5
GCAGTGGAATGTTAACTACGTGG	4	1	1	0	1	1	0

Table 5: Efficiency of RALB sgRNAs

Target sequence	Target exon	On target efficiency		Strand
		CHO-CHOP	CRISPRko	
AACCATGATCACCTTGTGGAGGG	2	59.96	59.96	Antisense
TTGTTTCCCACGACGAGCAGTGG	4	58.57	58.57	Antisense
GGAGACGTCAGCGAAGACCCGGG	4	69.3	69.3	Sense

Table 6: RALB sgRNAs off-target prediction

Target sequence	Target exon	CHOP-CHOP			CRISPRko		
		MM1	MM2	MM3	MM1	MM2	MM3
AACCATGATCACCTTGTGGAGGG	2	0	0	3	7	11	25
TTGTTTCCCACGACGAGCAGTGG	4	0	0	1	1	1	5
GGAGACGTCAGCGAAGACCCGGG	4	0	0	6	1	6	3

3.2.3 Cloning of RALA and RALB sgRNAs

A suitable vector backbone is required to deliver sgRNAs and Cas9 to make stable KOs. We used pSpCas9(BB)-2A-GFP and pSpCas9(BB)-2A-Puro vectors for cloning as they provide *S. Pyogenes* Cas9 cloned in the backbone, selectable marker (GFP

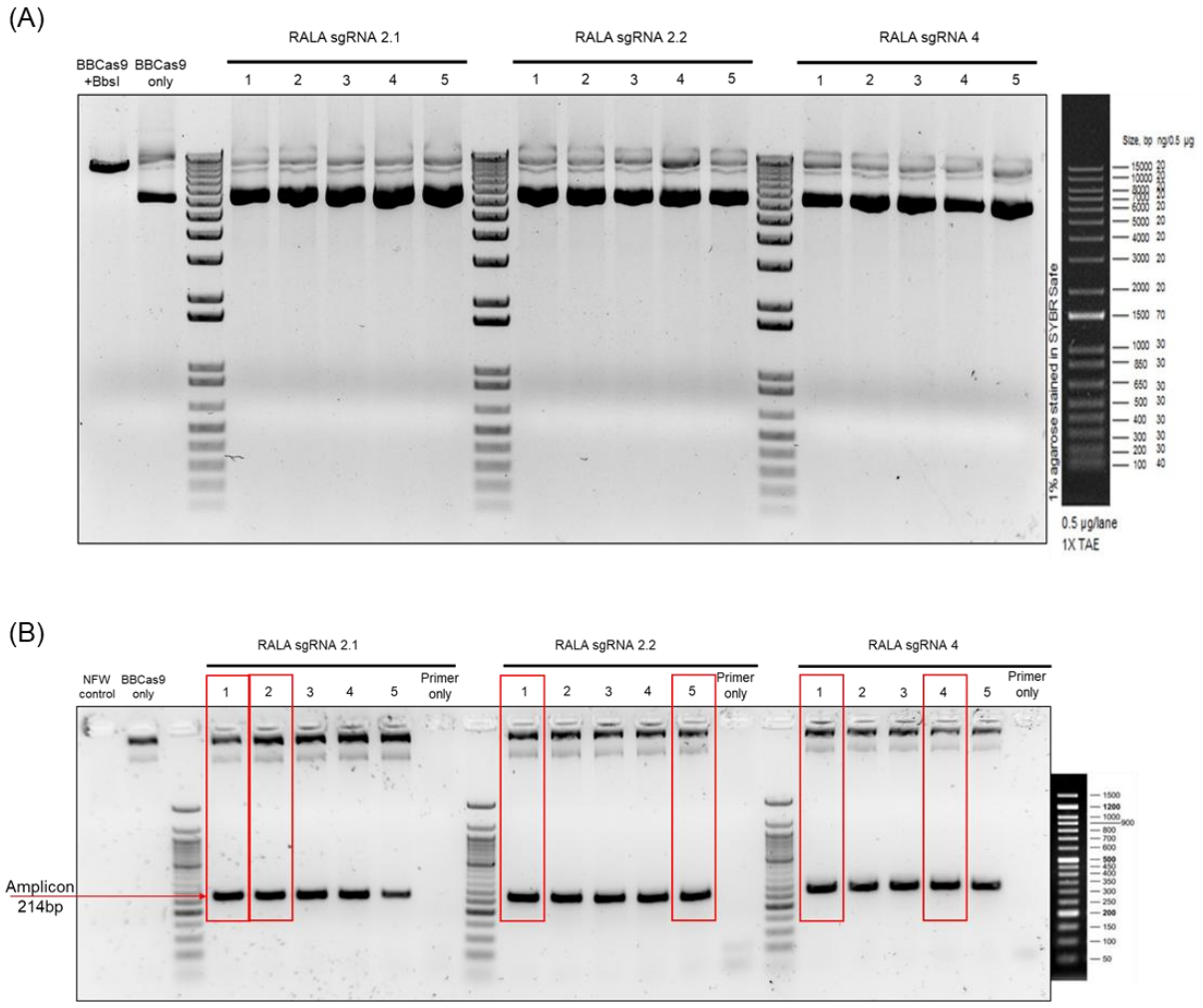

Figure 3.3: Colony screening to check cloning of RALA sgRNAs in pSpCas9(BB)-2A-Puro vector

(A) Agarose gel image showing pSpCas9(BB)-2A-Puro vector size after digestion with BbsI enzyme and control reaction. (B) Agarose gel image showing amplicon size of PCR product amplified with RALA sgRNA primers and pSpCas9(BB)-2A-Puro vector. Red boxed represents colonies selected for further confirmation.

and Puromycin, respectively). The cloning protocol for sgRNA in these vectors is also well-optimized (Ran *et al.*, 2013). We added suitable overhangs (CACC) into the sgRNA sequences for cloning into the pSpCas9(BB)-2A-GFP and pSpCas9(BB)-2A-Puro vectors. We cloned RALA sgRNAs in both pSpCas9(BB)-2A-GFP and pSpCas9(BB)-2A-Puro vectors, and RALB sgRNAs only in pSpCas9(BB)-2A-GFP vector.

To clone RALA in the pSpCas9(BB)-2A-Puro vector, we digested the backbone with the BbsI enzyme to generate sticky ends for cloning. A pair of sgRNAs (100uM) were annealed and used at 1:200 dilution for ligation. Cloning sgRNAs in pSpCas9(BB)-2A-Puro backbone disrupts the BbsI restriction site, and positive colonies, when screened, will not be digested by BbsI. Upon ligation and transformation, we screened 5 colonies per sgRNAs by digesting them with BbsI enzyme. All selected colonies were resistant to enzymatic digestion (Figure 3.3 A), confirming the cloning of RALA sgRNAs in pSpCas9(BB)-2A-Puro backbone. PCR amplification of part of pSpCas9(BB)-2A-Puro backbone using sequencing primer and sgRNA reverse primer in all selected colonies further confirmed this cloning (Figure 3.3 B). We confirmed the sequence specificity of sgRNAs by DNA sequencing of the cloned backbone (Figure 3.4)

We used the same method to clone RALA and RALB sg RNAs in the pSpCas9(BB)-2A-GFP vector. Upon ligation and transformation, we screened 5 colonies per sgRNA for RALA and RALB by PCR to confirm the cloning (Figure 3.5 A and B). We selected 2 colonies for each sgRNA for further confirmation by BbsI digestion. All colonies except RALB sgRNA 4.2 showed resistance to digestion by the BbsI enzyme, confirming the cloning (Figure 3.5 C). RALB sgRNA 4.2 had a BbsI restriction site in the sgRNA sequence, making it susceptible to digestion by the BbsI enzyme despite the cloning of the sgRNA.

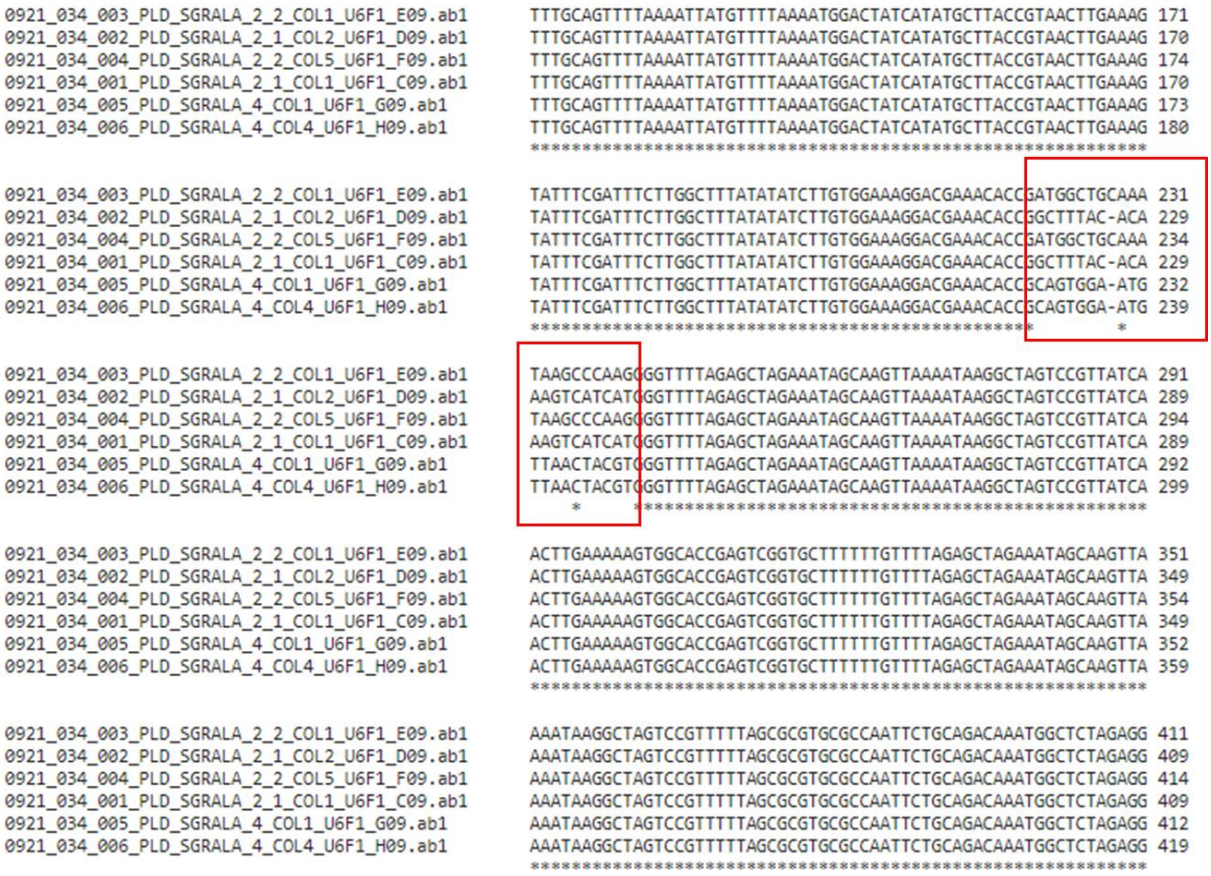

Figure 3.4: DNA sequencing to confirm cloning of RALA sgRNAs in pSPCas9(BB)-2A-Puro vector. The image represents the sequence alignment for DNA sequencing data of RALA sgRNA. This confirmed the cloning of RALA sgRNA in correct position in pSPCas9(BB)-2A-Puro vector. (red box indicate sgRNA sequences)

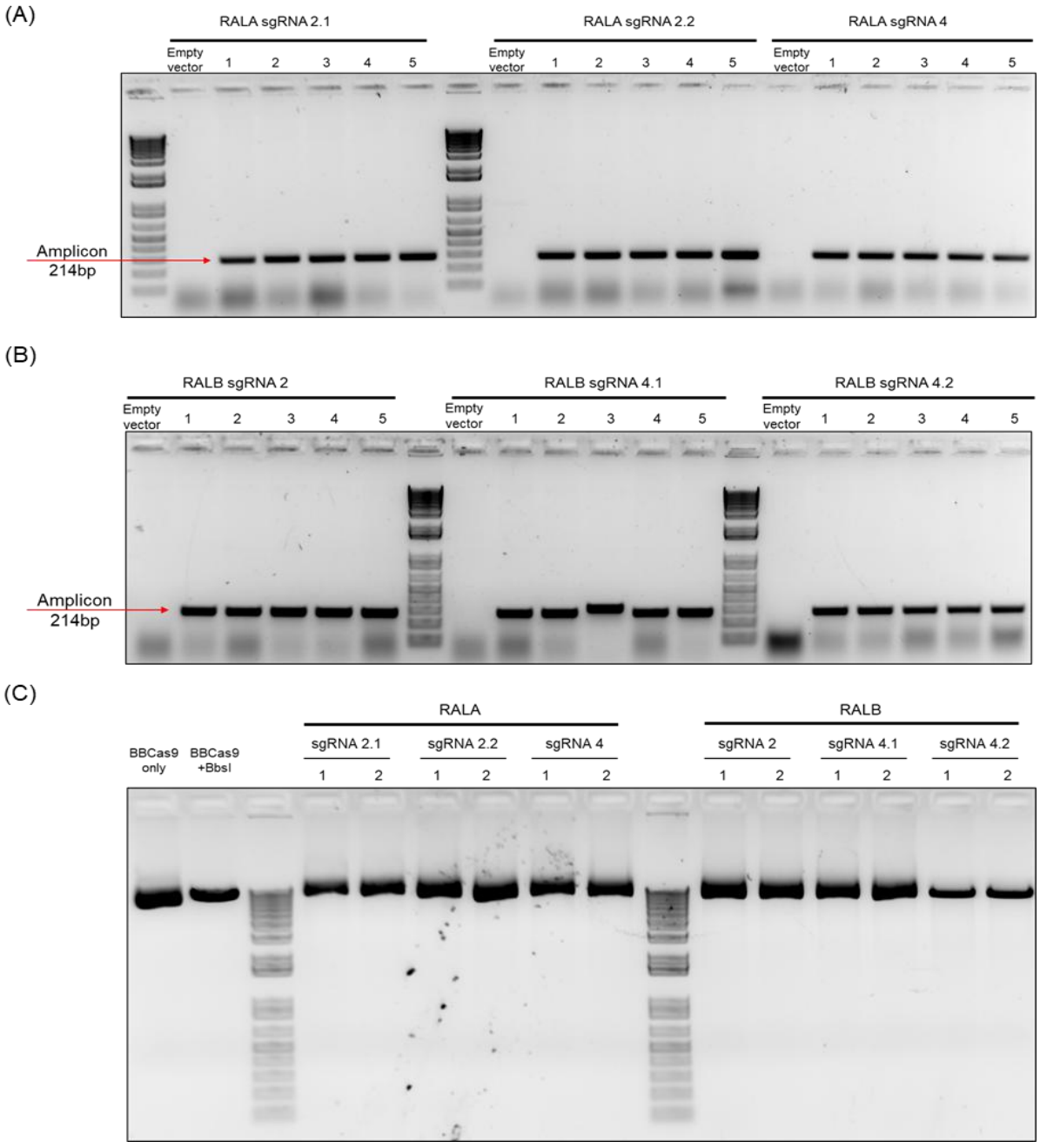

Figure 3.5: Colony screening to confirm cloning of RALA and RALB sgRNAs in pSpCas9(BB)-2A-GFP vector. Agarose gel image showing amplicon size of PCR product amplified with RALA (A) and RALB (B) sgRNA primers and pSpCas9(BB)-2A-Puro vector. Red line represents expected amplicon size. (C) Agarose gel image showing pSpCas9(BB)-2A-Puro vector size after digestion with BbsI enzyme and control reaction.

3.2.4 Making of RALA KO in cancer cell lines

To knockout RALA in cancer cells, we transfected them with all three sgRNAs and the pSpBBCas9-GFP vector as a marker for transfection. Transfected cells were sorted as single cells, and clones were expanded from single cells and tested for RALA expression. Preliminary screening was done by checking for RALA vs RALB expression using Western blot detection. One clone each for MCF7, SKOV3 and T24 and two clones for UMUC3 and MiaPaCa2, showing the highest loss of RALA without affecting RALB, were then probed for the expression of RALB, AURKA, AURKB and phosphorylation of AURKA and AURKB. Together, this confirmed the loss of RALA in MCF7, SKOV3, T24, UMUC3 (clone 2), and MiaPaCa2 (clone 2) without affecting RALB, AURKA and AURKB expression. These clones also showed no detectable change in the basal phosphorylation of AURKA, AURKB and other proteins, including AKT, AMPK and ERK (Figure 3.6 A, B and Figure 3.7 A, C, E).

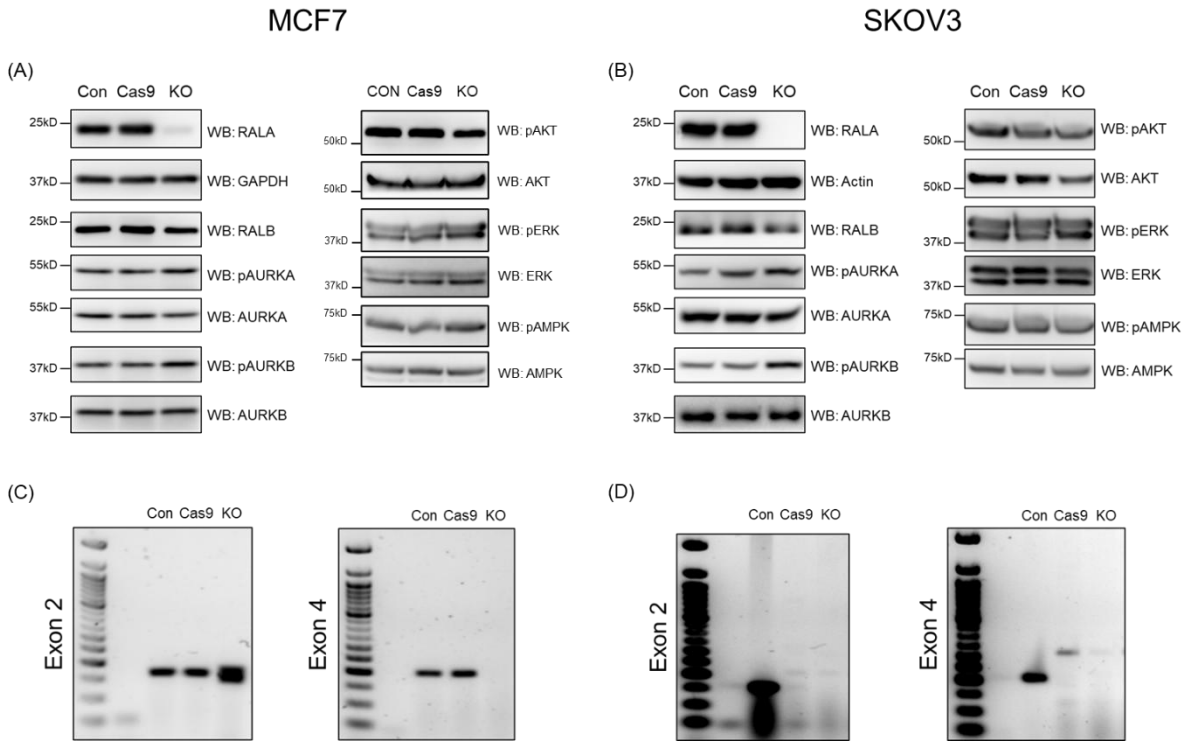

Figure 3.6: CRISPR-Cas9 mediated RalA KO in RAS-independent cancer cells (MCF7 and SKOV3). (A,B) Western blotting in MCF7 and SKOV3 cells confirmed CRISPR-Cas9 mediated RalA KO to be specific and with no effect on other signaling pathways. (C,D) Genotyping PCR for exon 2 and 4 was performed to confirm physical cut on RalA gene.

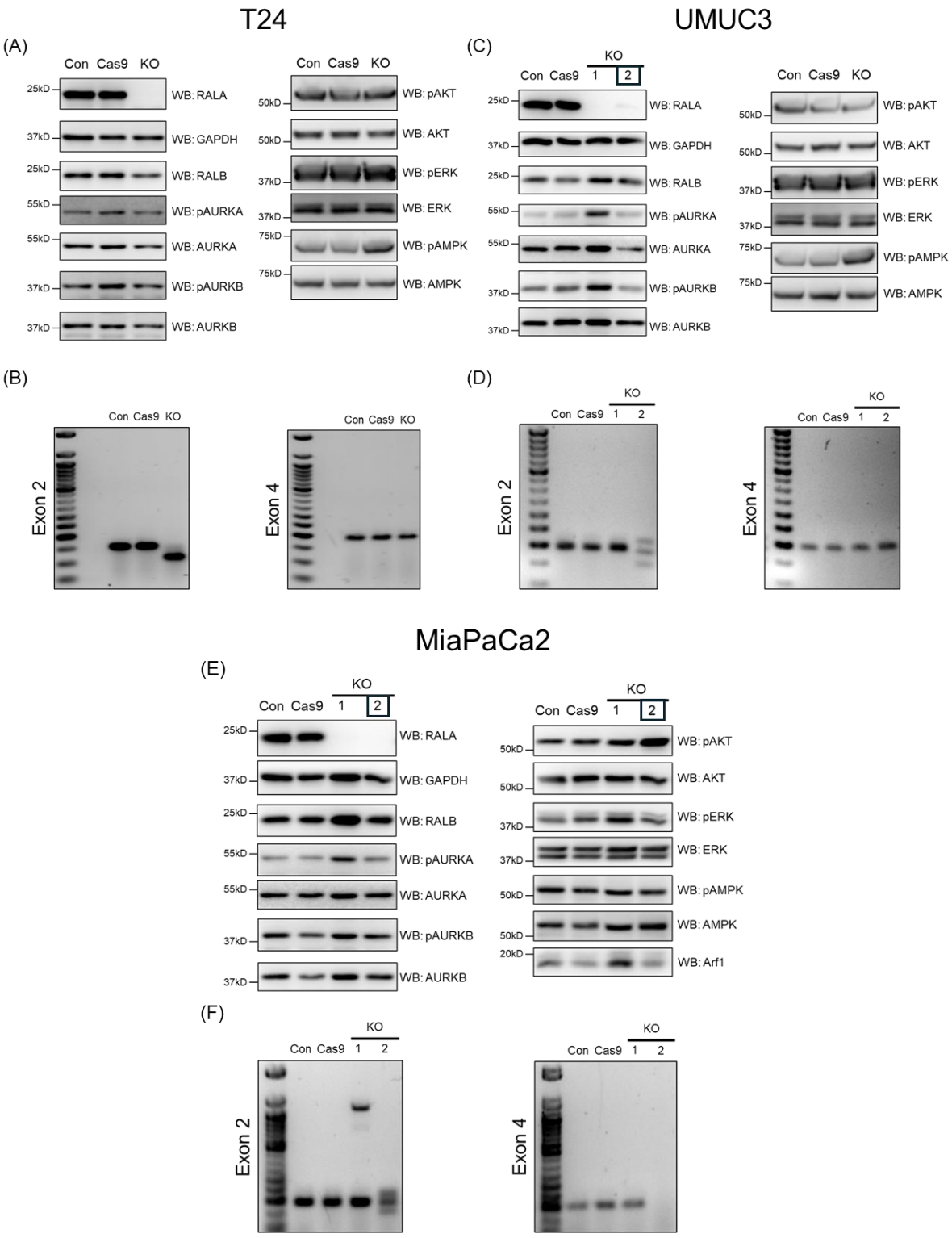

Figure 3.7: CRISPR-Cas9 mediated RalA KO in RAS-dependent cancer cells (T24, UMUC3 and MiaPaCa2) (A,C,E) Western blotting in T24, UMUC3 and MiaPaCa2 cells confirmed CRISPR-Cas9 mediated RalA KO to be specific and with no effect on other signaling pathways. (B,D,F) Genotyping PCR for exon 2 and 4 was performed to confirm physical cut on RalA gene. (box represents clones selected for further study)

Genotyping PCR to detect a physical break in exon 2 and/or exon 4 of RALA (reflected as a loss or shift in the size of the PCR amplicon) confirmed the KO status of the selected clones for MCF7, T24, UMUC3 (clone 2) and MiaPaCa2 (clone 2) (Figure 3.6 B and Figure 3.7 B, D, F). The lack of a detectable loss or shift in amplicon for UMUC3 (clone 1) and MiaPaCa2 (clone 1) and its effects on expression and phosphorylation of proteins tested (AURKA, AURKB, AKT, AMPK and ERK) made them unusable (Figure 3.7 C, D, E, F). Despite multiple attempts with multiple primers for genotyping PCR in SKOV3 cells, we did not get any amplification of RALA exons in SKOV3 Cas9 control or RALA KO cells. Additionally, several non-specific bands were observed in the PCR for SKOV3 control, Cas9 control and RALA KO cells, making it difficult to comment on genotyping data (Figure 3.6 D). Genotyping detects a cut on exon 2 in MCF7, T24, UMUC3 (clone 2) and MiaPaCa2 (clone 2). MCF7 and MiaPaCa2 also detect a cut on exon 4. This provided us with one confirmed RALA KO clone for RAS-independent cell line MCF7 and RAS-dependent cell lines T24, UMUC3 and MiaPaCa2.

3.3 Summary and Conclusion

CRISPR-Cas9 can be used to make stable RALA KO in multiple cancer cell lines. Knocking down RALA in cancer cell lines does not affect the expression and activation of other proteins, including RALB, AURKA and AURKB. We find that genomic verification combined with western blot is needed to authenticate these knockouts. This revealed that verifiable KOs were obtained for further use in MCF7, T24, UMUC3 (clone 2) and MiaPaCa2 (clone 2). This allows us to test these clones for the phosphorylation status of RALA and its regulation by AURKA.

Chapter 4

Evaluation of pS194 RALA detection by anti-phospho-RALA antibody (S194) in RAS-independent and RAS-dependent cancer cell lines

4.1 Rationale

Our objective in making CRISPR-Cas9 RALA KO in cancer cells has been to use these to evaluate the role of S194 RALA phosphorylation in regulating cancer cell tumorigenesis. Stable reconstitution of RALA KO cells with WT / S194A / S194D mutants should help evaluate this. The detection of RALA phosphorylation with anti-phospho-RALA Antibody (Ser194) (Merck-Millipore, Cat no- 07-2119) has been vital in assessing its role and regulation in cells. The anti-phospho-RALA Antibody (Ser194) from MERCK-Millipore we and others have used is raised against KLH-conjugated linear peptide corresponding to human RALA phosphorylated at S194. There, however, have been concerns about the specificity of this antibody. Despite the knockdown of RALA in PANC-1 cells, this antibody continues to detect pS194 RALA (Neel *et al.*, 2014). A lack of specificity and resulting variations in detection of pS194 RALA phosphorylation in western blotting by this antibody could significantly affect the understanding of pS194 RALA-dependent signaling and its regulation by AURKA-RALA crosstalk in literature.

In this chapter, we evaluated the detection of pS194 RALA in western blot studies by anti-phospho-RALA Antibody (Ser194) (Merck-Millipore, Cat no- 07-2119) across cancer cell lines. With the help of AURKA inhibitor MLN8237 encapsulated in nanovesicle (V_{MLN}), we also evaluated the role of AURKA-RALA crosstalk in regulating RALA activation and AIG in RAS-independent and RAS-dependent cancer cell lines.

4.2 Results

4.2.1 Evaluating pS194 RALA detection in RAS-independent and RAS-dependent RALA KO cells

To test the detection issue faced with this antibody, we used confirmed stable RALA KO clones of MCF7, T24, UMUC3 and MiaPaCa2 (evaluated in Chapter 3). Although the genotyping PCR did not work in SKOV3 cells, a clear absence of RALA was seen in western blotting studies (Figure 3.6 B); thus, we also decided to use the SKOV3 RALA KO clones to test anti-phospho-RALA Antibody (Ser194). pS194 RALA detection using anti-phospho-RALA Antibody (Ser194), no detectable band for pS194

RALA was seen in RALA KO RAS-independent MCF7 and SKOV3 cells (Figure 4.1). However, in RALA KO RAS-dependent T24, UMUC3 and MiaPaCa2 cells, despite the visible absence of RALA, a distinct pS194 RALA band was detected by the antibody at the expected size (Figure 4.1).

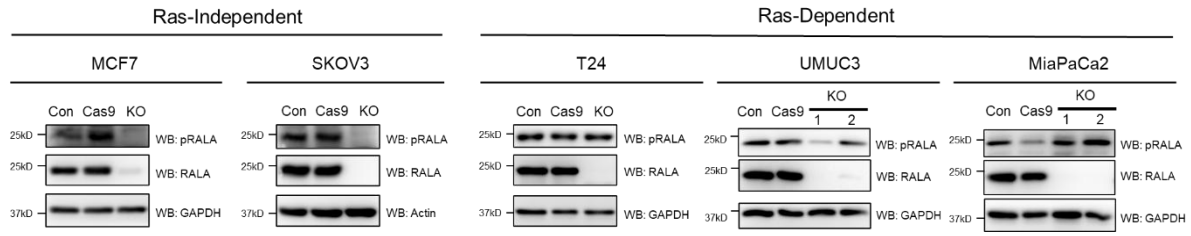

Figure 4.1: pS194 RALA detection in RALA KO cancer cell lines. Western blot detection of pRALA (RALA S194 phosphorylation) in cell lysate from untreated control (CON), Cas9 control (Cas9) and RALA KO cells using anti-phospho-RALA Antibody (Ser194) (Merck-Millipore, Cat no- 07-2119) in Ras-independent (MCF7 and SKOV3) and Ras-dependent (T24, UMUC3 and MiaPaCa2) cancer cells.

4.2.2 Evaluating pS194 RALA detection in MiaPaCa2 upon RALA KD

To further confirm this finding, we used a known RALA-specific siRNA (Pawar *et al.*, 2016) to knock it down (KD) and tested the detection of pS194 RALA in MiaPaCa2 cells. We detected pS194 RALA in RALA KO and KD cells side by side to compare the effect of KO and KD on the detection of pS194 RALA. Despite the siRNA causing a ~80% drop in RALA protein levels and no detectable RALA protein being observed in

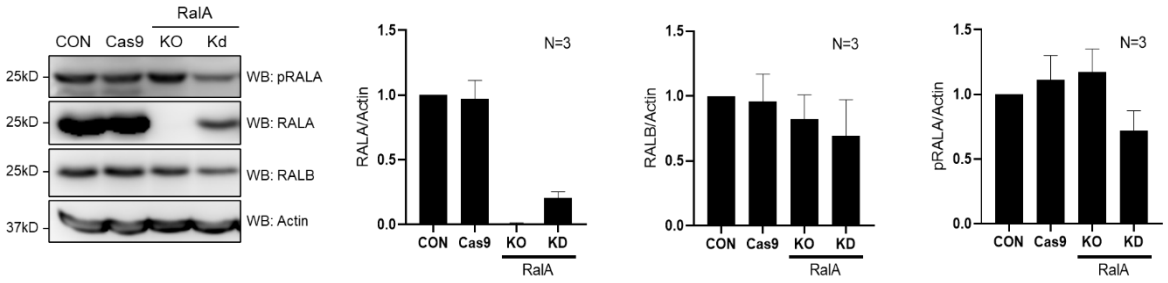

Figure 4.2: pS194 RALA detection in RALA KO and RALA KD MiaPaCa2 cell line Western blot detection of pRALA (RALA S194 phosphorylation) in the cell lysate of control (CON), Cas9 control (Cas9), siRNA mediated RALA KD and CRISPR-Cas9 RALA KO MiaPaCa2 cells. Blots were also probed for RALA, RALB and actin. Blots were quantitated, and the ratio of band intensities for RALA, pRALA and RALB normalized to actin as mean ± SE from three independent experiments. Statistical analysis was done using the one sample T-test, compared to control p values, if significant, are represented in the graph (* $p < 0.05$, ** $p<0.01$, *** $p<0.001$).

RALA KO cells, the pS194 RALA band is detectable in RALA KD and KO cells, comparable to control cell lysates (Figure 4.2).

This reveals that in RAS-dependent MiaPaCa2 cells, the pS194 RALA antibody detects a non-specific band that seemingly runs at a molecular weight close enough to RALA. It also explains why this would be difficult to ascertain without probing RALA lacking cell lysate, as shown above.

4.2.3 Evaluating the pS194 RALA detection upon AURKA inhibition in RAS-independent and RAS-dependent cancer cell lines

An additional approach to evaluate the specificity of the pS194 RALA band detected in these cell lysates is to test the effect inhibition of AURKA (known to phosphorylate RALA at S194) has on the detected pS194 RALA band. Previous studies from the lab have developed a dextran nano-vesicle encapsulated MLN8237 (V_{MLN}) that inhibits AURKA without affecting AURKB (Inchanalkar *et al.*, 2018b). We inhibited AURKA with V_{MLN} MCF7, SKOV3, T24, UMUC3 and MiaPaCa2 cells to check its effect on pS194 RALA. The V_{MLN} uptake in these cells was confirmed using Rhodamine (RhB) encapsulated nano-vesicles (Figure 4.3).

V_{MLN} mediated AURKA inhibition detected using the pThr288-AURKA was better than free MLN8237 across these cell lines and significant in MCF7, SKOV3 and MiaPaCa2 (Figure 4.4). Interestingly, AURKA inhibition causes a significant decrease in detectable pS194 RALA band in MCF7 and SKOV3 cells (RAS-independent) but not in T24, UMUC3 and MiaPaCa2 cells (Figure 4.5). This further suggests that the pS194 RALA band detected in these RAS-dependent cell lines could be non-specific. This restricts the use of this antibody in studying the role of S194 RALA phosphorylation in RAS-dependent cancer cells. It also suggests using S194 site-specific RALA mutant could be a better way to evaluate their role in these cancers.

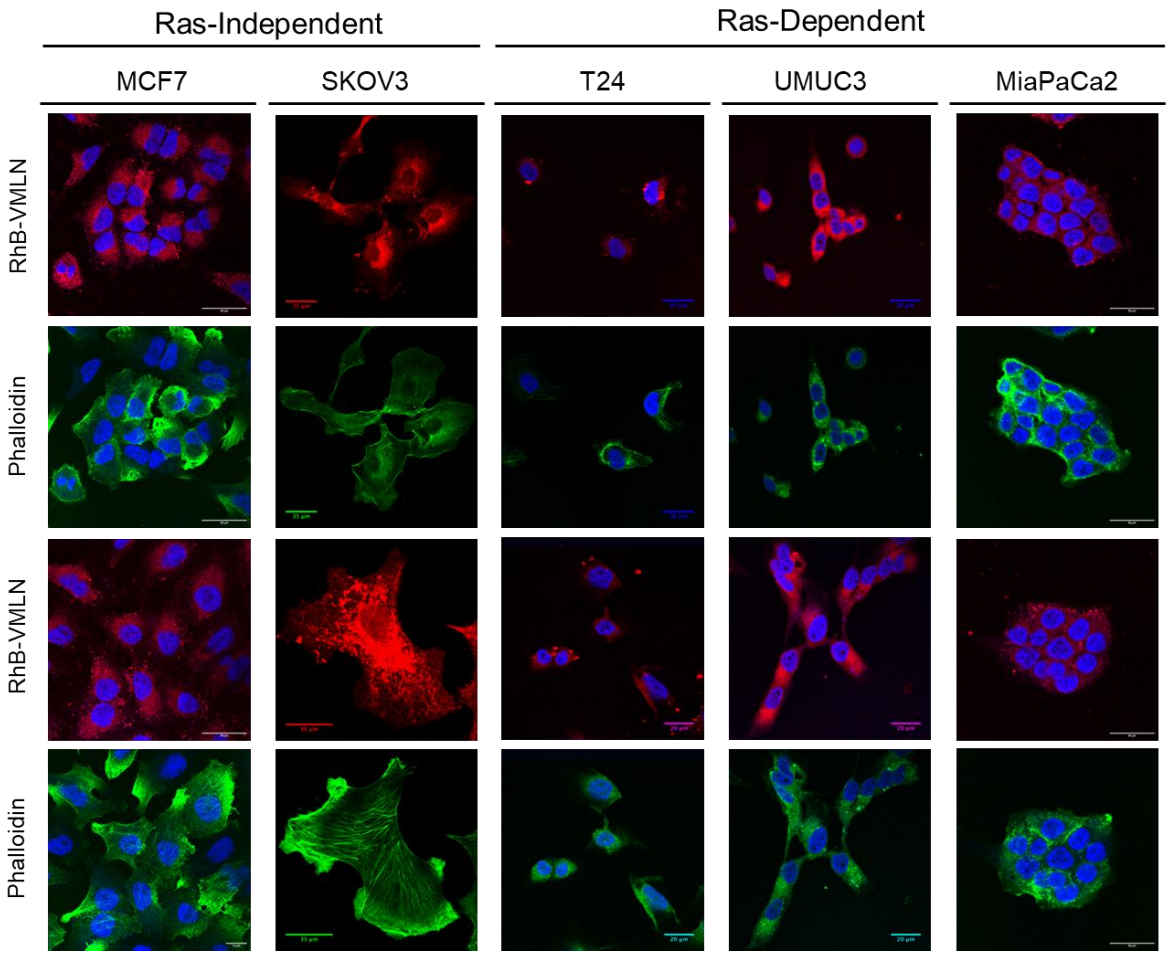

Figure 4.3: Uptake of $V_{MLN+RhB}$ in cancer cells. Uptake of DEX nano-vesicle with RhB (1.37 μM) and MLN8237 (0.5 μM) ($V_{MLN+RhB}$) was visualized by confocal microscopy in cells treated for 48hours. The actin cytoskeletal network stained with phalloidin was conjugated to Alexa-488 and nucleus was counterstained with DAPI. The images shown are representative of two independent experiments that gave similar results.

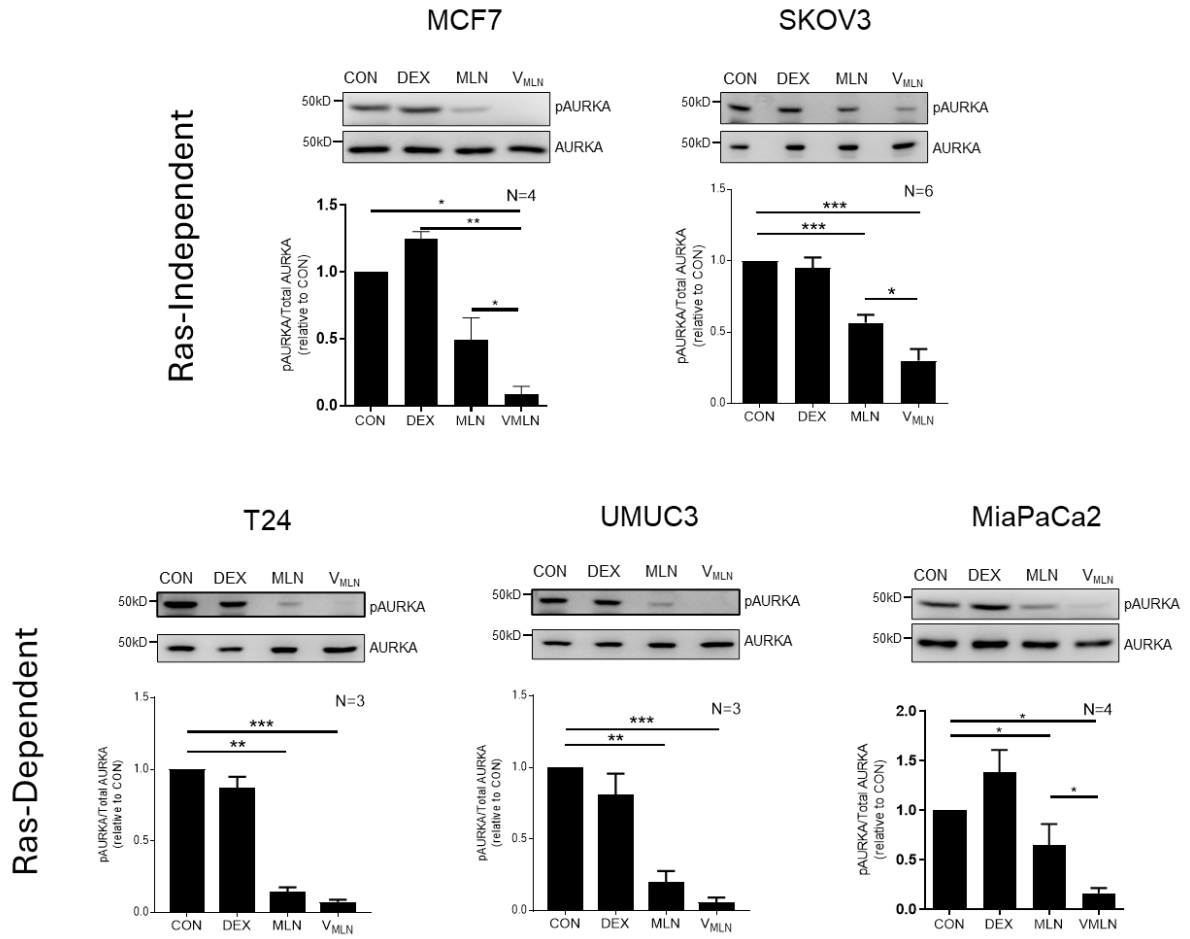

Figure 4.4: Inhibition of AURKA by V_{MLN} in RAS-independent and RAS-dependent cancer cell lines. Western blot detection (upper panel) and quantitation (lower panel) of phosphorylation of Threonine 288 residue (pThr288 AURKA) and total AURKA, from lysates of MCF7, SKOV3, T24, UMUC3 and MIAPaCa2 treated with 0.02μM Free MLN (MLN) or 0.02μM encapsulated MLN (V_{MLN}). DMSO (CON) and empty nano-vesicle scaffold (DEX) were used as controls for MLN and V_{MLN}, respectively. The ratio of pAURKA/AURKA in each cell line was normalized to their respective controls (CON) (equated to 1) and were represented in the graph as mean ± SE from at least three independent experiments. Statistical analysis was done using one sample T-test, and p values, if significant, are represented in the graph (* $p < 0.05$, ** $p<0.01$, *** $p<0.001$).

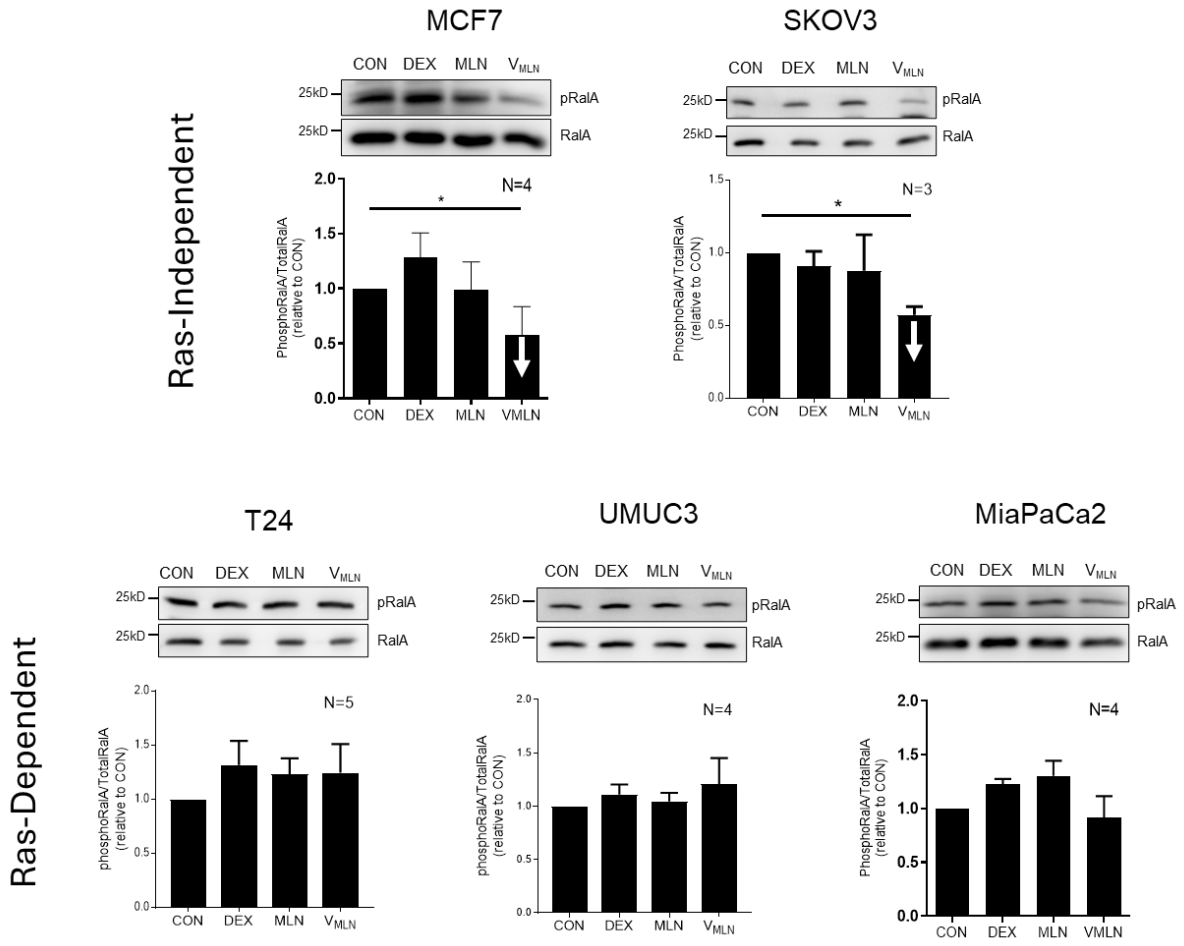

Figure 4.5: Effect of AURKA inhibition using V_{MLN} on pS194 RALA detection in Ras-independent and Ras-dependent cancer cell lines. Western blot detection (upper panel) and quantitation (lower panel) of phosphorylation of Serine 194 residue (pS194 RALA) and total RALA, from lysates of MCF7, SKOV3, T24, UMUC3 and MIAPaCa2 cells treated with 0.02μM Free MLN (MLN) or 0.02μM encapsulated MLN (V_{MLN}). DMSO (CON) and empty nano-vesicle scaffold (DEX) were used as controls for MLN and V_{MLN}, respectively. The ratio of pRALA/TotalRALA in each cell line was normalized to their respective controls (CON) (equated to 1) and were represented in the graph as mean ± SE from at least three independent experiments. Statistical analysis was done using one sample T-test, and p values, if significant, are represented in the graph (* $p < 0.05$, ** $p<0.01$, *** $p<0.001$).

4.2.4 Evaluating the role of AURKA-RALA crosstalk in regulating RALA activation and AIG

As a first step to understanding the AURKA-RALA crosstalk in cancer, we used V_{MLN} as a tool to test its regulation of RALA activation and AIG in RAS-independent (MCF7 and SKOV3) and RAS-dependent (T24, UMUC3 and MiaPaCa2) cancer cells. Ral activity assay was performed using GST-Sec5 fusion protein linked to sepharose beads. RBD (Ral binding domain) of Sec5 helps in binding of active RalA and GST domain helps in linking with beads. Using this design we were able to pull down active RalA from cell lysates. Upon AURKA inhibition, the GST-Sec5 pulldown assay detected a drop in RALA activation in only SKOV3 and not in any other cell lines (Figure 4.6). This drop in SKOV3 cells was seen for free MLN8237 and V_{MLN}, though the drop was significant only on V_{MLN} treatment. This could reflect the efficiency of AURKA inhibition in SKOV3 cells, as V_{MLN} showed better inhibition than free MLN8237 (Figure 4.4). This suggests that AURKA-RALA crosstalk is present only in SKOV3 cells and not in other cell lines.

AURKA inhibition with V_{MLN} showed a significant drop in colony numbers in SKOV3 and MiaPaCa2 cell lines, and no effect in AIG was observed for MCF7, T24 and UMUC3 cell lines (Figure 4.7). In MiaPaCa2, since no effect on RALA activation was observed, the impact on AIG could only be the result of AURKA inhibition. Since a drop in AIG was observed only with V_{MLN}, it suggests that the extent of AURKA inhibition (independent of RALA) could be responsible for its effect on MiaPaCa2 (Figure 4.4).

This suggests that the AURKA-RALA crosstalk could contribute differently to SKOV3 and MiaPaCa2 cells. This difference could also result from our interpretation of how AURKA does not affect pS194 RALA phosphorylation in MiaPaCa2 cells. This could result from the pS194 RALA antibody detecting a non-RALA protein in the RAS-dependent cancer cells. Also, in the case of MCF7, although pS194 RALA phosphorylation was affected, no effect was observed on RALA activation or AIG, suggesting that in this particular cell line, pS194 RALA phosphorylation may not regulate RALA activation. Mutant studies with pS194 RALA phosphomutants will help us address this question.

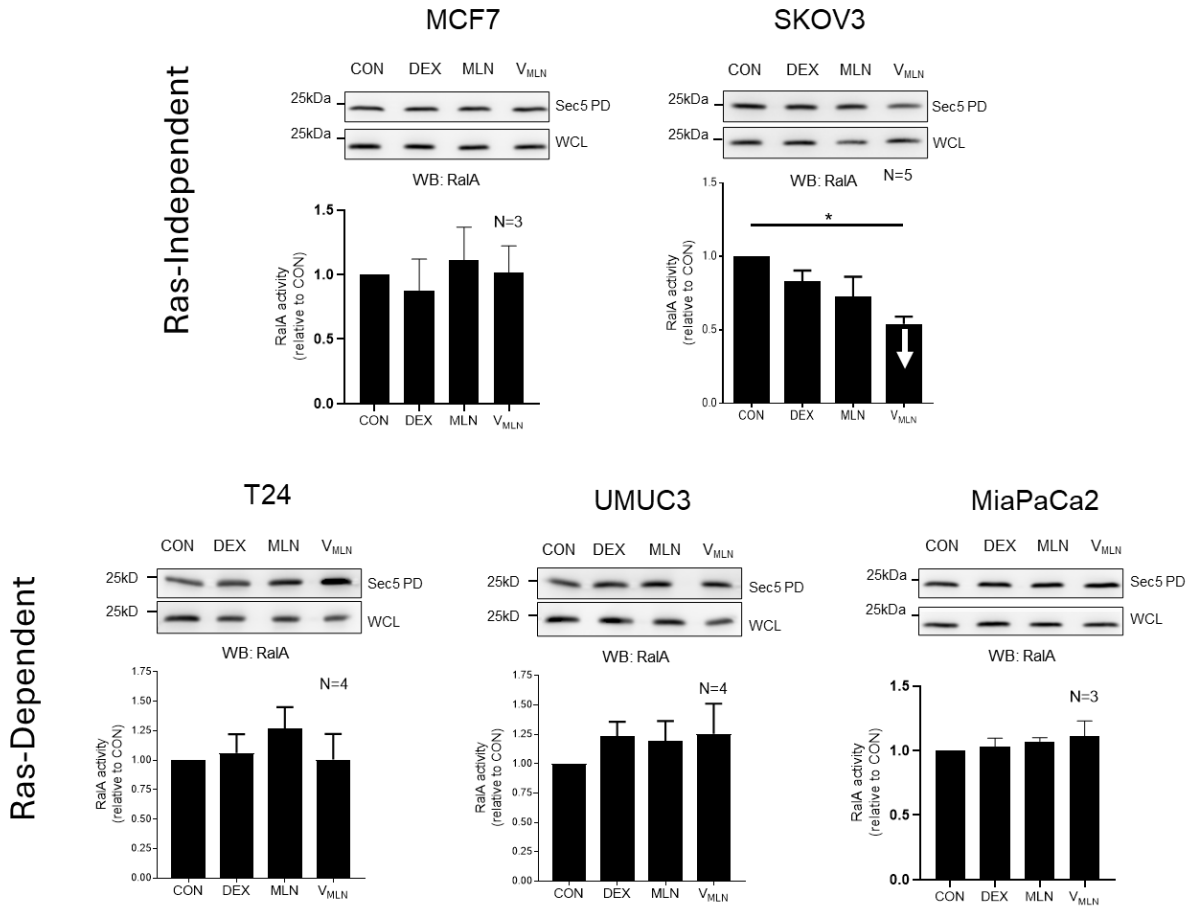

Figure 4.6: Effect of AURKA inhibition using V_{MLN} on RALA activation in RAS-independent and RAS-dependent cancer cell lines. Western blot detection (upper panel) and quantitation (lower panel) of Active RALA from Sec5 pulldown lysate (Sec5 PD) and total RALA, from whole cell lysates (WCL) of MCF7, SKOV3, T24, UMUC3 and MiaPaCa2 cells treated with DMSO (CON), empty nano-vesicle scaffold (DEX), 0.02μM Free MLN or V_{MLN}. The active RALA were normalized to their respective controls (equated to 1) and are represented in the graph as mean ± SE from four independent experiments. Statistical analysis was done using one sample T-test, and p values, if significant, are represented in the graph (* $p < 0.05$, ** $p<0.01$, *** $p<0.001$).

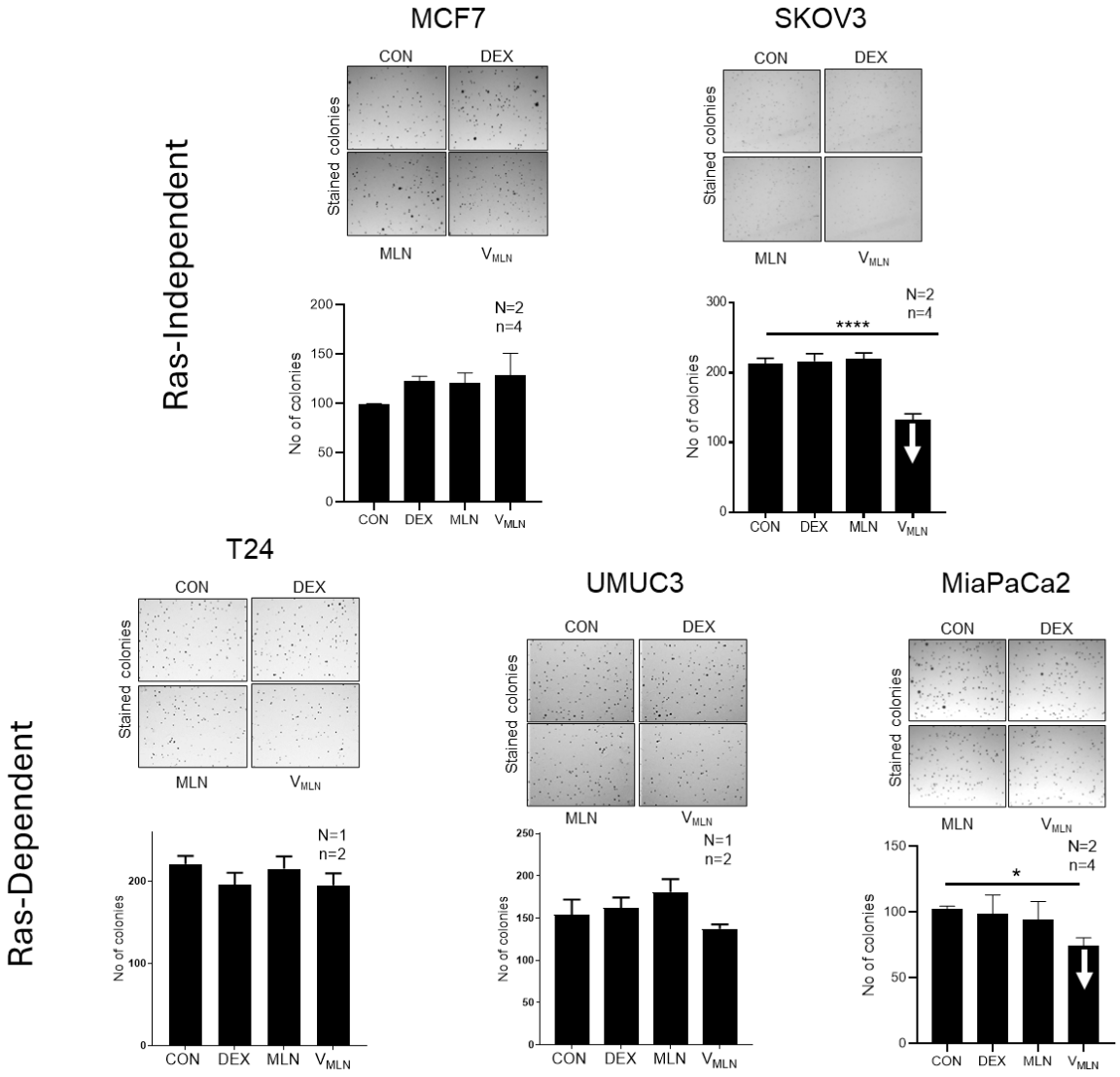

Figure 4.7: Effect of AURKA inhibition using V_{MLN} on AIG in RAS-independent and RAS-dependent cancer cell lines. DMSO-treated CON, empty Dextran nano-vesicle scaffold (DEX), 0.02 μM MLN8237 (MLN), and V_{MLN}-treated MCF7, SKOV3, T24, UMUC3 and MiaPaCa2 cells were embedded in the agarose gel and incubated for up to 15 days with DMSO, DEX, MLN, or V_{MLN}, and the colonies formed were stained and counted as described in methods section. The graph represents mean ± SE data from at least two independent experiments (N), 'n' represents technical replicates. Statistical analysis was done using mann-whitney test, and p values, if significant, are represented in the graph (**** $p < 0.0001$).

4.3 Summary and Conclusion

pS194 RALA detection by anti-phospho-RALA Antibody (Ser194) from MERCK-Millipore while seen in both RAS-independent (MCF7 and SKOV3) and RAS-dependent (T24, UMUC3 and MiaPaCa2) cancer cell lines, was differentially affected by RALA KO. In RAS-independent cancer cells, loss of RALA causes a loss of pS194 RALA band, as expected. However, neither RALA KO nor siRNA KD caused the band detected by the pS194 RALA antibody to be lost in RAS-dependent cancer cell lines (T24, UMUC3 and MiaPaCa2). The band detected in these KO cells also matched in size and intensity with the control cells. This questions the specificity of the anti-phospho-RALA Antibody (Ser194) and limits its use in RAS-dependent cancer cell lines. It also raises queries about conclusions made from previous studies using this antibody. We observed the same trend on V_{MLN} treatment where the detectable inhibition of AURKA in RAS-independent cancer cell lines affects pS194 RALA detection. No such effect was observed in RAS-dependent cancer cell lines, confirming our above findings. What protein is being detected by anti-phospho-RALA Antibody used in RAS-dependent cancer cell lines on the loss of RALA remains an open question. Why this antibody does not pick up this protein in western blots of RAS-independent cells also remains perplexing.

In RAS-independent cancer cell lines, AUKRA inhibition (using V_{MLN}) affected RALA phosphorylation in MCF7 and SKOV3 cells, but RALA activation and AIG were only affected in SKOV3 cells. It isn't clear what causes this distinction, as AURKA inhibition and the resulting drop in pS194RALA levels (that we know to be specific in these cells) were comparable. No effect of AURKA inhibition (using V_{MLN}) was seen on RALA activation in RAS-dependent T24, UMUC3 and MiaPaCa2 cells. Specificity issues with the detection of RALA phosphorylation means we are not evaluating its levels in these cells. AIG was, however, affected in MiaPaCa2 cells ONLY, possibly reflecting AURKA-dependent, RALA-independent regulation of growth in these cells.

This suggests that AURKA-RALA crosstalk is variable in cancer cell lines, and its impact on RALA activation and AIG could also be variable. The presence or absence of oncogenic RAS also does not produce a consistent effect on the AURKA-RALA crosstalk.

The takeaway from these studies, which looked for a conserved pattern of regulation and its effect on RALA function, was that this could be very cell type specific and must be studied accordingly. Using RALA phospho-mutants (S194A, S194D) might be the most effective way of evaluating the impact AURKA-RALA crosstalk has in individual cancers.

Chapter 5

Reconstitution of RALA S194 mutants (WT, S194A, S194D) in RALA KO RAS-independent cells and RALA KO RAS-dependent cells

5.1 Rationale

The detection of pS194 RALA with anti-phospho-RALA Antibody (Ser194) was an issue in RAS-dependent cancer cell lines, as was the variability in regulation and role of the AURKA-RALA crosstalk in both RAS-independent and RAS-dependent cancer cells. This meant that the regulation and role of this crosstalk could be cell type specific. Testing each cancer cell line using S194 phospho-mutants in the RALA KO backgrounds might be the only way to effectively study the role of RALA S194 phosphorylation (and hence the AURKA-RALA) crosstalk in AIG and tumorigenesis.

We have stable RALA knockouts verified in MCF7, T24, UMUC3 and MiaPaCa2 cells. We first chose MCF7 and MiaPaCa2 KO cells for reconstitution with RALA WT and S194 mutants (S194A/S194D). Their RAS-independent and RAS-dependent status was also a consideration when making this choice. To create stable RALA S194 phospho-mutant cells, we used the retroviral transduction method for the delivery and stable integration of RALA WT and S194 mutants (S194A/S194D) in RALA KO cell lines.

5.2 Results

5.2.1 Cloning of RALA in pBABE puro vector

To reconstitute the RALA in RALA KO cells, we began by selecting suitable vectors for the cloning of RALA. pBABE Puro vector was chosen as it has been extensively used for stable DNA insertions. RlaA was cloned from a flag MCV4 vector (Flag Tagged), into pBABE Puro. Six colonies were selected for colony PCR using cloning primers, and all six tested positive, showing amplification of RALA (Figure 5.1 A). Four of these colonies were further screened for insert release of RALA upon digestion with BamHI and SalI, and all showed release of RALA (Figure 5.1 B). Colonies 1 and 4 showed some shift in backbone size, while colonies 2 and 3 had backbone of the correct size (Figure 5.1 B). Colony 3, when sequenced, confirmed no undesired mutation in RALA (Figure 5.2) and was chosen for further study.

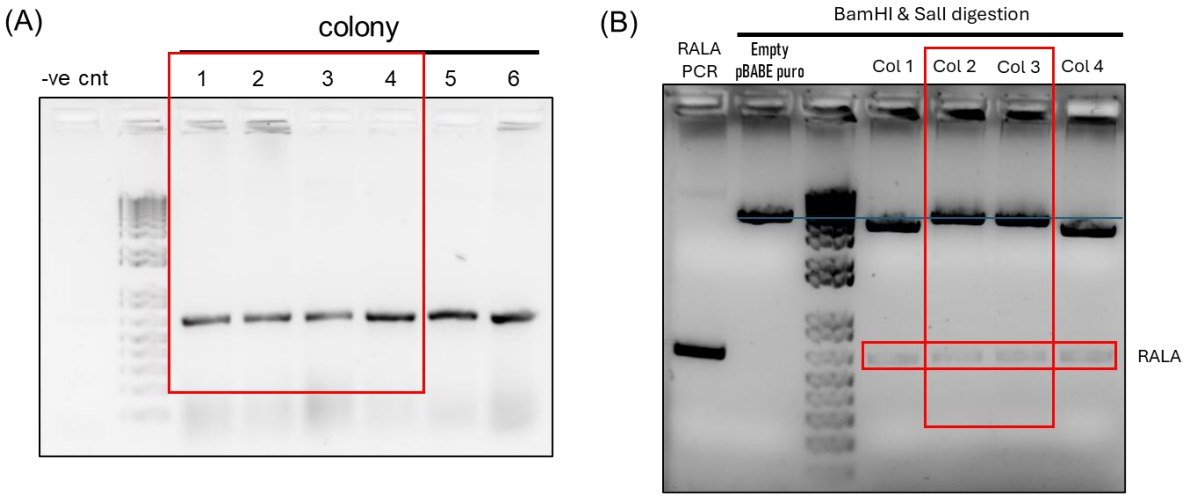

Figure 5.1: Colony screening to confirm cloning of RALA in pBABE Puro vector. (A) Agarose gel image showing the amplicon size of RALA from colony PCR od selected colonies. (B) Agarose gel image showing the size of pBABE Puro vector after digestion with BamHI and SalI enzyme.

5.2.2 Making of RALA S194 mutants in pBABE Puro

After cloning the WT RALA gene in the pBABE Puro vector, we did SDM (Side Directed Mutagenesis) PCR to make RALA S194 mutants, as described in the Materials and Methods section. Once we introduced S194A and S194D mutations in RALA with SDM PCR, they were cloned in an empty pBABE Puro vector, as mentioned earlier, for WT RALA. We screened five colonies each for S194A and S194D mutants by inserting release by restriction digestion (BamHI and SalI). For the RALA S194A mutant, four out of five colonies tested positive, while for the RALA S194D mutant, all five colonies tested positive (Figure 5.3 A). Positive colonies were sequenced to confirm the S194 mutation and check for undesired mutations (Figure 5.3 B).

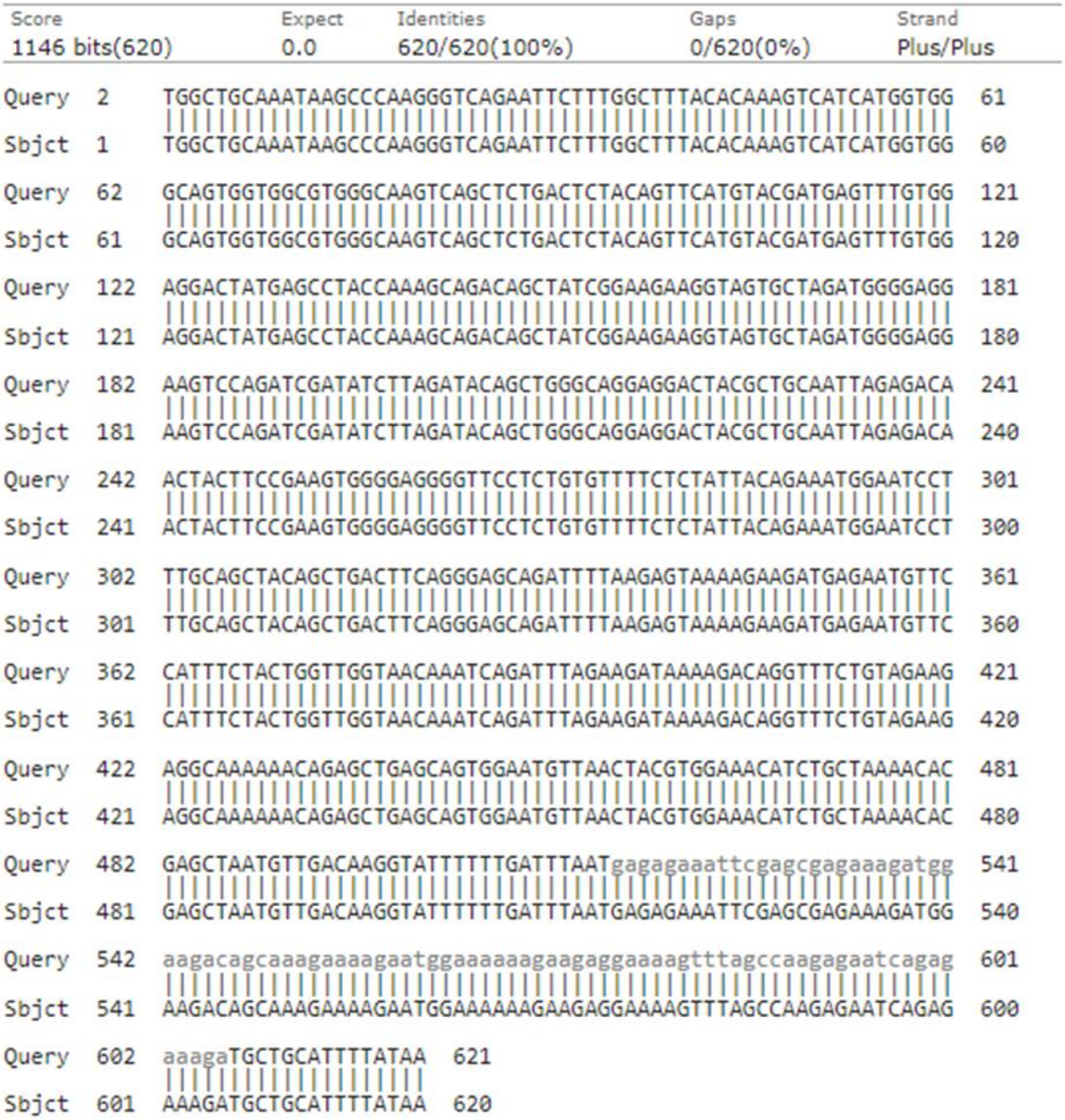

Score	Expect	Identities	Gaps	Strand
1146 bits(620)	0.0	620/620(100%)	0/620(0%)	Plus/Plus

```
Query  2    TGGCTGCAAATAAGCCCAAGGGTCAGAATTCTTTGGCTTTACACAAAGTCATCATGGTGG  61
            ||||||||||||||||||||||||||||||||||||||||||||||||||||||||||||
Sbjct  1    TGGCTGCAAATAAGCCCAAGGGTCAGAATTCTTTGGCTTTACACAAAGTCATCATGGTGG  60

Query  62   GCAGTGGTGGCGTGGGCAAGTCAGCTCTGACTCTACAGTTCATGTACGATGAGTTTGTGG  121
            ||||||||||||||||||||||||||||||||||||||||||||||||||||||||||||
Sbjct  61   GCAGTGGTGGCGTGGGCAAGTCAGCTCTGACTCTACAGTTCATGTACGATGAGTTTGTGG  120

Query  122  AGGACTATGAGCCTACCAAAGCAGACAGCTATCGGAAGAAGGTAGTGCTAGATGGGGAGG  181
            ||||||||||||||||||||||||||||||||||||||||||||||||||||||||||||
Sbjct  121  AGGACTATGAGCCTACCAAAGCAGACAGCTATCGGAAGAAGGTAGTGCTAGATGGGGAGG  180

Query  182  AAGTCCAGATCGATATCTTAGATACAGCTGGGCAGGAGGACTACGCTGCAATTAGAGACA  241
            ||||||||||||||||||||||||||||||||||||||||||||||||||||||||||||
Sbjct  181  AAGTCCAGATCGATATCTTAGATACAGCTGGGCAGGAGGACTACGCTGCAATTAGAGACA  240

Query  242  ACTACTTCCGAAGTGGGGAGGGGTTCCTCTGTGTTTTCTCTATTACAGAAATGGAATCCT  301
            ||||||||||||||||||||||||||||||||||||||||||||||||||||||||||||
Sbjct  241  ACTACTTCCGAAGTGGGGAGGGGTTCCTCTGTGTTTTCTCTATTACAGAAATGGAATCCT  300

Query  302  TTGCAGCTACAGCTGACTTCAGGGAGCAGATTTTAAGAGTAAAAGAAGATGAGAATGTTC  361
            ||||||||||||||||||||||||||||||||||||||||||||||||||||||||||||
Sbjct  301  TTGCAGCTACAGCTGACTTCAGGGAGCAGATTTTAAGAGTAAAAGAAGATGAGAATGTTC  360

Query  362  CATTTCTACTGGTTGGTAACAAATCAGATTTAGAAGATAAAAGACAGGTTTCTGTAGAAG  421
            ||||||||||||||||||||||||||||||||||||||||||||||||||||||||||||
Sbjct  361  CATTTCTACTGGTTGGTAACAAATCAGATTTAGAAGATAAAAGACAGGTTTCTGTAGAAG  420

Query  422  AGGCAAAAAACAGAGCTGAGCAGTGGAATGTTAACTACGTGGAAACATCTGCTAAAACAC  481
            ||||||||||||||||||||||||||||||||||||||||||||||||||||||||||||
Sbjct  421  AGGCAAAAAACAGAGCTGAGCAGTGGAATGTTAACTACGTGGAAACATCTGCTAAAACAC  480

Query  482  GAGCTAATGTTGACAAGGTATTTTTTGATTTAATgagagaaattcgagcgagaaagatgg  541
            ||||||||||||||||||||||||||||||||||||||||||||||||||||||||||||
Sbjct  481  GAGCTAATGTTGACAAGGTATTTTTTGATTTAATGAGAGAAATTCGAGCGAGAAAGATGG  540

Query  542  aagacagcaaagaaaagaatggaaaaaagaagaggaaaagtttagccaagagaatcagag  601
            ||||||||||||||||||||||||||||||||||||||||||||||||||||||||||||
Sbjct  541  AAGACAGCAAAGAAAAGAATGGAAAAAAGAAGAGGAAAAGTTTAGCCAAGAGAATCAGAG  600

Query  602  aaagaTGCTGCATTTTATAA  621
            ||||||||||||||||||||
Sbjct  601  AAAGATGCTGCATTTTATAA  620
```

Figure 5.2: DNA sequencing to confirm the insertion of RALA in pBABE Puro vector. Sequence alignment data showing the comparison of sequence of RALA sequence obtained from NCBI database (subject) and clones RALA sequence obtained from pBABE Puro vector (query).

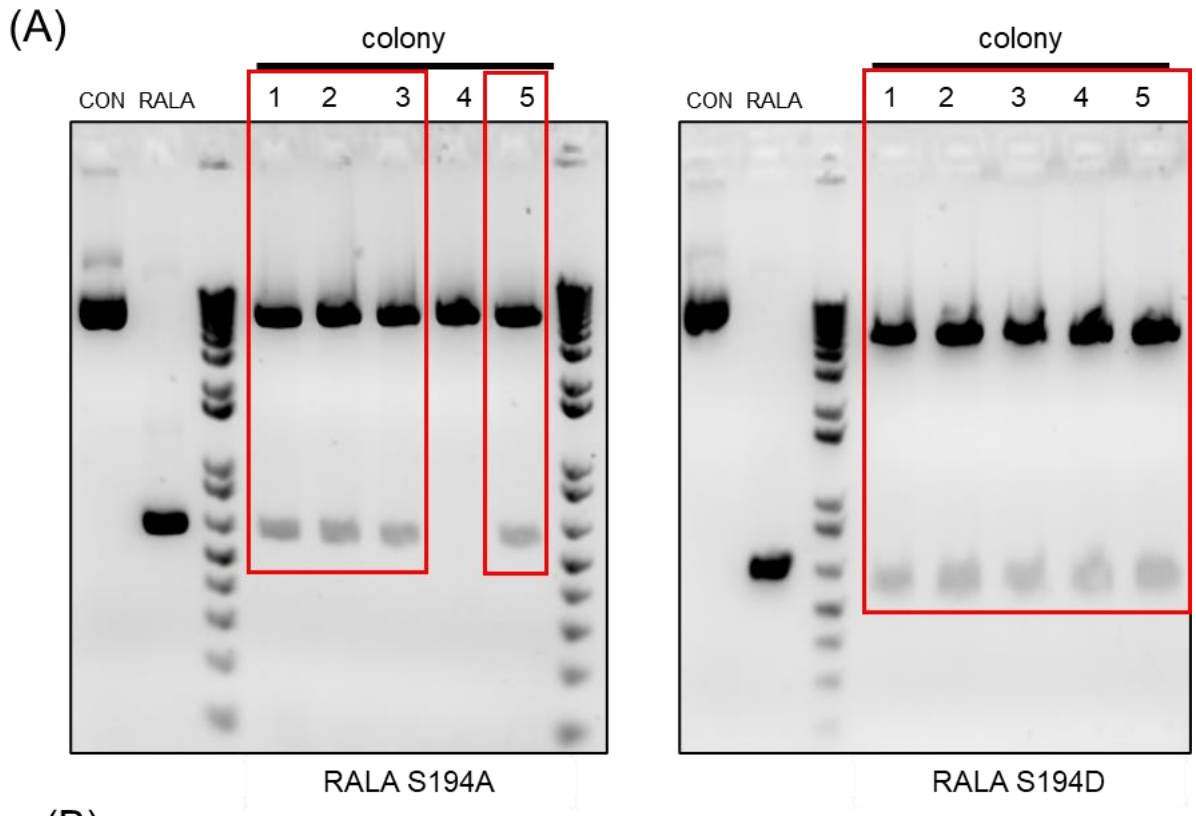

(B)

RALA S194A cloning (AGT > GCT)

```
RALA WT      545 acagcaaagaaaagaatggaaaaaagaagaggaaaagtttagccaagagaatcagagaaa 604
S194A Col-5  552 ..................................GC..................... 611
S194A Col-2  553 ..................................GC..................... 612
S194A Col-1  556 ..................................GC..................... 615
```

RALA S194D cloning (AGT > GAT)

```
RALA WT      542 aagacagcaaagaaaagaatggaaaaaagaagaggaaaagtttagccaagagaatcagag 601
S194D Col-2  551 ....................................GA.................... 610
S194D Col-1  545 ....................................GA.................... 604
S194D Col-5  542 ....................................GA.................... 601
S194D Col-4  542 ....................................GA.................... 601
S194D Col-3  543 ....................................GA.................... 602
```

Figure 5.3: Colony screening to confirm cloning of RalA S194A and S194D mutants in pBABE Puro vector (A) Agarose gel image showing insert release of RalA S194A and S194D mutants clones in pBABE Puro vector after digestion with BamHI and SalI enzyme. (B) DNA sequences for S194A and S194D RALA mutants isolated from positive transformed colonies were compared to known WT RALA sequences (human mRNA NCBI database). The AGT base pair codon for Ser194 is marked in the WT RALA sequence and, when compared, shows distinct mutations in base pair codons for S194A (GCT) and S194D (GAT) mutants. Red color indicates colonies selected for further studies.

5.2.3 Reconstitution of RALA S194 mutants in MCF7 RALA KO cells and MiaPaCa2 RALA KO cells

We used a retroviral approach to reconstitute the RALA (WT/S194A/S194D) mutants in RALA KO cells. To optimize and monitor the production of virus particles, we used an empty pMIG-GFP vector as a marker for transfection and transduction. HEK293T cells were transfected with pBABE Puro RALA (WT/S194A/S194D) and envelope plasmid (pVSVG) and packaging plasmid (pGagPol) and pMIG-GFP (in control) (Figure 5.4 A). 60 hours after transfection in HEK293T cells, virus particles were collected and added to the MCF7 RALA KO cells and MiaPaCa2 RALA KO cells. We began the puromycin selection after the expression of GFP in pMIG-GFP transduced cells was detectable (Figure 5.4 B).

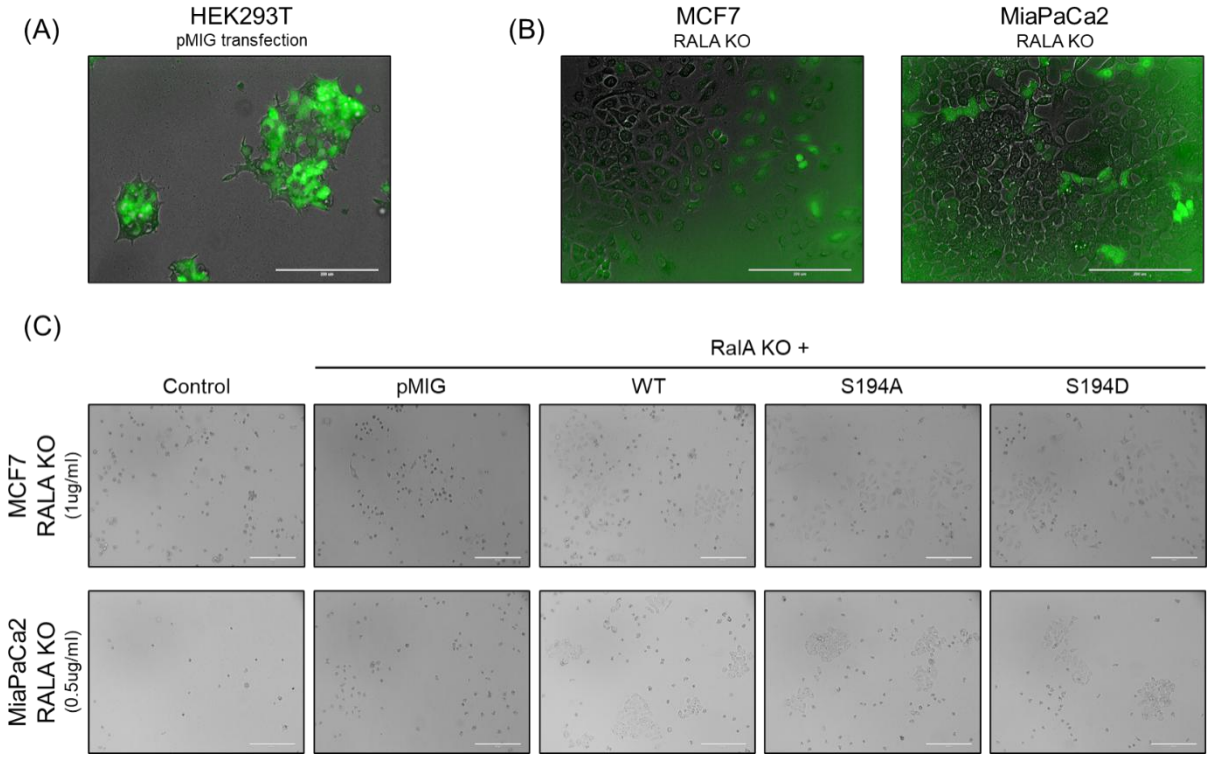

Figure 5.4: Reconstitution of RALA WT, S194A and S194D mutants in MCF7 and MiaPaCa2 cells. (A) Visualization of transfection efficiency with the help of pMIG vector in HEK293t cells for generation of viral particles. (B) Visualization of transduction efficiency in MCF7 and MiaPaCa2 cells with the help of pMIG vector. (C) Puromycin selection was carried out to select cells transduced with RALA WT, S194A and S194D mutants in MCF7 and MiaPaCa2 cells. Selection was continued till all cells in control and pMIG only control is dead.

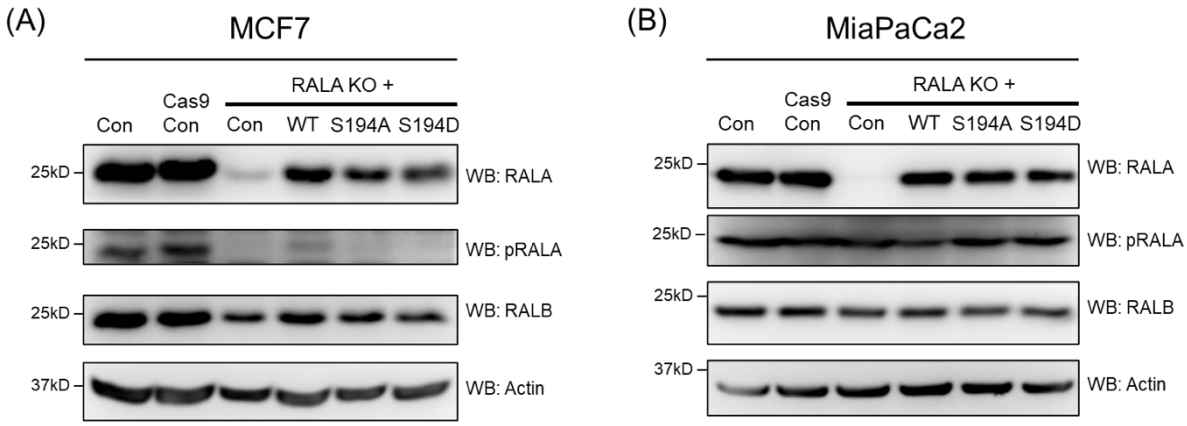

Figure 5.5: Reconstitution of RALA WT, S194A and S194D mutants in MCF7 and MiaPaCa2 cells (A,B) Western blot detection of RALA S194 phosphorylation (pRALA), total RALA, RALB and Actin in MCF7 and MiaPaCa2 control (CON), Cas9 control (Cas9 CON), RALA KO (KO) and RALA KO expressing WT-RALA (WT), S194A-RALA (S194A) and S194D-RALA (S194D) mutants.

Puromycin selection continued until all cells in control and pMIG transduced dishes were dead, and surviving cells in RALA (WT/S194A/S194D) transduced dishes were cultured further (Figure 5.4 C). The reconstitution of RALA WT, S194A and S194D was confirmed with western blotting in both MCF7 RALA KO cells and MiaPaCa2 RALA KO cells (Figure 5.5 A and B). The stable expression of WT-RALA and RALA mutants (S194A/S194D) in RALA KO MCF7 and MiaPaCa2 cell lines were comparable when detected with total RALA antibody. However, their expression levels were less than endogenous RALA in both cell types. Knowing the anti-phospho-RALA Antibody (Ser194) was more specific in its detection of pS194 RALA in MCF7 cells, we probed reconstituted RALA (WT/S194A/S194D) MCF7 cell lysates. As shown earlier, the RALA KO cells did not detect a band when probed. Reconstitution of WT-RALA in RALA KO cells restores the pS194 RALA detection, which is missing in RALA S194A and S194D reconstituted cells (Figure 5.5 A). In MiaPaCa2 cells the the pS194RALA band stays detected in the RALA KO cells and is the reconstituted mutants (Figure 5.5 B).

5.3 Summary and Conclusion

We successfully cloned RALA in the pBABE Puro vector and made RALA S194A and S194D mutants, which were confirmed by sequencing. Using retroviral transduction, stable reconstitution of these mutants was done in RALA KO MCF7 and MiaPaCa2 cells. The expression of WT-RALA, S194A and S194D mutants were comparable in the reconstituted MCF7 and MiaPaCa2 cells. These were almost always less than the expression of RALA in the untransfected Control or Cas9 Control cells. The mutants also did not affect RALB expression in reconstituted cells.

In MCF7 cells, phosphorylation of reconstituted WT-RALA was detectable and distinctly reduced in S194A and S194D mutant-expressing cells. In MiaPaCa2 cells, WT-RALA, S194A and S194D mutant expressing cells were all seen to detect a band of comparable size and intensity as seen in CON or Cas9Con and KO cells using the anti-phospho-RALA Antibody (Ser194). Together, they further confirm the issues raised earlier (Chapter 4) regarding the lack of specificity for this antibody in RAS-dependent cancers. This prevents us from using this antibody for any further evaluation in RAS-dependent cancers. The RALA KO and reconstituted with WT-RALA, S194A-RALA and S194D-RALA MCF7 and MiaPaCa2 cells are validated for use in mice tumorigenesis study.

Chapter 6

Evaluating the role of RALA and RALA S194 phosphorylation in tumorigenesis

6.1 Rationale

RALA is overexpressed and activated in a wide range of human cancer cells. RALA overexpression has been suggested to be associated with poor prognosis and survival in cancer patients. Downstream of RAS, activation of RALA is critical for cancer cell tumorigenesis mediated through RALGEFs. The understanding of RALA in cancer is based on previous studies on loss of function (LOF) with the help of siRNA/shRNA and RALA inhibitors (Richardson *et al.*, 2022). Only one study has been reported to use RALA CRISP-Cas9 KO to test the effect of true LOF phenotype of RALA on tumorigenesis. Having RALA knocked out in multiple cancer cell lines would provide a unique opportunity to understand how the absence of RALA can impact cancer tumorigenesis. They also offer a unique tool to evaluate the role of RAL in cellular functions.

RALA function mainly depends upon its localization and activation in the cell, and it is primarily regulated by RALGEFs and PTMs (Post-translational modifications). *In-vitro* kinase assay studies showed AURKA phosphorylates RALA at Serine 194 residue (S194) but did not affect RALB (Wu *et al.*, 2005). Whether RALA phosphorylation at S194 can regulate RALA activity and, thus, function is still unclear. One *In-vitro* study using anti-phospho-RALA antibody (Ser194) (Merck-Millipore, Cat no- 07-2119) suggests PKA to also mediate RALA phosphorylation at S194 (Neel *et al.*, 2014), though the role of this regulatory crosstalk in cells remains untested. Various studies have evaluated the role of RALA S194 phosphorylation in regulating RALA activation, AIG, localization and tumorigenesis; however, most of the studies were carried out with immortalized non-transformed cells (Wu *et al.*, 2005; Lim, Donita C. Brady, *et al.*, 2010), and a handful of studies were done in cancer cells (Lim, Donita C. Brady, *et al.*, 2010). The results from these studies are also variable, making it difficult to clearly define if and how RALA S194 phosphorylation regulates RALA function.

Considering there might be inconsistencies in the detection, role and even the kinase that could phosphorylate RALA in the S194 residue, evaluating its role in RALA function can be challenging. Our earlier studies with V_{MLN} mediated AURKA inhibition

in RAS-dependent MCF7, SKVO3 and RAS-independent T24, UMUC3 and MiaPaCa2 cells have only further highlighted some of these inconsistencies. Keeping all of these in mind, we concluded that the stable KO of RALA and their stable reconstitutions with WT-RALA, RALA S194A and RALA S194D mutants might be the best (and maybe the only way) to test the role of the AURKA-RALA crosstalk in individual cancers.

6.2 Results

6.2.1 Evaluating the role of RALA and its S194 phosphorylation in tumorigenesis

To evaluate the role of RALA KO and RALA S194 phosphorylation stable, reconstituted MCF7 and MiaPaCa2 cells were used for mice xenograft tumor assay (as described in methods). The control cells (Con) and Cas9 control (Cas9) (to make sure Cas9 had no effect on tumor formation) in both MCF7 and MiaPaCa2 cells formed tumors of decent size (Figure 6.2). The MCF7 and MiaPaCa2 cells with RALA KO formed significantly smaller tumors than control cells (Figure 6.2). Reconstitution of KO cells with WT RALA, S194A RALA (phosphodeficient) and S194D RALA (phosphomimetic) mutants showed their expression to be comparable and slightly less than the endogenous RALA expression in the CON and Cas9 cells (Figure 5.5). Their expression is tumor lysates (from male and female mice) show levels of RALA in KO cells to be marginally enhanced (relative to the cells used to make tumors (Figure 5.5), possibly reflecting the recruitment of RALA-containing cells from neighboring tissue or circulation. In MCF7 and MiaPaCa2 tumors the expression of WTRALA, S194ARALA and S194D RALA were comparable (Figure 6.1).

Reconstitution of MCF7 and MiaPaCa2 KO cells with WT RALA partially restored their tumor size (Figure 6.2 A and B). This partial rescue could reflect the restored WT RALA levels in these cells being less than endogenous RALA levels (in Con and Cas9-Con cells). The rescue in tumor size is also marginally better for WT-RALA expressing MiaPaCa2 tumors than MCF7 tumors, possibly reflecting their relative expression of WT-RALA protein (Figure 5.5). Together, this does highlight the importance of RALA in tumor formation for both RAS-dependent and RAS-independent cancer cells.

Tumors formed by MCF7 and MiaPaCa2 RALA S194A (phosphodeficient) mutant reconstituted cells were comparable to their RALA KO tumors in size (Figure 6.2). The tumors formed by RALA S194D (phosphomimetic) mutant reconstituted cells were also comparable to those made by RALA S194A mutants in both MCF7 and MiaPaCa2 cells (Figure 6.2). This could mean the RALA S194D phosphomimetic mutant may not be as effective in mimicking the function of phosphorylation in tumor formation. An earlier study by Lim et.al. has reported the S194D mutant to behave similar to S194A mutants in regulating RALA activation in HEKTtH cells (Lim, Donita C. Brady, *et al.*, 2010).

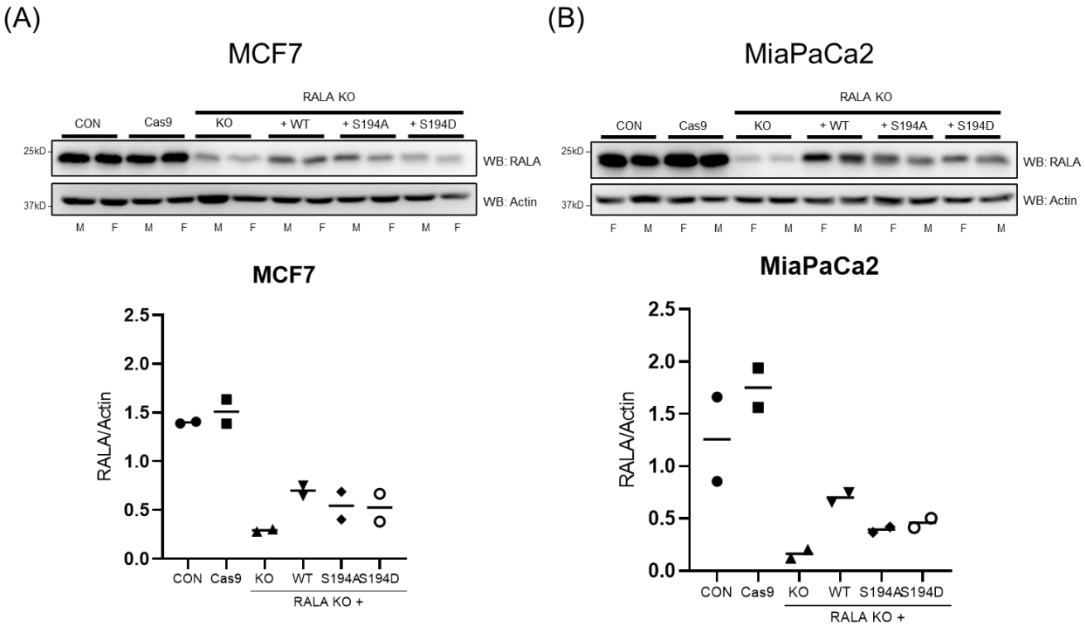

Figure 6.1: Detection of RALA and Actin in tumor lysates (A,B) (Upper panel) RALA and Actin was detected using western blotting from harvested tumors to confirm the RALA KO and reconstitution. (Lower panel) Graph represents the mean value of RALA/Actin from tumor lysates. Statistical analysis was done using mann-whitney test, and p values, if significant, are represented in the graph (**** $p < 0.0001$).

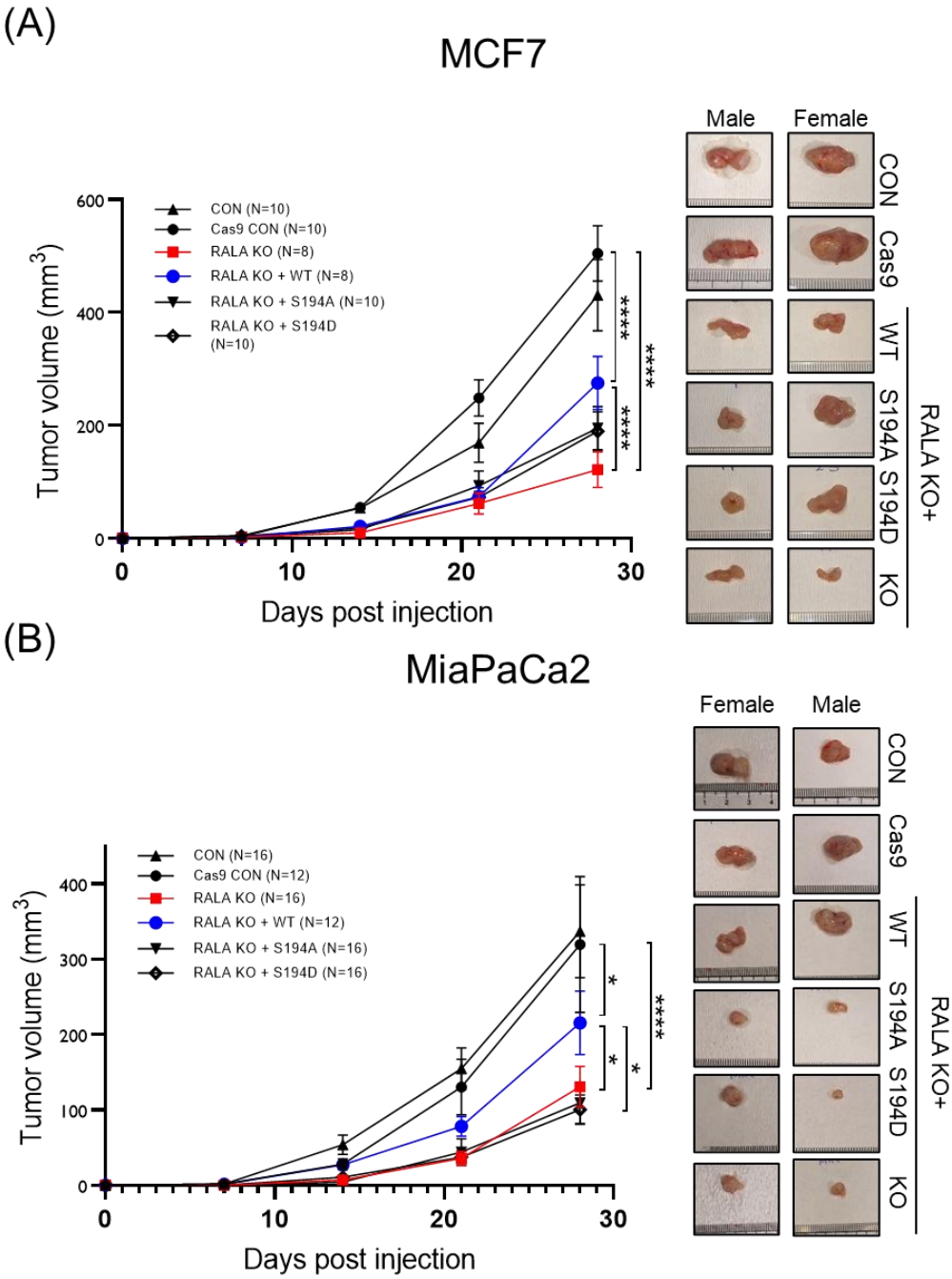

Figure 6.2: Role of RALA and its S194 phosphorylation in regulating tumor formation in MCF7 and MiaPaCa2 cells. (A) Tumor volume (mm^3) ± SE versus time (days) of MCF7 control cells (▲), Cas9 treated cells (●), RALA KO cells (■) or RALA KO cells expressing RALA WT (●) or RALA S194A (▼) or RALA S194D (◊) mutants injected into a flank of immunocompromised mice. (B) Tumor volume (mm^3) ± SE versus time (days) of MiaPaCa2 control cells (▲), Cas9 treated cells (●), RALA KO cells (■) or RALA KO cells expressing RALA WT (●) or RALA S194A (▼) or RALA S194D (◊) mutants injected into a flank of immunocompromised mice. Statistical analysis was done using Two-Way ANOVA comparing rows within each column and p Values if significant are represented in graph (* $p < 0.05$, **** $p < 0.0001$)..

6.2.2 Evaluating the role of RALA S194 phosphorylation on RAL activation

Since RALA S194 phosphorylation affected tumorigenesis, we checked whether this effect comes from a change in RALA activation. GST-Sec5 pulldown of active RALA from reconstituted MCF7 and MiaPaCa2 cells showed no significant difference in the activation status of WT RALA, S194A RALA and S194D RALA mutants (Figure 6.3 A and B). This suggests that RALA S194 phosphorylation does not affect RALA activation (detected by its effector binding capability) in RAS-independent (MCF7) or RAS-dependent (MiaPaCa2) cancer cell lines. In both cell types targeting this phosphorylation site by mutation does affect tumor formation. RALB activation was shows a small but nonsignificant increase on RALA KO or reconstitution with WT or Mutant RALA in both MCF7 and MiaPaCa2 cells (Figure 6.3 A and B).

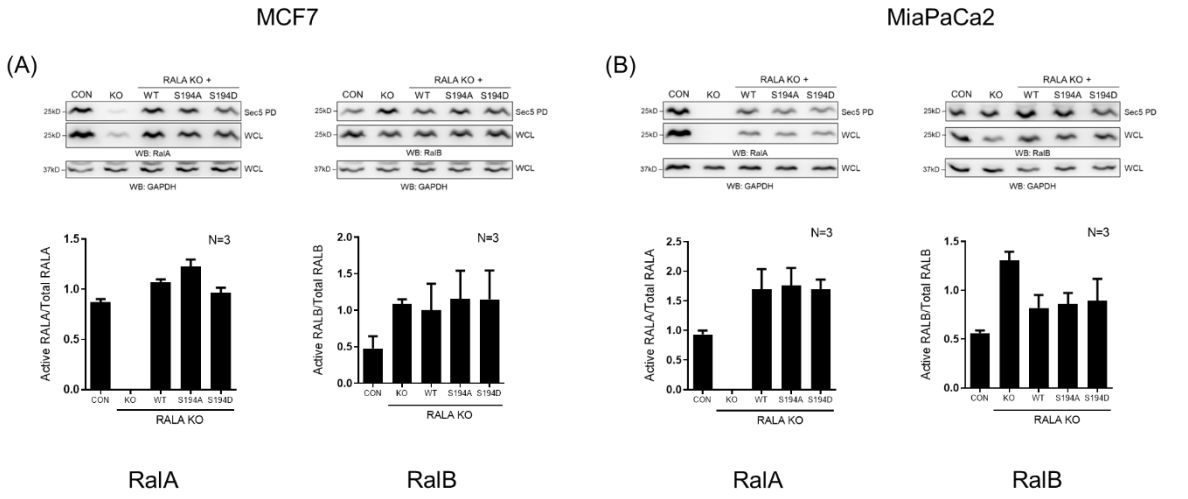

Figure 6.3: Role of RALA and its S194 phosphorylation in regulating RAL activation in MCF7 and MiaPaCa2 cells. (A,B) Western blot detection (upper panel) and quantitation (lower panel) of Active RALA, active RALB, RALA and total RALB, from lysates of Control, Cas9 control, RALA KO, KO+WT, KO+S194A, KO+S194D of MCF7 and MiaPaCa2 cells. The graphs represents ratio of active/total Ral as mean ± SE from at least three independent experiments. Statistical analysis was done using mann-whitney test, and p values, if significant, are represented in the graph (* $p < 0.05$, ** $p<0.01$, *** $p<0.001$).

6.2.3 Evaluating the role of RALA S194 phosphorylation on RALA localization

Since RALA S194 phosphomutants did not affect RALA activation, we looked at their localization in cells. We performed IFA experiments to examine the RALA localization

in RALA WT, S194A and S194D mutant reconstituted cells. In MCF7 reconstituted cells, the WT-RALA showed distinct perinuclear localization and occasional localization in membrane ruffles. S194A-RALA mutant lacked this spatial clarity in cells, being more homogeneously distributed. Fluorescence images, when comparably thresholded and intensities above the set threshold marked (in red), confirmed this difference in spatial localization of WT vs S194A-RALA mutant (Figure 6.4). This localization difference in MCF7 cells was difficult to evaluate in MCF7 cells as they spread distinctly less. The localization of RALA and its regulation by RALA

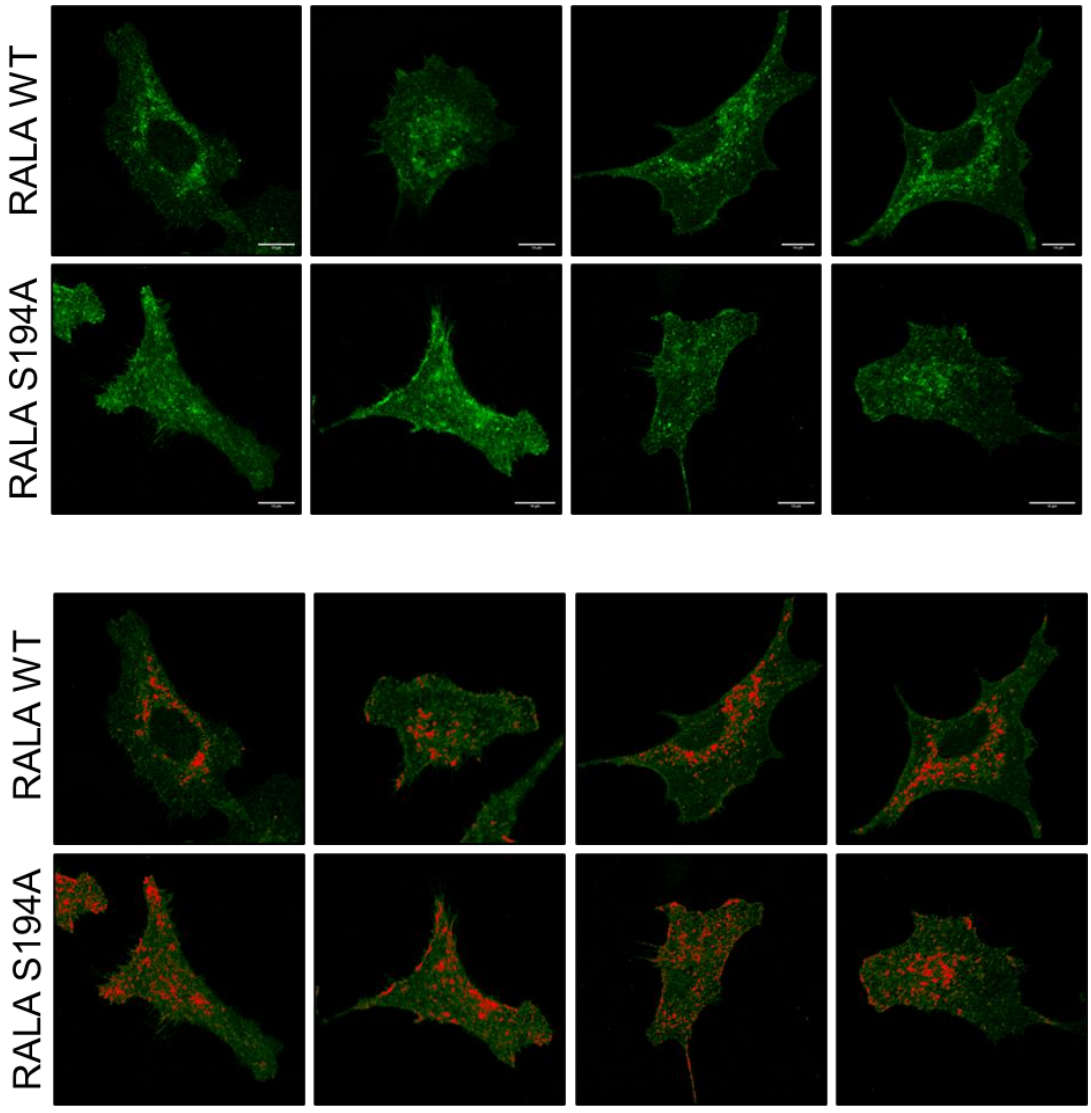

Figure 6.4: Effect of RalA S194 phosphorylation on RalA localization in MCF7 cells Immunofluorescence detection of RALA in MCF7 RALA KO cells reconstituted with WT-RALA (top row) and S194-RALA mutant (bottom row). Fluorescence images were comparably thresholded, and intensities above the set threshold were marked in red to highlight their localization. (Data Credit – Tushar Sherkhane)

S194 phosphorylation could, in the absence of any effect on RALA activation, be the mediators for regulating tumor growth.

6.3 Summary and Conclusion

We evaluated the role of RALA and its S194 phosphorylation in tumorigenesis of RAS-independent (MCF7) and RAS-dependent (MiaPaCa2) cancer cell lines. RALA and its S194 phosphorylation both are important in regulating tumorigenesis in MCF7 and MiaPaCa2 cells. Reconstitution of RALA KO cells with WT-RALA partially restores tumor growth possibly reflecting its expression profile in these tumors. The expression of S194A-RALA mutant is not able to rescue the RALA KO phenotype in these cells. The S194D-RALA mutant behaves like the S194A-RALA mutant, suggesting it might be a poor mimic of this phosphorylation. The lack of any visible effect on RALA activity of S194A and S194D mutants also supports this claim. It also suggests the role this phosphorylation could have in regulating RALA function in tumors, could come through its localization or effector interaction more than activation.

Chapter 7:

Evaluating the role of AURKA and RGL1 in regulating RALA and RALB

7.1 Rationale

RAL GTPases (RALA and RALB) are essential in cell spreading, migration, and actin organization downstream of adhesion. The function of small GTPase, RALA and RALB depends on their activation and localization. RALGEFs regulate RAL GTPases activation (that can be classified as RAS-dependent RALGEFs and RAS-independent RALGEFs) and RALGAPs. Their localization, which is dependent on PTMs (Post Translational modifications), is also vital to their regulation.

The way regulatory pathways can differentiate RALA and RALB is only beginning to be understood, and it is an essential element of their regulation. Recently, AURKA has emerged as a novel regulator that can distinguish between RALA and RALB. AURKA phosphorylates RALA at S194 residue, but not RALB, which can regulate RALA localization and activation in some cells (Sablina *et al.*, 2007). However, AURKA is a mitotic kinase that can't directly cause RALA activation. It must work through RALGEFs or RALGAPs to mediate the same. AURKA has previously been shown to phosphorylate RalGDS (Wang et al., 2010); however, the effect of this interaction on RALA activation was not evaluated. This suggests that AURKA-mediated regulation of GEFs is an attractive regulatory pathway worth exploring for other RAL GEFs / GAPs. Cell matrix adhesion affects RALA but not RALB activation (Balasubramanian *et al.*, 2010) (Figure 7.1), making it a beautiful system to evaluate their variable regulation and the role of AURKA in mediating this.

This chapter evaluates if and how AURKA and RALGEFs work together to regulate adhesion-dependent RALA vs RALB activation.

7.1.1 Regulation of RALA and RALB by AURKA and RGL1 in Early Adhesion

To evaluate RALA activation in response to early cell-matrix adhesion, earlier studies from the lab had performed a suspension and re-adhesion assay in WTMEFs. It found RALA activation to drop in suspension, recovering upon replating cells on fibronectin (Figure 7.1 A), confirming its regulation by adhesion. RALB activation was largely unaffected by suspension and replating (Figure 7.1 B).

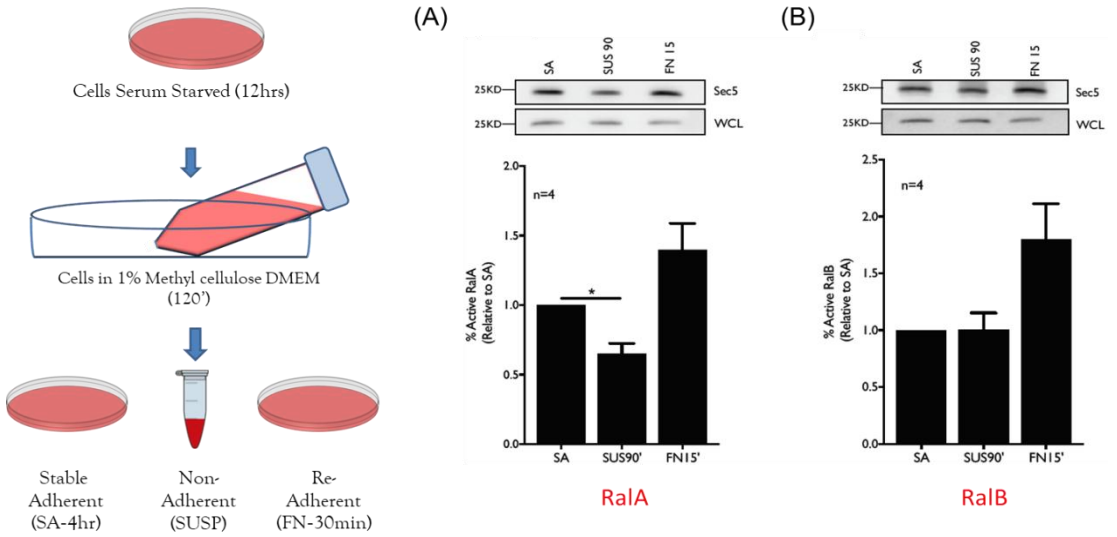

Figure 7.1: Adhesion dependent regulation of RAL GTPases. Suspension assay was performed as shown in schematic to evaluate the adhesion dependent regulation of RAL GTPases. (A,B) Western blot detection (upper panel) and quantitation (lower panel) of active RALA and RALB pulled down by GSTSec5 beads and total RALA and RALB in WCL in the lysates from serum-starved WT-MEFs stable adherent (SA), suspended for 30 mins (SUS 30') and re-adherent on fibronectin for 15 mins (FN 15'). The ratios of percent active RALA and RALB were normalized to respective SA (equated to 1), and these values are represented in the graph as mean ± SE from at least three independent experiments. Statistical analysis of all the above data was done using the one sample t-test for normalized and two-tailed unpaired student's t-test for non-normalized data and significance if any was represented in graph (* p-value <0.05, ** p-value <0.01, *** p-value <0.0001). ***Data credit: Siddhi Inchanalkar, Schematic by Archana Pawar***

Once we confirmed the adhesion-dependent regulation of RALA in WTMEFs, we checked if RALGEFs and AURKA can influence the adhesion-dependent RALA activation. siRNA-mediated knockdown of RALGEFs (RalGPS1, RalGDS and RGL1) was seen to affect re-adhesion mediated RALA recovery. This effect was significantly higher on RGL1 KD, suggesting downstream of adhesion RGL1 is a major RALGEF that regulated RALA activation (Figure 7.2 A). Reconstitution of RGL1 KD cells with siRNA-resistant human RGL1 (hRGL1) restored RALA activation in re-adherent cells (Figure 7.2 B). This confirmed RGL1 to regulate RALA activation in early adhesion. Our studies then tested AURKA activation downstream of adhesion, finding it to

increase on suspension and returning to basal level upon replating (Figure 7.2 C). This is distinctly opposite of RALA activation observed (Figure 7.1 A). RALA S194 phosphorylation, when tested in suspension assay by expressing human RALA (since the S194A antibody does not detect mouse RALA) finds pS194 RALA levels to increase on loss of adhesion (Figure 7.2 D), when AURKA activity increases (Figure 7.2 C) and RALA activity drops (Figure 7.1 A). On re-adhesion, AURKA activation and pS194 RALA drop slightly to basal levels as RALA activity recovers.

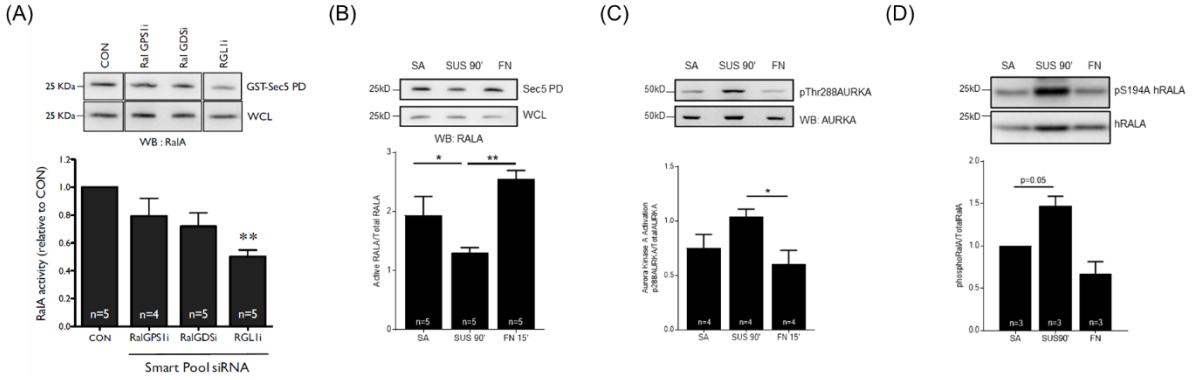

Figure 7.2: Regulation of RALA by RGL1 and AURKA in early adhesion. Western blot detection (upper panel) and quantitation (lower panel) of (A,B) Active RALA pulled down by GST-Sec5, and the total RALA in WCL in lysates from serum starved Control (CNT/CON) and RGL1 knockdown (RGL1i) WT-MEFs re-adherent on fibronectin for 15 min (FN150min). (C) phosphorylation on Threonine 288 residues of AURKA (pThr288AURKA) and total AURKA (D) phosphorylation on Serine 194 residues of human RALA (pSer194hRALA) and total human RALA in lysates from serum starved WT-MEFs stable adherent (SA), suspended for 60 mins + 30mins with V_{MLN}/Empty DEX (SUS 90') and re-adherent on fibronectin for 15mins with V_{MLN}/Empty DEX (FN 15'). The graph represents the mean ± SE data from four independent experiments. Statistical analysis was done using the one sample t-test and p values, if significant, are represented in the graph (* $p < 0.05$). ***Data credit: Siddhi Inchanalkar***

This suggests that AURKA-mediated regulation of S194 RALA phosphorylation might be decoupled from its adhesion-dependent activation. V_{MLN} (described in Chapter 4) treatment of cells inhibited AURKA and RALA S194 phosphorylation in suspension and re-adherent cells (Figure 7.3 A), affecting the recovery of RALA activation in re-adherent WTMEFs (Figure 7.3 B).

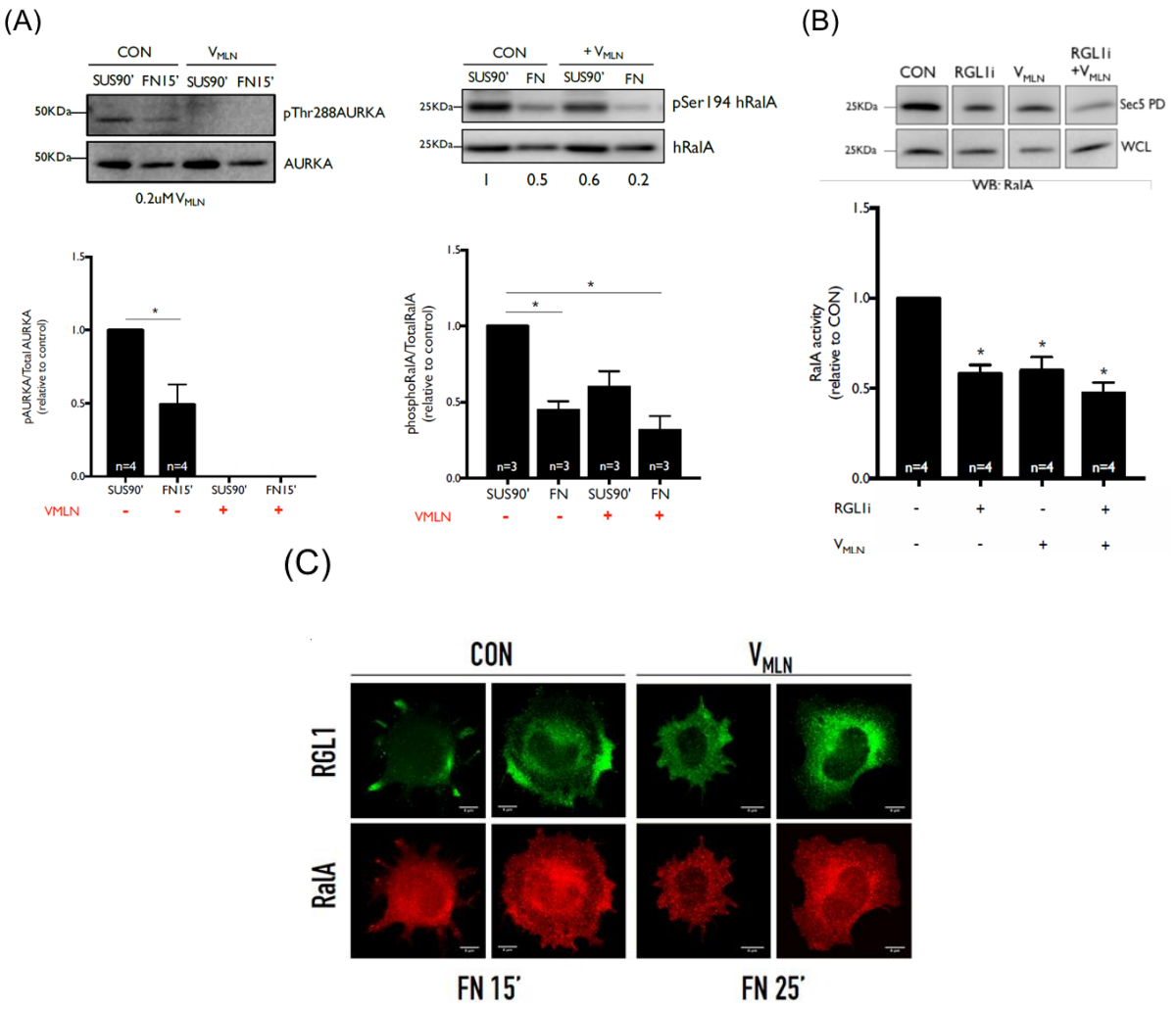

Figure 7.3: AURKA-RGL1 in regulating RALA in early adhesion. Western blot detection (upper panel) and quantitation (lower panel) of (A) phosphorylation on Threonine 288 residues of AURKA (pThr288AURKA) and total AURKA, and phosphorylation on Serine 194 residues of human RALA (pSer194hRALA) and total human RALA in lysates from serum starved WT-MEFs stable adherent (SA), suspended for 60 mins + 30mins with V_{MLN}/Empty DEX (SUS 90') and re-adherent on fibronectin for 15mins with V_{MLN}/Empty DEX (FN 15'). (B) Western blot for active RALA pulled down by GST-Sec5, and the total RALA in WCL in lysates from serum-starved, control or RGL1 knockdown WT-MEFs, suspended for 60 mins + 30mins with V_{MLN}/Empty DEX and re-adherent on fibronectin for 15mins with V_{MLN}/Empty DEX. The graph represents the mean ± SE data from atleast three independent experiments. Statistical analysis was done using the single-sample t-test and p values, if significant, are represented in the graph (* $p < 0.05$). (C) Re-adherent WT-MEFs expressing Myc-tagged RGL1 detected with an anti-myc antibody (Myc-RGL1) and endogenous RALA with the anti-RALA antibody (RALA) shows their co-localization in membrane ruffles and membrane protrusions in control cells which are altered in V_{MLN} treated WT-MEFs. Data is representative of 30 cells from three independent experiments. Scale bars in images are set at 8 µm. ***Data credit: Siddhi Inchanalkar***

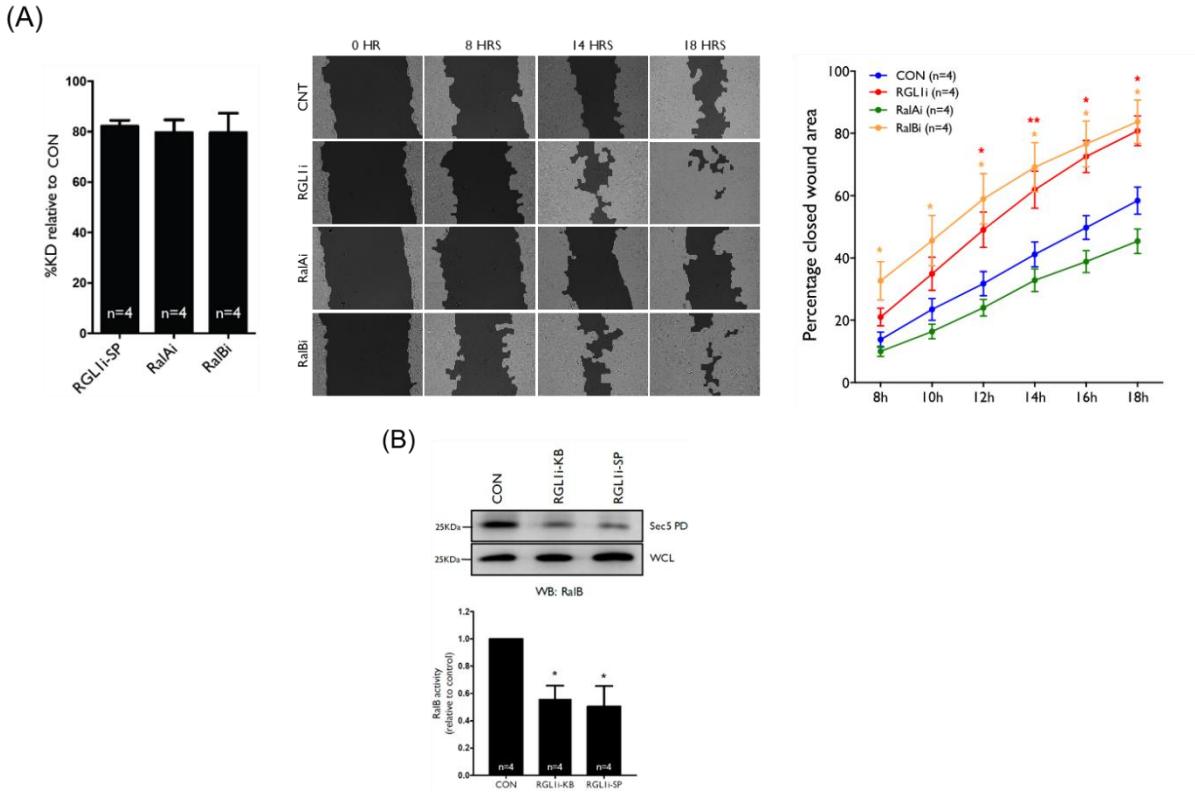

Figure 7.4: Effect of RGL1, RALA and RALB knockdown on the migration of WT-MEFs in wound healing assay. (A) Healed and representative ROI and Calculated percentage wound area are shown from smart pool siRNA treated Control (CON), RGL1 (RGL1i), RALA (RALAi) and RALB (RALBi) knockdown WT-MEFs post 8, 14 and 18hours of scratch formation. Aleast three beacons per group were analyzed for each experiment. Data was obtained from results of four independent experiments. Student t test was used to calculate significance (* $p < 0.05$, ** $p < 0.01$) ***Data credit: Neha Deshpande***. (B) active RALB pulled down by GST-Sec5 (Sec5 PD) and total RALA/RALB in the whole-cell lysate (WCL) was done from control (CON), individual siRNA (RGL1i-KB) and smart pool siRNA (RGL1i-SP) targeting RGL1 treated WT-MEFs (in presence of serum). Calculated percentage of active RALA/RALB levels were normalized to respective control (CON) (equated to 1). The graph represents the mean ± standard error from four independent experiments. Statistical analysis of all data was done using the single sample T-Test and P values are as indicated (* $p<0.05$). ***Data credit: Siddhi Inchanalkar***

Because the drop in RALA activation with AURKA and RGL1 was comparable in re-adherent WTMEFs, we asked if RGL1 and AURKA can work synergistically to mediate this regulation. A joint inhibition of AURKA and RGL1 did not show any additive effect on RALA activation in re-adherent WTMEFs (Figure 7.3 B). This suggests they work along the same pathway to regulate adhesion-dependent RALA activation. Since PTMs regulate RALA localization, we hypothesized that AURKA may regulate the RALA and RGL1 localization downstream of adhesion. To test this hypothesis, we checked the RALA and RGL1 localization in re-adherent cells in the presence and absence of V_{MLN}. On re-adhesion, RGL1 and RALA co-localise at membrane protrusions, with V_{MLN} disrupting this localization and cell spreading (Figure 7).

7.1.2 Regulation of RALA and RALB in cell migration by AURKA and RGL1

Since both RALA and RALB are known to regulate cell migration, we had tested if and how AURKA and RGl1 could differentially regulate RALA and RALB in cell migration. However, in absence of serum, neither RGL1 Kd or RALA/RALB Kd had any effect on cell migration (data not shown), indicating presence of serum or growth factors along with cell-matrix adhesion could influence the RGL1 dependent regulation of RALA and RalB.

In the presence of serum growth factors comparable specific knockdown of RALA, RALB and RGL1 (Figure 7.4 A) shows RGL1 and RALB loss to cause cells to migrate significantly faster than control WTMEFs. On loss of RALA no effect on migration was seen (Figure 7.4 A). This suggested that RGL1 could regulate RALA-dependent migration in the absence of serum and RALB dependent migration in the presence of serum. GST-Sec5 pulldown of control and RGL1 KD cells shows it affects RALA activity in the absence of serum and RALB activity in the presence of serum (Figure 7.4 B).

As a part of this understanding a small part of my thesis work has focused on using V_{MLN} mediated targeting of AURKA to test the role this could have in serum-dependent migration of cells.

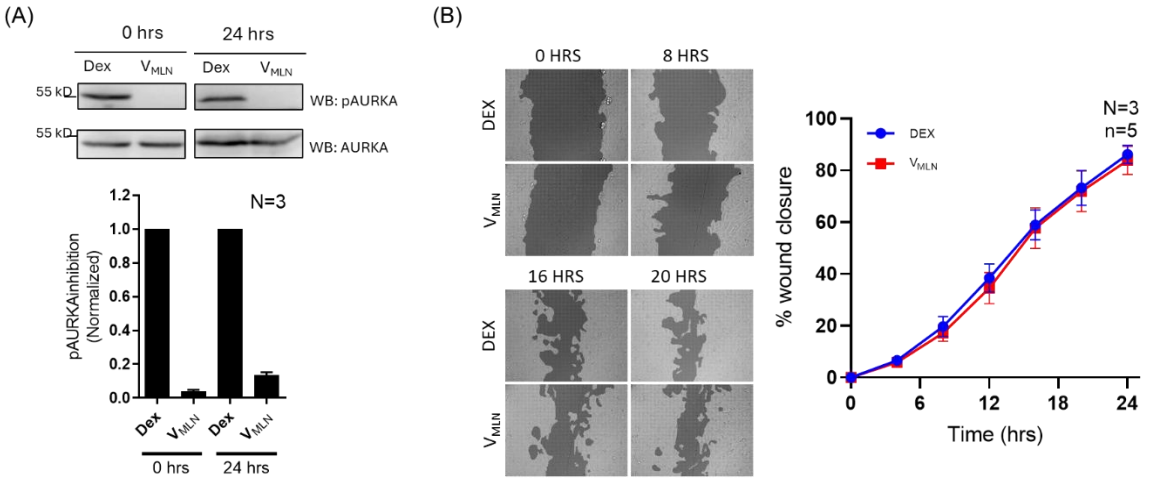

Figure 7.5: Effect of AURKA inhibition using V_{MLN} on the migration of WT-MEFs in wound healing assay. (A) Western blot detection (upper panel) and quantitation (lower panel) of phosphorylation on Threonine 288 residues of AURKA (pThr288AURKA) and total AURKA were done from lysates of control (CON) and 0.06μM V_{MLN} treated (V_{MLN}) WT-MEFs in presence of serum at end of migration assay. The calculated ratio of pAURKA/TotalAURKA was normalized to respective control (CON). The graph represents the mean ± standard error from three independent experiments. Statistical analysis of all data was done using the single sample T-Test and P values are as indicated (***p<0.001). (B) Calculated percentage wound area healed and representative ROI are shown from Control and V_{MLN} treated WT-MEFs post 8, 16 and 20hours of scratch formation.

7.2 Results

7.2.1 Role of AURKA in regulating Ral-dependent migration.

To test the role of AURKA in regulating serum-dependent migration in WTMEFs, we used V_{MLN} to inhibit AURKA (0.2μM for 1 hour), followed by a scratch assay with 0.06μM V_{MLN} for the wound healing experiment. AURKA inhibition was confirmed before and after making the scratch (Figure 7.5 A). AURKA inhibition we find did not affect the rate of wound closure (over 24 hours) compared to control cells (Figure 7.5 B). It also did not affect RALA (Figure 7.6 B) or RALB (Figure 7.6 C) activation in these cells. This confirms the AURKA mediated regulation of RALA activation is not observed in the presence of serum. Expectedly it is not involved in regulating RALB activation in these cells.

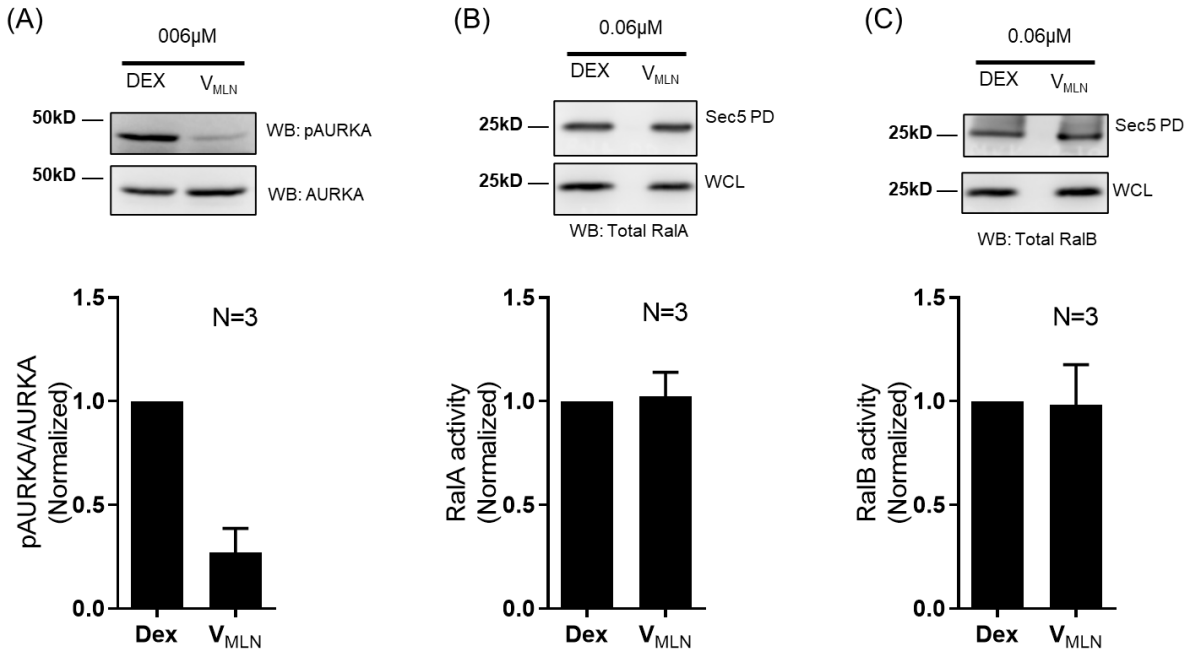

Figure 7.6: Effect of AURKA inhibition on RAL activation in actively migrating WTMEFs. Western blot detection (upper panel) and quantitation (lower panel) of (a) phosphorylation on Threonine 288 residues of AURKA (pThr288AURKA) and total AURKA (b) Active RALA and (c) Active RALB pulled down by GST-Sec5, and the total RALA/RALB in the whole-cell lysate (WCL) was done from control (CON) and VMLN (0.06μM) treated (VMLN) WT-MEFs in presence of serum. Calculated percentage of active RALA/RALB levels and theratio of pAURKA/TotalAURKA were normalized to respective control (CON) (equated to 1). The graph represents the mean ± standard error from three independent experiments. Statistical analysis of all data was done using the single sample T-Test and p-values if significant areindicated in the graph (* $p<0.05$, ** $p<0.01$).

7.2.2 Identification of AURKA phosphorylation site on RGL1

Since in early adhesion, AURKA and RGL1 seem to work together to regulate the RALA activation, there might be a way for AURKA to indirectly or directly regulate RGL1 localization or function. This direct association we wanted to evaluate and as a first step to doing this we used online kinase prediction tools to test for potential AURKA phosphorylation site on RGL1.

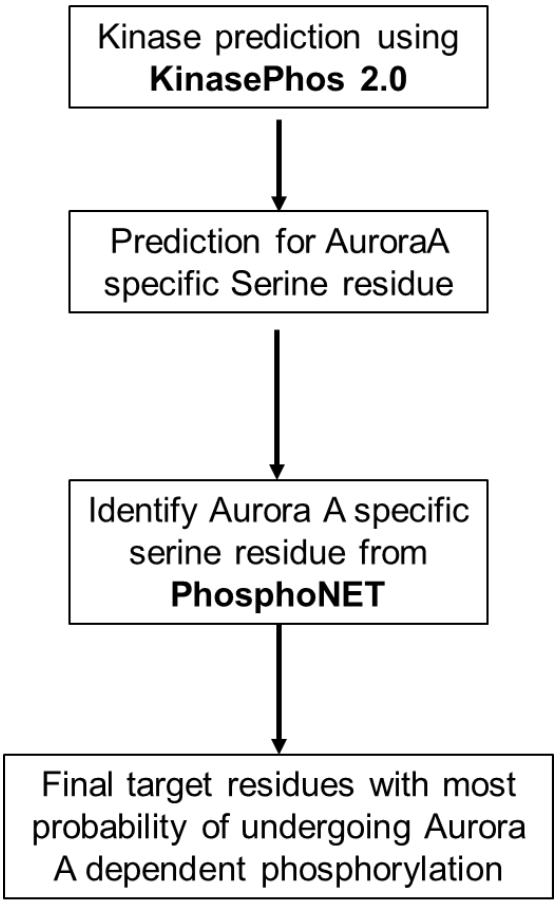

Figure 7.7: Strategy to identify AURKA phosphorylatio site on RGL1 .Pipeline showing use of online kinase prediction tools (KinasePhos 2.0 and PhosphoNET) to identify the AURKA phosphorylation site on RGL1.

Using online kinase prediction tools KinasePhos 2.0 and PhosphoNET, we developed a pipeline (Figure 7.7) that can predict the AURKA phosphorylation sites on RGL1. This pipeline helps us select the common predicted AURKA phosphorylation site for a target protein (RGL1). AURKA kinase-specific sites, predicted by KinasePhos 2.0, were manually searched in PhosphoNET (which predicts all Aurora kinase family sites) to identify AURKA-specific sites. We then validated this pipeline with known AURKA substrates to check if it correctly identifies known phosphorylation sites (data not shown). This was done for multiple substrates, and the accuracy of the pipeline developed was confirmed. Using this pipeline, we identified possible phosphorylation sites on RGL1 and were left with three potential sites, i.e. S339, S514 and S627 (Figure 7.8).

Out of these three predicted sites, the first site i.e. S339 is located in CDC25 domain (232-501 aa) of RGL1 which is known to be responsible for its GEF activity (Shirakawa and Horiuchi, 2015). This region is also involved in autoinhibition by binding with its REM domain (65-196 aa) (Nakhaeizadeh *et al.*, 2016). Hence, phosphorylation of RGL1 at S339 by AURKA could affect its GEF activity and function. According to UNIPROT, the remaining sites S514 and S627 are located near a region rich in polar residue which are generally required for maintaining stability of protein structure and interaction with small molecules (Zhou *et al.*, 2001; Illergård, Kauko and Elofsson, 2011). These sites may hence affect RGL1 stability and hence levels to affect its function.

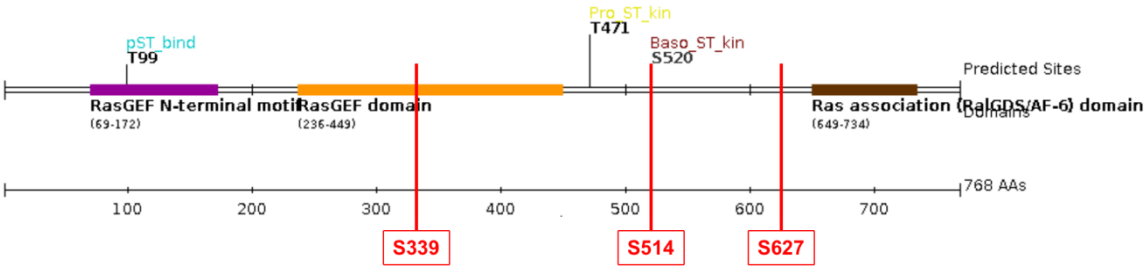

Figure 7.8: Identification of AURKA phosphorylation site on RGL1. Three AURKA phosphorylation sites were identified on RGL1 using online kinase prediction tools (KinasePhos 2.0 and PhosphoNET). Image showing the identified residue and location on RGL1.

7.3 Summary and Conclusions

In this chapter, my work has helped evaluate the possible role of AURKA in regulating RALGEF, RGL1 dependent RAL activation. AURKA inhibition using V_{MLN} revealed it can regulate RALA S194 phosphorylation and activation downstream of adhesion in WTMEFs. This we find regulates early adhesion-dependent cell spreading (regulated by RALA) but does not affect serum-dependent cell migration (regulated by RALB). This supports the involvement of the AURKA-RALA crosstalk in early adhesion events. Knowing RGL1 has a role in regulating RALA in early adhesion suggests the possible presence of an AURKA-RGL1-RALA pathway downstream of adhesion. Potential AURKA phosphorylation sites in RGL1 identified by *in-silico* studies make testing for

the above regulatory pathway with RGL1 phospho-mutants a realistic possibility. Ongoing work in the lab aims to evaluate the same.

Chapter 8:

Discussion

The work presented in this thesis focuses on understanding the regulation and role of RALA S194 phosphorylation in tumorigenesis in cancer cells. Phosphodeficient mutant studies reveal that S194 phosphorylation of RalA is required for RALA-dependent tumorigenesis, making it an attractive candidate for targeting tumor growth and RALA localization and downstream effector interaction rather than RALA activation may play more important role in this regulation. However, AURKA-mediated regulation of S194 phosphorylation of RALA and its effect on RALA activation and function are seen to be cell type specific and not affected by oncogenic RAS. This work has also raised important questions about the specificity of the pS194A-RalA antibody, which has implications for our understanding of its role and regulation. Our studies also explore the possibility that AURKA by phosphorylating RalGEFs, like RGL1, could regulate adhesion-dependent RALA activation. Together, they suggest the AURKA-RALA crosstalk could be more complex than initially imagined, and a careful and complete evaluation across cancers might be needed to understand its role better.

8.1 Making of CRISPR-Cas9 mediated RALA KO in cancer cells

Evaluation of the role of RAL (RALA and RALB) in cancer has been understandably focused on malignancies with RAS mutation, such as lung and pancreatic cancers. The inconsistency in RAL function across various cancer types illustrates the critical need to thoroughly evaluate their contribution and regulation in cancers. RALA and RALB share 82% structural similarity (Richardson *et al.*, 2022), are both involved in cancer progression but have distinctly different cellular functions (Richardson *et al.*, 2022). Multiple studies suggest RALB is majorly involved in tumor invasion and metastatis and RALA is majorly involved in tumor growth (Ward *et al.*, 2001; Falsetti *et al.*, 2007; Male *et al.*, 2012; Neel *et al.*, 2012; Wang *et al.*, 2013; Thies *et al.*, 2021). This could, in part, be mediated by the differential regulation of RAL activation by RALGEFs or their localization. For RALA this could be mediated by its phosphorylation at the serine194 residue or post-translational modifications at its C-terminal domain.

The best way to establish and understand the pS194 mediated regulation of RALA would be to make cancer cell lines with RALA that can (expressing WT-RALA) or cannot (expressing S194A-RALA mutant) be phosphorylated. This will also allow us to bypass inconsistencies in the extent of phosphorylation physiological kinases acting on S194 phosphorylation might have. While AURKA might be the major mediator of this phosphorylation a role for other kinases (like PKA) (Neel *et al.*, 2014)cannot be ruled out when investigating its role in RALA function. Mutants will overcome this limitation focusing instead on how complete phosphorylation (S194D) or lack thereof (S194A) affects RALA function and tumorigenesis.

These studies will first require stable knockdown (KD) or knockout (KO) of endogenous RALA in cancer cells, which can then be reconstituted with RALA (WT/S194A/S194D) mutants. This KD or KO of RALA could be achieved using siRNA, shRNA, or CRISPR-Cas9 system. Although RNAi provides flexibility in making transient knockdowns, off-target effects have been a growing concern. Recent studies have shown that imperfect matches between mRNA 3'-UTR and siRNA can induce silencing by translational repression and/or degradation (Jackson *et al.*, 2006; Carthew and Sontheimer, 2009; Sigoillot and King, 2011). Since siRNA and shRNA interfere with endogenous RNAi systems governed by microRNAs, flooding the system with exogenous siRNA can dislocate microRNAs from the RISC complex. It can thus impair the functions of endogenous microRNA, leading to changes in transcription (Khan *et al.*, 2009). Also, incomplete silencing is possible with RNAi, and residual protein can always interfere with the phenotype observed. The development of CRISPR-Cas9 allows for the silencing of genes at the DNA level. Since CRISPR works on the DNA level, enable us to generate complete loss of function (LOF) or null phenotype. Like RNAi, CRISPR-Cas9 also shows off-target binding. Mismatches in the seed region of sgRNA and PAM sites are essential in determining the specificity of Cas9 (Cong *et al.*, 2013; Hsu *et al.*, 2013). While non-specific binding of dCas9 or Cas9 appears to be a concern, it should be noted that its function (activation/silencing/ds breaks) depends on its genomic location and the sgRNA sequence used (Gilbert *et al.*, 2014; Frock *et al.*, 2015; Tsai *et al.*, 2015). Considering everything we know, a recent study showed that RNAi has much more significant off-target effects than CRISPR-Cas9 (Smith *et*

al., 2017). Also, since CRISP-Cas9 ideally leaves no residual endogenous protein that could interfere with overexpressed mutants. This, again, makes it the preferred choice for our KO and reconstitution studies. However, only one previous study in MDA MB 231 uses CRISP-Cas9 KO of RALA to study its function (Thies *et al.*, 2021).

To make a RALA KO in cancer cell lines using CRISPR-Cas9, we began by selecting the exons for targeting using sgRNA. Choosing a target region is vital to get a clean and consistent KO in multiple cancer cell lines. We selected the target region based on the openness of chromatin structure (based on DNAse1 sensitivity), the presence of exon in all splice variance and the role of that exon in coding for the functional part of the protein. This strategy has been used previously to make a clean KO (Ran et al., 2013), and with this, we were able to get clean RALA KO in multiple cancer cell lines. We also designed and used multiple sgRNAs to increase the probability of getting dsDNA breaks to get RALA KO. Two sgRNAs were designed against exon 2, and one against exon 4. Genotyping showed all (MCF7, T24, UMUC3 and MiaPaCa2) cell lines had a cut in exon 2 while only MCF7 and MiaPaCa2 had a cut in exon 4, indicating designing at least two sgRNAs does increase the probability of Cas9 making dsDNA breaks. In SKOV3 cells, despite clean detectable loss of RALA in western blot studies, genotyping PCR data failed to detect amplicons of expected size for exon 2 and exon 4. These amplifications were done using primers designed to bind intron-exon boundaries of exon 2 and exon 4, respectively. The same primers were used and seen to work well for all other cell lines, making a lack of amplification in SKVO3 unlikely to be due to issues with design of primers. Additional new primers were also designed for exon2 and exon 4 to be tested in SKOV3. They also failed to give a detectable amplicon in genotyping PCR (data not shown). Why this happens repeatedly in SKOV3 cells only is still unclear to us, but it made the RALA KO SKOV3 cells unsuitable for use in our study.

While RALA KO in cells is genotypically authenticated for MCF7, T24, UMUC3 and MiaPaCa2, there are concerns about the impact this has on genes and pathways closely associated with RALA. To help address this, we confirmed western blot detection of the levels of a panel of proteins related to RALA that are of interest for this

study (RALB, AURKA, AURKB, ERK, AKT, AMPK). We also checked to see if the activation status of (RALB, AURKA, AURKB, ERK, AKT, AMPK) is altered by the loss of RALA. Except for RALB showing a slight increase, no significant change in the basal activation status of these proteins was observed. RALA KD not having any significant effect on other signaling pathways has been previously reported in myeloma cells (Seibold *et al.*, 2020). Similarly, shRNA-mediated RALA KD or RALA inhibition by GGTI-2147 did not affect the expression of Erk, PDI, Calnexin, Exo84, PERK and other proteins (Balasubramanian et al., 2010; Ginn et al., 2016; Sowalsky et al., 2010).

CRISPR-Cas9 KO of RALA in MDA MB 231 cells reported earlier in the literature showed that RALA KO increases RALB expression (Thies et al., 2021). No such increase in RALB levels was observed in our study, but we did see a modest increase in RALB activation. It thus provides us with stable RALA lacking cancer cells suited for evaluation and reconstitution.

8.2 pS194 RALA detection in western using anti-phospho-RALA Antibody (Ser194) (Merck-Millipore, Cat no- 07-2119) is different in RAS-independent and RAS-dependent cancer cells

To study the regulation and function of RALA S194 phosphorylation in cancer cells, it is crucial to detect this phosphorylation. anti-phospho-RALA Antibody (Ser194) (Merck-Millipore, Cat no- 07-2119) is the only commercially available antibody to detect RALA S194 phosphorylation in western blot studies. Many studies have used this antibody to understand the regulation of RALA S194 phosphorylation in cells. However, few inconsistencies have been observed in pS194 RALA detection using this antibody. When used in PANC1 cells, the band detected by the pS194 RALA antibody continued to be detected even upon RALA KD (Neel *et al.*, 2014). Also, AURKA inhibition using MLN8237 in multiple cancer cell lines did not affect pS194 RALA detection (Neel *et al.*, 2014). This suggests that careful evaluation of this antibody to confirm its specificity could be vital to understanding this phosphorylation, its regulation, and its role in cancers.

Probing of the RALA knockout RAS-dependent cancer cell line (T24, UMUC3 and MiaPaCa2) lysates using the anti-phospho-RALA Antibody (Ser194) shows it continues to detect a band of similar size and intensity as the control cells. This strongly supported our view that this antibody likely detects a non-specific band in these lysates. V_{MLN} mediated AURKA inhibition in these cells also does not visibly affect this detection, neither does the siRNA mediated knockdown of RALA. Together they make a strong case for this antibody being non-specific in these cell types. Interestingly under similar conditions, pS194 RALA antibody detects a band of the expected size in RAS-independent cancer cell lines (MCF7 and SKOV3) that is lost on RALA knockout and in V_{MLN} mediated AURKA inhibition. This hence suggests the lack of specificity for this antibody could be variable, and cell-type specific. Could this lack of specificity have something to do with the expression of RAS in cancer cells? As our data seems to suggest, this remains an open question. Expression of oncogenic RAS in RAS-independent cancers could help address this. The non-specific protein being detected as a phospho-protein whose levels might be differentially modulated in RAS-dependent cancers may be one likely explanation. This may not just account for the variable results in some cancers (like PANC1 - (Neel *et al.*, 2014)), but also impact our understanding of the regulation and role of pS194RALA (Neel *et al.*, 2014). What protein is non-specifically detected by anti-phospho-RALA Antibody (Ser194) in RAS-dependent cancer cell lines remains to be established and will be a vital question to address. Immunoprecipitation using pS194 RALA antibody in RAS-independent and RAS-dependent cancer cells combined with LC-MS would help us identify this non-specific target.

8.3 AURKA-RALA crosstalk to regulate RALA activation, localization and AIG is variable in normal and cancer cells

In evaluating the AURKA-RALA crosstalk in normal cells (WTMEFs), RAS-independent (MCF7 and SKOV3) and RAS-dependent (T24, UMUC3 and MiaPaCa2) cancer cells our studies show V_{MLN} mediated inhibition of AURKA does affect RALA activation and function variably. V_{MLN} in RAS-independent cancer cell lines (MCF7 and SKOV3) and WTMEFs showed it can affect pS194 RALA phosphorylation suggesting the AURKA-RALA crosstalk to be function here. However, this crosstalk variably affects RALA activation and function (AIG) in MCF7 and SKOV3 cells,

suggesting this role and regulation could be affected by changes beyond just this phosphorylation. In MCF7 cell tumor formation, RALA and its S194 phosphorylation are both found to be required. Some of this could depend on the tissue type from which these cells are derived. MCF7 and SKVO3, with comparable effects on RALA phosphorylation but variable effects on RALA activation and anchorage-independent growth, could provide an attractive system to test and compare the regulation and outcome of AURKA-RALA crosstalk. Stable reconstitution of RALA KO cells with WT vs S194A RALA mutants could offer a direct way for testing this. While we have not successfully made genotype verified SKVO3 RALA KO cells, trying to get these made and reconstituted will be useful for such a comparative study.

Since we don't see an effect of S194A mutation on RALA activation in MCF7 and MiaPaC2 cells but see a significant inhibition of tumor growth, we can speculate the role this phosphorylation in regulating RALA function in tumor formation may stem from its effect on RALA localization. Study in HEKTtH RALA knockdown cells reconstituted with WT-RALA vs S194-RALA mutant suggest a change in their localization to internal membranes, also seen in fractionation studies. This study also indicate that S194 phosphorylation can influence the interaction of RALA with downstream effector molecules such as RALBP1 (Lim *et al.*, 2010), which could affect its role in tumorigenesis. Kashatus et. al. also showed that RALA and RALBP1 localize to the mitochondria and this localization is dependent on S194 phosphorylation (Kashatus *et al.*, 2011). In this study, we found that in MCF7 cells, RALA S194 mutant indeed showed distinctly different localization as compared to WT-RALA. This localization can regulate tumor growth in the absence of major changes in WT vs S194 RALA activation. One possibility is this change in RALA localization may change the nature in which RALA interact with its downstream effectors as observed previously with RALA S194D mutant in HEKTtH cells that localizes in internal membrane and shows increased interaction with RalBP1 (Lim et al. 2010).

V_{MLN} treatment in all RAS-dependent cancer cell lines we tested, T24, UMUC3 and MiaPaCa2, did not affect RALA activation but affected AIG in MiaPaCa2 cells. This could suggest this effect might be AURKA dependent but RALA independent. If

AURKA does regulate RALA phosphorylation in these cells, which we are limited in detecting with the anti-pS194RALA antibody currently available, this crosstalk could contribute to its effect on AIG and tumorigenesis. In MiaPaCa2 cell tumor formation, RALA and its S194 phosphorylation are both found to be required.

In WTMEFs expressing human RALA, V_{MLN} treatment showed a distinct drop in its pS194 RALA levels. V_{MLN} also inhibits endogenous RALA activity and RALA dependent early cell spreading. Together, they suggest the presence of an AURKA-RALA crosstalk that affects RALA function, as seen in SKOV3 cells. The possible role RALGEFs could have in this regulatory pathway could be worth testing in WTMEFs, as discussed later.

8.4 AURKA mediated Regulation of RALA: What do the RALA S194 phosphorylation mutants reveal?

As discussed above there does seem to be much variability in how AURKA regulates RALA activation and function. This is complicated because the detection of pS194RALA phosphorylation might also be plagued by specificity issues across cell types. Stable RALA KO with stable reconstitution with WT RALA vs S194A RALA vs S194D RALA mutants might be the best way to test what this phosphorylation means to cells and tumors. Based on our understanding, this needs to be a cell-type-specific evaluation. Even though we have been able to do this for only two (MCF7 and MiaPaCa2) of the five cancer cell lines we have explored, this data carries significant relevance for our and other studies. Such an evaluation might also be needed to develop a consensus on what this phosphorylation site does for RALA and RALA-dependent tumorigenesis.

Our finding shows that when compared to WTRALA reconstituted cells, RALA S194A mutation did not affect RALA activation in MCF7 and MiaPaCa2 cells. Considering that the pS194 RALA antibody works in MCF7 cells, V_{MLN} mediated inhibition of this phosphorylation and its lack of any effect on RALA activation agree with what the

phospho-mutant shows. Could this be the 'real' phospho-RALA phenotype we have sought?

In earlier studies, the expression of kinase-dead AURKA reduces RALA activation (NIH3T3 and MDCK cells) (Wu *et al.*, 2005). In HEK2393 cells WT AURKA expression increases RALA S194 phosphorylation and activation (Lim, Donita C. Brady, *et al.*, 2010), while overexpression of kinase-active AURKA^{Thr288} increases RALA S194 phosphorylation without affecting RALA activation (Lim, Donita C. Brady, *et al.*, 2010). This suggests that the nature of AURKA activation (its kinetics and localization) and the resulting regulation of RALA S194 phosphorylation may affect its activation differently. The nature of AURKA activation could also impact additional regulatory pathways, like its possible regulation of a RALGEF, to affect RALA activation. *In-vitro* kinase assays have shown the phosphorylation of RalGDS by AURKA (Wu et al., 2005), which could regulate RALA activation and function. A similar regulation by AURKA of RALGEF, RGL1, as suggested in our studies, may hence not be too speculative.

While the role of RALA in tumor formation is well-established in the literature, how RALA S194 phosphorylation affects tumorigenesis is expectedly more variable (Lim et al., 2010). The only known study testing this uses RALA knockdown pancreatic cancer cells (CFPac-1, HPAC, Capan1) reconstituted with WT-RALA or S194A-RALA mutant. This showed loss of RALA affects tumor formation, which is restored by WT-RALA reconstitution in all 3 cell types. S194A-RALA mutant, however, had variable cell type specific effects. In Capan-1 and HPAC tumors, phosphorylation was required for tumor formation. In CFPac-1, phosphorylation was NOT needed for tumor formation (Lim et al., 2010). In our study in both MCF7 and MiaPaCa2, phosphorylation was required for tumor formation. A consolidated figure comparing data from Lim et al. with data from these studies highlights the cell type nature of this regulation across cancers (Figure 8.1). All of these cells, except MCF7, express oncogenic RAS, further supporting the S194 RALA-mediated regulation of tumorigenesis to be RAS-independent. It is also worth noting that when compared to RALA KO, the S194A tumors are comparable in size in some (Capan-1 and MiaPaCa2) and slightly bigger

in others (HPAC and MCF7). The similarities in the nature of this regulation between their and our study are hence striking.

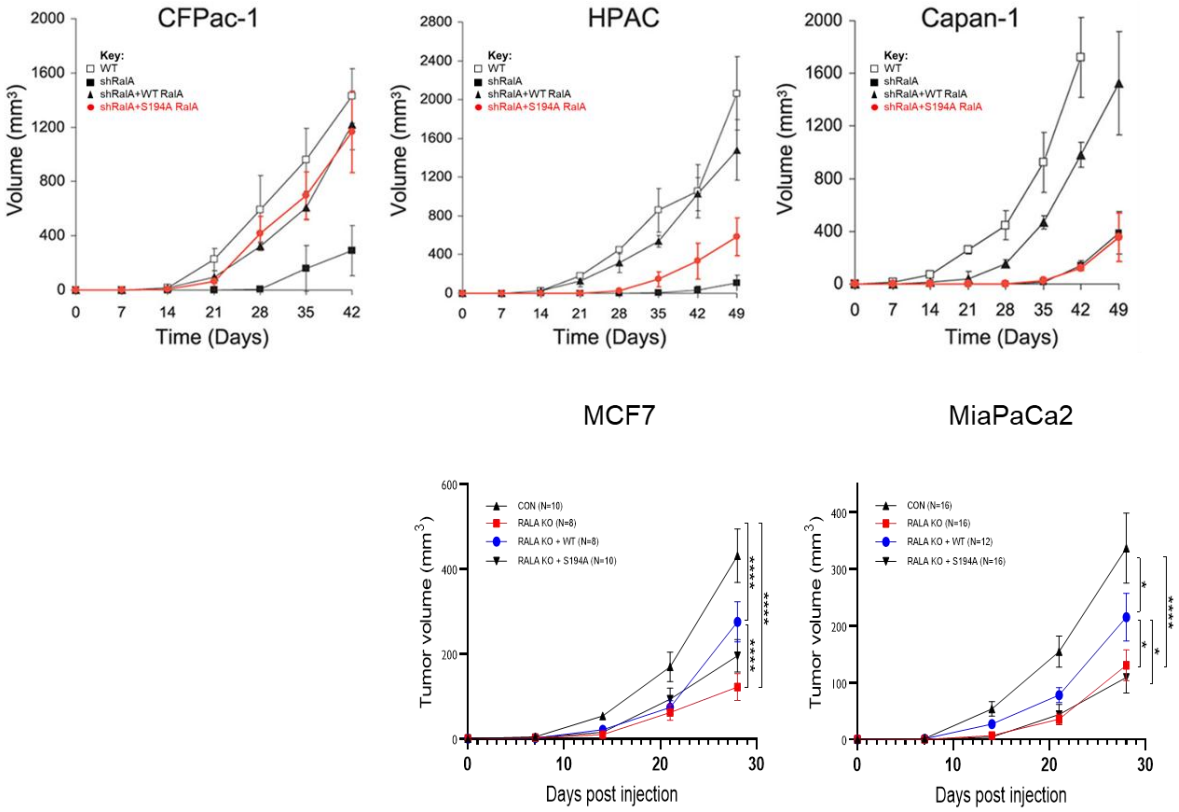

Figure 8.1: Variable role of RALA S194 phosphorylation in regulating tumor formation in cancer cells. This figure represents the variation in role of RALA S194 phosphorylation in regulating tumor formation by CFPac-1, HPAC, Capan-1 (adapted from Lim et al. 2010), MCF7 and MiaPaCa2.

In our studies, the RALA S194D mutant doesn't effectively mimic phosphorylation. Its effect on MCF7 and MiaPaCa2 tumors is comparable to S194A and RALA KO. We have also looked at RALA activation for these mutants and seen no effect of the S194A or S194D mutant on RALA activation in both MCF7 and MiaPaCa2 cells. Lim et al. are testing the S194D mutant in non-transformed HEKTtH cells and have reported its behavior to be similar to S194A mutants in regulating RALA activation (Lim et al., 2010). They both have a marginal effect on RALA activation that hasn't been quantitated in the study (Lim *et al.*, 2010). Hence, both these studies suggest that the

S194D mutant may not be relevant to evaluating the role of this phosphorylation in RALA function.

Since we don't see an effect of S194A mutation on RALA activation in MCF7 and MiaPaC2 cells but see a significant inhibition of tumor growth, we can speculate the role this phosphorylation could have in tumor formation may stem from its effect on RALA localization. Studies in HEKTtH RALA knockdown cells reconstituted with WTRALA vs S194RALA mutant suggest a change in their localization to internal membranes, also seen in fractionation studies. These studies also indicate that S194 phosphorylation can influence the interaction of RALA with downstream effector molecules such as RALBP1 (Lim *et al.*, 2010), which could affect its role in tumorigenesis. LC-MS evaluation of binding partners for WT vs S194A mutant probing for downstream effectors that they differentially bind could have valuable clues for what regulatory pathways they target based on their localization to affect tumor growth.

Thus, despite the complex nature of its regulation, the need for Serine-194 phosphorylation of RALA to support tumor formation is evident. The schematic in Fig 8.2 represents the AURKA-RALA regulatory pathway in cancer cells. This regulation and its implications for tumorigenesis might be cell type specific. The role AURKA or other kinases have in mediating this phosphorylation needs careful evaluation, which may be limited by the availability of pS194 RALA-specific antibody. Since S194 phosphorylation is vital for RALA-dependent tumor formation, targeting this site can also carry therapeutic advantages. Could AURKA targeting be an effective way to block RALA-dependent tumor growth is a question worth addressing.

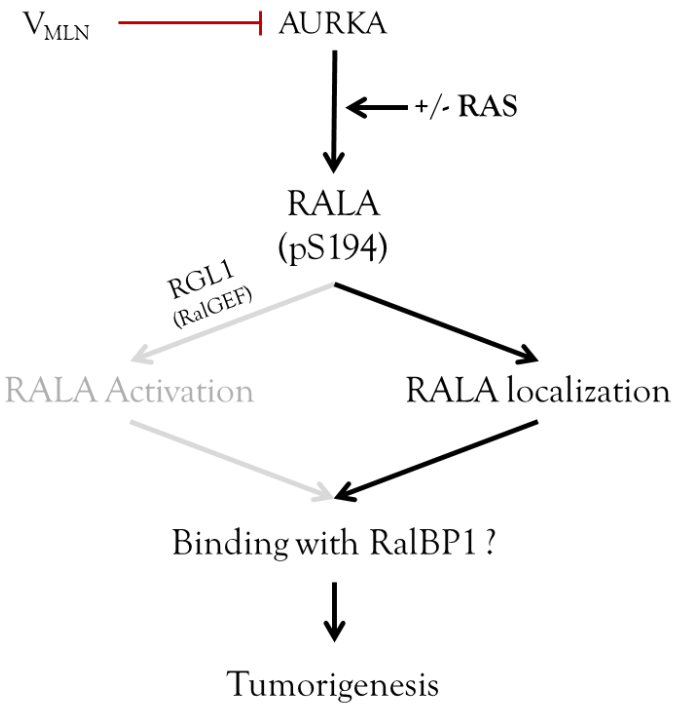

Figure 8.2: Schematic representing the AURKA-RALA regulatory pathway in cancer cells

Conclusion

The work carried out in my thesis has helped us understand the role and regulation of RALA and its S194 phosphorylation in normal and cancer cells. Our major finding was that AURKA-RALA crosstalk exists (in the form of RALA S194 phosphorylation) in normal and RAS-independent cancer cells. However, it may not always regulate RALA activation and RALA function depending on the cell type. This regulation does seem to be independent of oncogenic RAS. Further, this study confirmed S194 phosphorylation to be required in tumorigenesis and this could be independent of RALA activation, possibly regulated by its spatial localization which could affect effector interaction. Finally, AURKA-RALA crosstalk may not be limited to RALA S194 phosphorylation but also involves interaction between AURKA and RALGEFs (RGL1 in the case of WTMEFs), which could regulate RALA function. Understanding the AURKA-RALA crosstalk could further have implications for targeting S194 phosphorylation to disrupt tumor growth in RALA-dependent cancers, which our ongoing studies are exploring.

Annexure 1

Preliminary studies to evaluate the stability, uptake and biodistribution of nanoparticles for delivery of MLN8237 in *in-vitro* and *in-vivo* model

Use of V_{MLN} to study AURKA-RALA crosstalk by inhibiting AURKA showed that nanovesicle mediated delivery of MLN8237 is efficient way to target AURKA in cancer cells. We wanted to further extend this study to animal model to target tumors using V_{MLN}. However, the V_{MLN} nanovesicle's delivery of MLN8237 in mice is limited by the loading of MLN8237 in these nanovesicles. Multiple attempts over the last few years were made to improve loading efficiency in these nanovesicles, as a collaborative project with Prof. Jayakannan's Lab. The best efficiency achieved using V_{MLN} was about 0.5% of MLN8237. Administering 10mg/KG of MLN8237 will require ~50mg of the nanovesicle (consider the 0.5% loading). The solubility of the nanovesicle makes it impossible to dissolve ~50mg of it in ~125ul of PBS for administering to mice in these studies. This severely limits the use of MLN8237-loaded nanovesicle (V_{MLN}) for studies in mice.

To overcome this limitation, we collaborated with Dr. Jayakannan's lab to test the ability of a new star-shaped unimolecular micelle developed in their lab to load MLN8237. After testing various combinations of polymer to feed ratio, we were able to increase drug loading capacity up to 4% (data not shown) which was 8 times higher than V_{MLN}. Later we loaded nanoparticles with IR780 dye (NP-IR780) which allowed us to evaluate its uptake and targeting in mice with tumors. The making of this MLN loaded and IR780 loaded nanoparticles is work by Kajal Singh a graduate student from the lab and will feature in her thesis. I am hence not discussing the same in detail here and sharing just the preliminary experiments that I have done to evaluate the uptake of the NP-IR780. IR780 dye was chosen for this study to allow us to visualize the uptake and targeting of the NP in mice.

Ax.1 : Materials and method

Tumorigenesis assay in NOD-SCID mice

To evaluate the stability and localization of nano-particles in tumors, we did xenograft assay in an equal number of male and female NOD-SCID mice. 1 x 10^6 cells of were injected subcutaneously in 5-6 week-old mice. Mice were observed over 4-5 weeks, and mice weight and tumor size were measured weekly. Once the tumor size grew up to 100mm^3, we injected mice with empty nanoparticles, free IR780 dye and nanoparticles loaded with IR780 dye with final dose concentration of 0.5mg/KG by either IP or IV injections. *In-vivo* imaging was performed every 24 hrs (excitation wavelength – 735nm for IR780).

Ax.2: Results and discussion

To test which mode of delivery was suitable for these nanoparticles, we injected NOD-SCID mice having MCF7 tumors of around 100 mm^3 size with nanoparticles loaded with IR780 (NP-IR780) by IV (intravenous) and IP (intraperitoneal) and free IR780 by IV only. We found that 48hrs after injection both free IR780 and NP-IR780 localizes to tumors (Fig Ax3 A), however, the accumulation of NP-IR780 in tumors was much higher as compared to free IR780 (Fig Ax1 B). Also, among IV and IP injections, IP performed slightly better than IV in terms of accumulation of IR780 in tumors (Fig Ax1 B).

Further, to check the stability of these nanoparticles, we injected PBS, free IR780 and NP-IR780 by IP injection only into NOD-SCID mice having MiaPaCa2 tumors of around 100 mm^3 size. Equal number of male and female mice were used for this study. We looked at IR780 localization in tumors over 10 days and found that mice injected with NP-IR780 had high IR780 retention over time (Fig Ax2 A, B). We harvested the tumor at the end of assay and compared the IR780 accumulation and as expected, NP-IR780 treated tumors had more IR780 as compared to free IR780 treated tumors. The size of tumors in both mice were largely comparable. Overall, these preliminary studies show that mice do tolerate these Nanoparticles well and they are targeted and retained in tumors reasonably well to tested for using MLN8237 containing nanoparticle to target AURKA in-vivo. This work is being continued by Kajal Singh in the lab as part of her PhD.

(A)

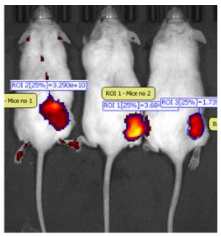

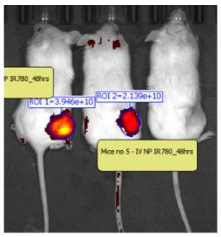

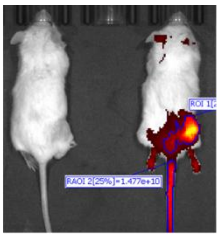

Mice no	1	2	3	4	5	6	7	8
Gender	M	M	M	F	F	F	M	M
Tumor size (mm^3)	95	109	76	107	297	141	37	10
Treatment	NP IR780	NP IR780	Free IR780	NP IR780	NP IR780	Empty NP	Empty NP	Free IR780
Mode of injection	IP	IV	IV	IP	IV	IV	IV	IV
Time post injections (hrs)	24	48	48	48	48	48	48	24

(B)

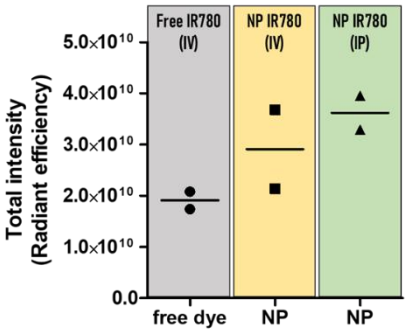

Figure Ax1: NP_{IR780} uptake and biodistribution in MCF7 tumours. (A) MCF7 tumour containing NOD-SCID mice were administered an intraperitoneal or intravenous injection of PBS, Free IR780 and NP_{IR780} and the distribution of the dye monitored for 48 hours. Upper panel represents *in-vivo* images showing biodistribution of IR780 and lower table showing experimental details. Tumours showed significantly better uptake and retention of Nanoparticle. (B) The graph represents mean of total intensity data from 2 independent mice.

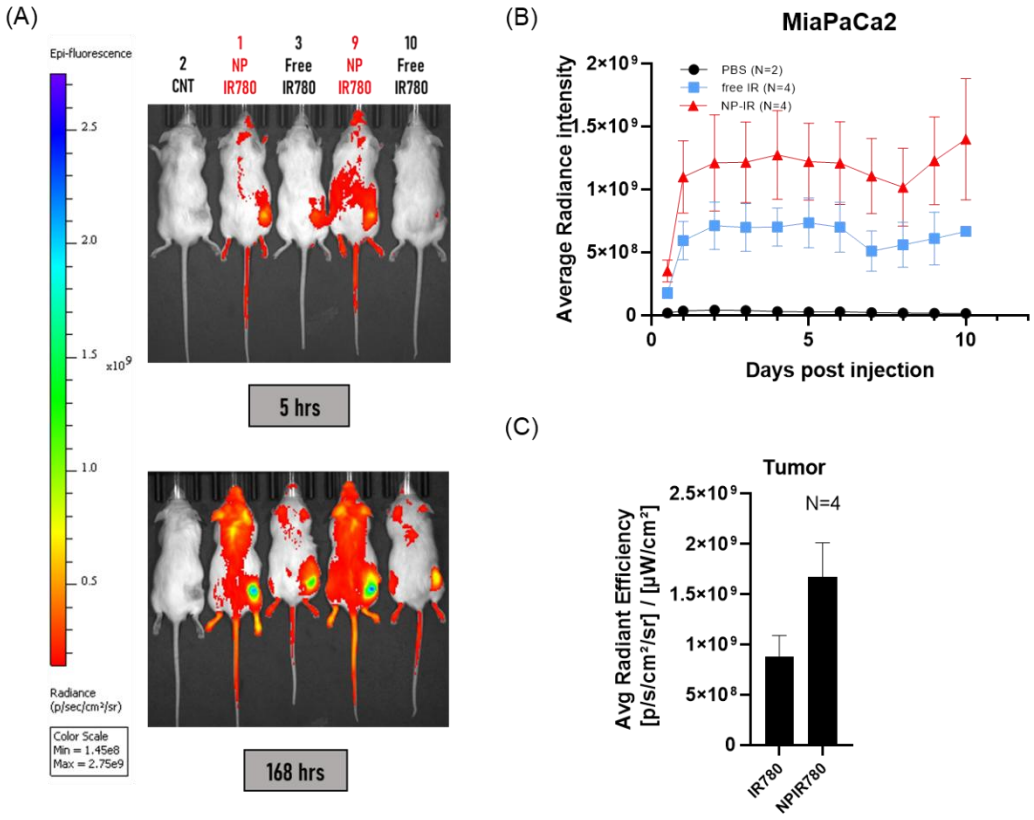

Figure Ax2: NP_{IR780} stability and biodistribution in MiaPaCa2 tumours

(A) MiaPaCa2 tumour containing NOD-SCID mice were administered an intraperitoneal injection of PBS, Free IR780 and NP_{IR780} and the distribution of the dye monitored for 168 hours. Tumours showed significantly better uptake and retention of Nanoparticle over the time. (B) The graph represents mean of average radiance intensity data from 4 independent mice (2 independent mice for PBS control). (C) The graph represents mean ± SE data from 4 independent mice. Statistical analysis was done using Mann Whitney test, and if significant, p values are represented in the graph (* $p < 0.05$, ** $p<0.01$, *** $p<0.001$, **** $p<0.0001$).

References:

1. Altman, B.J., Stine, Z.E. and Dang, C. V. (2016) 'From Krebs to clinic: Glutamine metabolism to cancer therapy', *Nature Reviews Cancer*. Available at: https://doi.org/10.1038/nrc.2016.71.

2. Awasthi, S. *et al.* (2001) 'Functional reassembly of ATP-dependent xenobiotic transport by the N- and C-terminal domains of RLIP76 and identification of ATP binding sequences', *Biochemistry*, 40(13). Available at: https://doi.org/10.1021/bi002182f.

3. Bache, K.G., Slagsvold, T. and Stenmark, H. (2004) 'Defective downregulation of receptor tyrosine kinases in cancer', *EMBO Journal*. Available at: https://doi.org/10.1038/sj.emboj.7600292.

4. Baker, R. *et al.* (2013) 'Site-specific monoubiquitination activates Ras by impeding GTPase-activating protein function', *Nature Structural and Molecular Biology*, 20(1). Available at: https://doi.org/10.1038/nsmb.2430.

5. Balasubramanian, N. *et al.* (2010) 'RalA-exocyst complex regulates integrin-dependent membrane raft exocytosis and growth signaling.', *Current Biology*, 20(1), pp. 75–79. Available at: https://doi.org/10.1016/j.cub.2009.11.016.

6. Bar-Sagi, D. and Feramisco, J.R. (1985) 'Microinjection of the ras oncogene protein into PC12 cells induces morphological differentiation', *Cell*, 42(3). Available at: https://doi.org/10.1016/0092-8674(85)90280-6.

7. Bartkova, J. *et al.* (2005) 'DNA damage response as a candidate anti-cancer barrier in early human tumorigenesis', *Nature*, 434(7035). Available at: https://doi.org/10.1038/nature03482.

8. Benito, M. *et al.* (1991) 'Differentiation of 3T3-L1 fibroblasts to adipocytes induced by transfection of ras oncogenes', *Science*, 253(5019). Available at: https://doi.org/10.1126/science.1857988.

9. De Berardinis, R.J. and Chandel, N.S. (2016) 'Fundamentals of cancer metabolism', *Science Advances*. Available at: https://doi.org/10.1126/sciadv.1600200.

10. Berndt, N., Hamilton, A.D. and Sebti, S.M. (2011) 'Targeting protein prenylation for cancer therapy', *Nature Reviews Cancer*. Available at: https://doi.org/10.1038/nrc3151.

11. Berrier, A.L. and Yamada, K.M. (2007) ‘Cell-matrix adhesion.’, *Journal of Cellular Physiology*, 213(3), pp. 565–573. Available at: https://doi.org/10.1002/jcp.21237.

12. Bister, K. and Duesberg, P.H. (1979) ‘Structure and specific sequences of avian erythroblastosis virus RNA: Evidence for multiple classes of transforming genes among avian tumor viruses’, *Proceedings of the National Academy of Sciences of the United States of America*, 76(10). Available at: https://doi.org/10.1073/pnas.76.10.5023.

13. Bister, K. and Jansen, H.W. (1986) ‘Oncogenes in retroviruses and cells: Biochemistry and molecular genetics’, *Advances in Cancer Research*, 47(C). Available at: https://doi.org/10.1016/S0065-230X(08)60199-2.

14. Bivona, T.G. *et al.* (2006) ‘PKC regulates a farnesyl-electrostatic switch on K-Ras that promotes its association with Bcl-XL on mitochondria and induces apoptosis’, *Molecular Cell*, 21(4). Available at: https://doi.org/10.1016/j.molcel.2006.01.012.

15. Buck, M.D.D. *et al.* (2016) ‘Mitochondrial Dynamics Controls T Cell Fate through Metabolic Programming’, *Cell*, 166(1). Available at: https://doi.org/10.1016/j.cell.2016.05.035.

16. Buhrman, G. *et al.* (2011) ‘Analysis of binding site hot spots on the surface of Ras GTPase’, *Journal of Molecular Biology*, 413(4). Available at: https://doi.org/10.1016/j.jmb.2011.09.011.

17. Burgering, B.M.T. and Coffer, P.J. (1995) ‘Protein kinase B (c-Akt) in phosphatidylinositol-3-OH kinase signal transduction’, *Nature*. Available at: https://doi.org/10.1038/376599a0.

18. Burnet, M. (1957) ‘Cancer--A Biological Approach: I. The Processes Of Control. II. The Significance of Somatic Mutation’, *BMJ*, 1(5022). Available at: https://doi.org/10.1136/bmj.1.5022.779.

19. Carmeliet, P. (2000) ‘Mechanisms of angiogenesis and arteriogenesis’, *Nature Medicine*. Available at: https://doi.org/10.1038/74651.

20. Carmeliet, P. and Jain, R.K. (2000) ‘Angiogenesis in cancer and other diseases’, *Nature*. Available at: https://doi.org/10.1038/35025220.

21. Carthew, R.W. and Sontheimer, E.J. (2009) ‘Origins and Mechanisms of miRNAs and siRNAs’, *Cell*, pp. 642–655. Available at: https://doi.org/10.1016/j.cell.2009.01.035.

22. Casalou, C., Ferreira, A. and Barral, D.C. (2020) ‘The Role of ARF Family Proteins and Their Regulators and Effectors in Cancer Progression: A Therapeutic Perspective’, *Frontiers in Cell and Developmental Biology*. Available at: https://doi.org/10.3389/fcell.2020.00217.

23. Cekan, P. *et al.* (2016) ‘RCC1-dependent activation of Ran accelerates cell cycle and DNA repair, inhibiting DNA damage-induced cell senescence’, *Molecular Biology of the Cell*, 27(8). Available at: https://doi.org/10.1091/mbc.E16-01-0025.

24. Chardin, P. and Tavitian, A. (1986) ‘The ral gene: a new ras related gene isolated by the use of a synthetic probe.’, *The EMBO journal*, 5(9). Available at: https://doi.org/10.1002/j.1460-2075.1986.tb04485.x.

25. Chua, C.E.L. and Tang, B.L. (2015) ‘The role of the small GTPase Rab31 in cancer’, *Journal of Cellular and Molecular Medicine*, 19(1). Available at: https://doi.org/10.1111/jcmm.12403.

26. Clough, R.R., Sidhu, R.S. and Bhullar, R.P. (2002) ‘Calmodulin binds RalA and RalB and is required for the thrombin-induced activation of Ral in human platelets.’, *The Journal of biological chemistry*, 277(32). Available at: https://doi.org/10.1074/jbc.M201504200.

27. Cong, L. *et al.* (2013) ‘Multiplex genome engineering using CRISPR/Cas systems’, *Science*, 339(6121). Available at: https://doi.org/10.1126/science.1231143.

28. Cooper, G.M. (2000) ‘The Cell: A Molecular Approach. 2nd edition - Intermediate Filaments’, *Sinauer Associates* [Preprint].

29. Cox, A.D. *et al.* (2014) ‘Drugging the undruggable RAS: Mission possible?’, *Nature Reviews. Drug Discovery*, 13(11), pp. 828–851. Available at: https://doi.org/10.1038/nrd4389.

30. Cox, A.D., Der, C.J. and Philips, M.R. (2015) ‘Targeting RAS Membrane Association: Back to the Future for Anti-RAS Drug Discovery?’, *Clinical Cancer Research*, 21(8), pp. 1819–1827. Available at: https://doi.org/10.1158/1078-0432.CCR-14-3214.

31. Craene, B. De and Berx, G. (2013) ‘Regulatory networks defining EMT during cancer initiation and progression’, *Nature Reviews Cancer*. Available at: https://doi.org/10.1038/nrc3447.

32. Crosas-Molist, E. *et al.* (2022) ‘RHO GTPase SIGNALING IN CANCER PROGRESSION AND DISSEMINATION’, *Physiological Reviews*. Available at: https://doi.org/10.1152/physrev.00045.2020.

33. Croucher, P.I., McDonald, M.M. and Martin, T.J. (2016) ‘Bone metastasis: The importance of the neighbourhood’, *Nature Reviews Cancer*. Available at: https://doi.org/10.1038/nrc.2016.44.

34. Culp, L.A. *et al.* (1998) ‘Earliest steps in primary tumor formation and micrometastasis resolved with histochemical markers of gene-tagged tumor cells’, in *Journal of Histochemistry and Cytochemistry*. Available at: https://doi.org/10.1177/002215549804600501.

35. Davis, J.E. *et al.* (2016) ‘ARF1 promotes prostate tumorigenesis via targeting oncogenic MAPK signaling’, *Oncotarget*, 7(26). Available at: https://doi.org/10.18632/oncotarget.9405.

36. Diori Karidio, I. and Sanlier, S.H. (2021) ‘Reviewing cancer’s biology: an eclectic approach’, *Journal of the Egyptian National Cancer Institute*. Available at: https://doi.org/10.1186/s43046-021-00088-y.

37. Donnem, T. *et al.* (2013) ‘Vessel co-option in primary human tumors and metastases: An obstacle to effective anti-angiogenic treatment?’, *Cancer Medicine*. Available at: https://doi.org/10.1002/cam4.105.

38. Duesberg, P.H., Bister, K. and Vogt, P.K. (1977) ‘The RNA of avian acute leukemia virus MC29’, *Proceedings of the National Academy of Sciences of the United States of America*, 74(10). Available at: https://doi.org/10.1073/pnas.74.10.4320.

39. Duesberg, P.H. and Vogt, P.K. (1970) ‘Differences between the ribonucleic acids of transforming and nontransforming avian tumor viruses.’, *Proceedings of the National Academy of Sciences of the United States of America*, 67(4). Available at: https://doi.org/10.1073/pnas.67.4.1673.

40. Dunn, G.P. *et al.* (2002) ‘Cancer immunoediting: From immunosurveillance to tumor escape’, *Nature Immunology*. Available at: https://doi.org/10.1038/ni1102-991.

41. Falsetti, S.C. *et al.* (2007) ‘Geranylgeranyltransferase I Inhibitors Target RalB To Inhibit Anchorage-Dependent Growth and Induce Apoptosis and RalA To Inhibit Anchorage-Independent Growth’, *Molecular and Cellular Biology*, 27(22). Available at: https://doi.org/10.1128/mcb.00057-07.

42. Faubert, B., Solmonson, A. and DeBerardinis, R.J. (2020) ‘Metabolic reprogramming and cancer progression’, *Science*. Available at: https://doi.org/10.1126/science.aaw5473.

43. Fernández-Medarde, A., De Las Rivas, J. and Santos, E. (2021) ‘40 years of RAS-a historic overview’, *Genes*, 12(5). Available at: https://doi.org/10.3390/genes12050681.

44. Fouad, Y.A. and Aanei, C. (2017) ‘Revisiting the hallmarks of cancer’, *American Journal of Cancer Research*.

45. Fraisl, P. *et al.* (2009) ‘Regulation of Angiogenesis by Oxygen and Metabolism’, *Developmental Cell*. Available at: https://doi.org/10.1016/j.devcel.2009.01.003.

46. Fritz, G. and Henninger, C. (2015) ‘Rho gtpases: Novel players in the regulation of the DNA damage response?’, *Biomolecules*. Available at: https://doi.org/10.3390/biom5042417.

47. Frock, R.L. *et al.* (2015) ‘Genome-wide detection of DNA double-stranded breaks induced by engineered nucleases’, *Nature Biotechnology*, 33(2). Available at: https://doi.org/10.1038/nbt.3101.

48. Gale, N.W. *et al.* (1993) ‘Grb2 mediates the EGF-dependent activation of guanine nucleotide exchange on Ras’, *Nature*, 363(6424). Available at: https://doi.org/10.1038/363088a0.

49. Gallego, C. *et al.* (1992) ‘Mitogen-activated protein kinase activation resulting from selective oncogene expression in NIH 3T3 and Rat 1a cells’, *Proceedings of the National Academy of Sciences of the United States of America*, 89(16). Available at: https://doi.org/10.1073/pnas.89.16.7355.

50. Gallucci, B.B. (1985) ‘Selected concepts of cancer as a disease: from the Greeks to 1900.’, *Oncology nursing forum*, 12(4).

51. Gentric, G., Mieulet, V. and Mechta-Grigoriou, F. (2017) ‘Heterogeneity in Cancer Metabolism: New Concepts in an Old Field’, *Antioxidants and Redox Signaling*. Available at: https://doi.org/10.1089/ars.2016.6750.

52. Giancotti, F.G. (2013) ‘XMechanisms governing metastatic dormancy and reactivation’, *Cell*. Available at: https://doi.org/10.1016/j.cell.2013.10.029.

53. Gilbert, L.A. *et al.* (2014) ‘Genome-Scale CRISPR-Mediated Control of Gene Repression and Activation’, *Cell*, 159(3). Available at: https://doi.org/10.1016/j.cell.2014.09.029.

54. Gildea, J.J. *et al.* (2002) ‘The role of Ral A in epidermal growth factor receptor-regulated cell motility’, *Cancer Research*, 62(4).

55. Ginn, K.F. *et al.* (2016) ‘RalA is overactivated in medulloblastoma’, *Journal of Neuro-Oncology*, 130(1). Available at: https://doi.org/10.1007/s11060-016-2236-4.

56. González-García, A. *et al.* (2005) ‘RalGDS is required for tumor formation in a model of skin carcinogenesis’, *Cancer Cell*, 7(3). Available at: https://doi.org/10.1016/j.ccr.2005.01.029.

57. Guo, H. *et al.* (2021) ‘Ral GEF with the PH Domain and SH3 Binding Motif 1 Regulated by Splicing Factor Junction Plakoglobin and Pyrimidine Metabolism Are Prognostic in Uterine Carcinosarcoma’, *Disease Markers*, 2021. Available at: https://doi.org/10.1155/2021/1484227.

58. Hajdu, S.I. (2011) ‘A note from history: Landmarks in history of cancer, part 1’, *Cancer*. Available at: https://doi.org/10.1002/cncr.25553.

59. Hajdu, S.I. (2012) ‘A note from history: Landmarks in history of cancer, part 4’, *Cancer*, 118(20). Available at: https://doi.org/10.1002/cncr.27509.

60. Hall, A. *et al.* (1983) ‘Identification of transforming gene in two human sarcoma cell lines as a new member of the ras gene family located on chromosome 1’, *Nature*, 303(5916). Available at: https://doi.org/10.1038/303396a0.

61. Hanahan, D. (2022) ‘Hallmarks of Cancer: New Dimensions’, *Cancer Discovery*. Available at: https://doi.org/10.1158/2159-8290.CD-21-1059.

62. Hanahan, D. and Weinberg, R.A. (2011) ‘Hallmarks of cancer: the next generation.’, *Cell*, 144(5), pp. 646–674. Available at: https://doi.org/10.1016/j.cell.2011.02.013.

63. Hancock, J.F., Paterson, H. and Marshall, C.J. (1990) ‘A polybasic domain or palmitoylation is required in addition to the CAAX motif to localize p21ras to the plasma membrane’, *Cell*, 63(1). Available at: https://doi.org/10.1016/0092-8674(90)90294-O.

64. Harvey, J.J. (1964) ‘An unidentified virus which causes the rapid production of tumours in mice [33]’, *Nature*. Available at: https://doi.org/10.1038/2041104b0.

65. Heider, D. *et al.* (2010) ‘Insights into the classification of small GTPases’, *Advances and Applications in Bioinformatics and Chemistry*, 3(1). Available at: https://doi.org/10.2147/aabc.s8891.

66. Hoda, S.A. and Hoda, R.S. (2020) ‘Robbins and Cotran Pathologic Basis of Disease’, *American Journal of Clinical Pathology*, 154(6). Available at: https://doi.org/10.1093/ajcp/aqaa163.

67. Hofer, F. *et al.* (1994) ‘Activated Ras interacts with the Ral guanine nucleotide dissociation stimulator’, *Proceedings of the National Academy of Sciences of the United States of America*, 91(23). Available at: https://doi.org/10.1073/pnas.91.23.11089.

68. Hsu, P.D. *et al.* (2013) ‘DNA targeting specificity of RNA-guided Cas9 nucleases’, *Nature Biotechnology*, 31(9). Available at: https://doi.org/10.1038/nbt.2647.

69. Huang, D. *et al.* (2022) ‘Cdc42 promotes thyroid cancer cell proliferation and migration and tumor-associated macrophage polarization through the PTEN/AKT pathway’, *Journal of Biochemical and Molecular Toxicology*, 36(8). Available at: https://doi.org/10.1002/jbt.23115.

70. Illergård, K., Kauko, A. and Elofsson, A. (2011) ‘Why are polar residues within the membrane core evolutionary conserved?’, *Proteins: Structure, Function and Bioinformatics*, 79(1). Available at: https://doi.org/10.1002/prot.22859.

71. Inchanalkar, S. *et al.* (2018a) ‘Polymer Nanovesicle-Mediated Delivery of MLN8237 Preferentially Inhibits Aurora Kinase A To Target RalA and Anchorage-Independent Growth in Breast Cancer Cells.’, *Molecular Pharmaceutics*, 15(8), pp. 3046–3059. Available at: https://doi.org/10.1021/acs.molpharmaceut.8b00163.

72. Inchanalkar, S. *et al.* (2018b) ‘Polymer Nanovesicle-Mediated Delivery of MLN8237 Preferentially Inhibits Aurora Kinase A To Target RalA and Anchorage-Independent Growth in Breast Cancer Cells.’, *Molecular Pharmaceutics*, 15(8), pp. 3046–3059. Available at: https://doi.org/10.1021/acs.molpharmaceut.8b00163.

73. Jackson, A.L. *et al.* (2006) ‘Widespread siRNA “off-target” transcript silencing mediated by seed region sequence complementarity’, *RNA*, 12(7), pp. 1179–1187. Available at: https://doi.org/10.1261/rna.25706.

74. Jullien-Flores, V. *et al.* (2000) 'RLIP76, an effector of the GTPase Ral, interactas with the AP2 complex: Involvement of the Ral pathway in receptor endocytosis', *Journal of Cell Science*, 113(16). Available at: https://doi.org/10.1242/jcs.113.16.2837.

75. Jura, N. *et al.* (2006) 'Differential modification of Ras proteins by ubiquitination', *Molecular Cell*, 21(5). Available at: https://doi.org/10.1016/j.molcel.2006.02.011.

76. Kardinal, C.G. and Yarbro, J.W. (1979) 'A conceptual history of cancer', *Seminars in Oncology*, 6(4).

77. Kashatus, D.F. *et al.* (2011) 'RALA and RALBP1 regulate mitochondrial fission at mitosis', *Nature Cell Biology*, 13(9). Available at: https://doi.org/10.1038/ncb2310.

78. Kelley, M.R., Logsdon, D. and Fishel, M.L. (2014) 'Targeting DNA repair pathways for cancer treatment: What's new?', *Future Oncology*. Available at: https://doi.org/10.2217/fon.14.60.

79. Khalili, A.A. and Ahmad, M.R. (2015) 'A Review of cell adhesion studies for biomedical and biological applications', *International Journal of Molecular Sciences*. Available at: https://doi.org/10.3390/ijms160818149.

80. Khan, A.A. *et al.* (2009) 'Transfection of small RNAs globally perturbs gene regulation by endogenous microRNAs', *Nature Biotechnology*, 27(6). Available at: https://doi.org/10.1038/nbt.1543.

81. Kim, M.P., Zhang, Y. and Lozano, G. (2015) 'Mutant p53: Multiple mechanisms define biologic activity in cancer', *Frontiers in Oncology*. Available at: https://doi.org/10.3389/fonc.2015.00249.

82. Kirschmann, D.A. *et al.* (2012) 'Molecular pathways: Vasculogenic mimicry in tumor cells: Diagnostic and therapeutic implications', *Clinical Cancer Research*. Available at: https://doi.org/10.1158/1078-0432.CCR-11-3237.

83. Koff, J.L., Ramachandiran, S. and Bernal-Mizrachi, L. (2015) 'A time to kill: Targeting apoptosis in cancer', *International Journal of Molecular Sciences*. Available at: https://doi.org/10.3390/ijms16022942.

84. Kontomanolis, E.N. *et al.* (2020) 'Role of oncogenes and tumor-suppressor genes in carcinogenesis: A review', *Anticancer Research*. Available at: https://doi.org/10.21873/anticanres.14622.

85. Kraemer, K.H. *et al.* (1994) 'The Role of Sunlight and DNA Repair in Melanoma and Nonmelanoma Skin Cancer: The Xeroderma Pigmentosum Paradigm', *Archives of Dermatology*, 130(8). Available at: https://doi.org/10.1001/archderm.1994.01690080084012.

86. Krishnan, P.D.G. *et al.* (2020) 'Rab gtpases: Emerging oncogenes and tumor suppressive regulators for the editing of survival pathways in cancer', *Cancers*. Available at: https://doi.org/10.3390/cancers12020259.

87. Kubiniok, P. *et al.* (2017) 'Time-resolved phosphoproteome analysis of paradoxical RAF activation reveals novel targets of ERK', *Molecular and Cellular Proteomics*, 16(4). Available at: https://doi.org/10.1074/mcp.M116.065128.

88. Lamas, I. *et al.* (2020) 'Optogenetics reveals Cdc42 local activation by scaffold-mediated positive feedback and Ras GTPase', *PLoS Biology*, 18(1). Available at: https://doi.org/10.1371/journal.pbio.3000600.

89. Lamouille, S., Xu, J. and Derynck, R. (2014) 'Molecular mechanisms of epithelial-mesenchymal transition', *Nature Reviews Molecular Cell Biology*. Available at: https://doi.org/10.1038/nrm3758.

90. Langbeheim, H., Shih, T.Y. and Scolnick, E.M. (1980) 'Identification of a normal vertebrate cell protein related to the p21 src of harvey murine sarcoma virus', *Virology*, 106(2). Available at: https://doi.org/10.1016/0042-6822(80)90252-4.

91. Lee, E.Y.H.P. and Muller, W.J. (2010) 'Oncogenes and tumor suppressor genes.', *Cold Spring Harbor perspectives in biology*. Available at: https://doi.org/10.1101/cshperspect.a003236.

92. De Leeuw, H.P.J.C. *et al.* (2001) 'Small GTP-binding protein Ral modulates regulated exocytosis of von Willebrand factor by endothelial cells', *Arteriosclerosis, Thrombosis, and Vascular Biology*, 21(6). Available at: https://doi.org/10.1161/01.ATV.21.6.899.

93. Lemmon, M.A. and Schlessinger, J. (2010) 'Cell signaling by receptor tyrosine kinases', *Cell*. Available at: https://doi.org/10.1016/j.cell.2010.06.011.

94. Lim, K.-H. *et al.* (2005) 'Activation of RalA is critical for Ras-induced tumorigenesis of human cells.', *Cancer Cell*, 7(6), pp. 533–545. Available at: https://doi.org/10.1016/j.ccr.2005.04.030.

95. Lim, K.-H. *et al.* (2006) 'Divergent roles for RalA and RalB in malignant growth of human pancreatic carcinoma cells.', *Current Biology*, 16(24), pp. 2385–2394. Available at: https://doi.org/10.1016/j.cub.2006.10.023.

96. Lim, K.-H., Brady, Donita C., *et al.* (2010) 'Aurora-A Phosphorylates, Activates, and Relocalizes the Small GTPase RalA', *Molecular and Cellular Biology*, 30(2), pp. 508–523. Available at: https://doi.org/10.1128/mcb.00916-08.

97. Lim, K.-H., Brady, Donita C, *et al.* (2010) 'Aurora-A phosphorylates, activates, and relocalizes the small GTPase RalA.', *Molecular and Cellular Biology*, 30(2), pp. 508–523. Available at: https://doi.org/10.1128/MCB.00916-08.

98. Liu, L. *et al.* (2021) 'KDM6A-ARHGDIB axis blocks metastasis of bladder cancer by inhibiting Rac1', *Molecular Cancer*, 20(1). Available at: https://doi.org/10.1186/s12943-021-01369-9.

99. Lopez, J. and Tait, S.W.G. (2015) 'Mitochondrial apoptosis: Killing cancer using the enemy within', *British Journal of Cancer*. Available at: https://doi.org/10.1038/bjc.2015.85.

100. Lopez, J.A. *et al.* (2008) 'The RalA GTPase is a central regulator of insulin exocytosis from pancreatic islet beta cells', *Journal of Biological Chemistry*, 283(26). Available at: https://doi.org/10.1074/jbc.M800321200.

101. Lorusso, G. and Rüegg, C. (2012) 'New insights into the mechanisms of organ-specific breast cancer metastasis', *Seminars in Cancer Biology*. Available at: https://doi.org/10.1016/j.semcancer.2012.03.007.

102. Luo, J.Q. *et al.* (1998) 'Functional association between ArF and RalA in active phospholipase D complex', *Proceedings of the National Academy of Sciences of the United States of America*, 95(7). Available at: https://doi.org/10.1073/pnas.95.7.3632.

103. Male, H. *et al.* (2012) 'Inhibition of RalA signaling pathway in treatment of non-small cell lung cancer', *Lung Cancer*, 77(2). Available at: https://doi.org/10.1016/j.lungcan.2012.03.007.

104. Malladi, S. *et al.* (2016) 'Metastatic Latency and Immune Evasion through Autocrine Inhibition of WNT', *Cell*, 165(1). Available at: https://doi.org/10.1016/j.cell.2016.02.025.

105. Malmberg, K.-J. (2004) ‘Effective immunotherapy against cancer’, *Cancer Immunology, Immunotherapy*, 53(10). Available at: https://doi.org/10.1007/s00262-004-0577-x.

106. Malumbres, M. and Barbacid, M. (2009) ‘Cell cycle, CDKs and cancer: A changing paradigm’, *Nature Reviews Cancer*. Available at: https://doi.org/10.1038/nrc2602.

107. Marshall, C.J., Hall, A. and Weiss, R.A. (1982) ‘A transforming gene present in human sarcoma cell lines’, *Nature*, 299(5879). Available at: https://doi.org/10.1038/299171a0.

108. Martin, G.S. (2004) ‘The road to Src’, *Oncogene*. Available at: https://doi.org/10.1038/sj.onc.1208077.

109. Martin, T.D. and Der, C.J. (2012) ‘Differential involvement of RalA and RalB in colorectal cancer.’, *Small GTPases*, 3(2), pp. 126–130. Available at: https://doi.org/10.4161/sgtp.19571.

110. McBride, O.W. *et al.* (1982) ‘Localization of the normal allele of T24 human bladder carcinoma oncogene to chromosome 11’, *Nature*, 300(5894). Available at: https://doi.org/10.1038/300773a0.

111. McCormick, F. (2022) ‘A brief history of RAS and the RAS Initiative’, in *Advances in Cancer Research*. Available at: https://doi.org/10.1016/bs.acr.2021.07.003.

112. Mulcahy, L.S., Smith, M.R. and Stacey, D.W. (1985) ‘Requirement for ras proto-oncogene function during serum-stimulated growth of NIH 3T3 cells’, *Nature*, 313(5999). Available at: https://doi.org/10.1038/313241a0.

113. Muller, L. *et al.* (2016) ‘Tumor-derived exosomes regulate expression of immune function-related genes in human T cell subsets’, *Scientific Reports*, 6. Available at: https://doi.org/10.1038/srep20254.

114. Nabi, I.R. *et al.* (1991) ‘Tumor cell autocrine motility factor receptor.’, *EXS*. Available at: https://doi.org/10.1007/978-3-0348-7494-6_11.

115. Nakashima, S. *et al.* (1999) ‘Small G protein Ral and its downstream molecules regulate endocytosis of EGF and insulin receptors’, *EMBO Journal*, 18(13). Available at: https://doi.org/10.1093/emboj/18.13.3629.

116. Nakhaeizadeh, H. *et al.* (2016) 'The RAS-effector interface: Isoform-specific differences in the effector binding regions', *PLoS ONE*, 11(12). Available at: https://doi.org/10.1371/journal.pone.0167145.

117. Neel, N.F. *et al.* (2011) 'The RalGEF-Ral Effector Signaling Network: The Road Less Traveled for Anti-Ras Drug Discovery.', *Genes & cancer*, 2(3), pp. 275–287. Available at: https://doi.org/10.1177/1947601911407329.

118. Neel, N.F. *et al.* (2012) 'The RalB Small GTPase Mediates Formation of Invadopodia through a GTPase-Activating Protein-Independent Function of the RalBP1/RLIP76 Effector', *Molecular and Cellular Biology*, 32(8). Available at: https://doi.org/10.1128/mcb.06291-11.

119. Neel, N.F. *et al.* (2014) 'Response to MLN8237 in pancreatic cancer is not dependent on RalA phosphorylation.', *Molecular Cancer Therapeutics*, 13(1), pp. 122–133. Available at: https://doi.org/10.1158/1535-7163.MCT-12-1232.

120. Niit, M. *et al.* (2015) 'Cell-cell and cell-matrix adhesion in survival and metastasis: Stat3 versus Akt.', *Biomolecular concepts*, 6(5–6), pp. 383–399. Available at: https://doi.org/10.1515/bmc-2015-0022.

121. Nikonova, A.S. *et al.* (2013) 'Aurora A kinase (AURKA) in normal and pathological cell division.', *Cellular and Molecular Life Sciences*, 70(4), pp. 661–687. Available at: https://doi.org/10.1007/s00018-012-1073-7.

122. Nyga, A. *et al.* (2023) 'The role of RAS oncogenes in controlling epithelial mechanics', *Trends in Cell Biology*. Available at: https://doi.org/10.1016/j.tcb.2022.09.002.

123. Pagès, G. *et al.* (1993) 'Mitogen-activated protein kinases p42mapk and p44mapk are required for fibroblast proliferation', *Proceedings of the National Academy of Sciences of the United States of America*, 90(18). Available at: https://doi.org/10.1073/pnas.90.18.8319.

124. Pamonsinlapatham, P. *et al.* (2009) 'P120-Ras GTPase activating protein (RasGAP): A multi-interacting protein in downstream signaling', *Biochimie*. Available at: https://doi.org/10.1016/j.biochi.2008.10.010.

125. Panciera, T. *et al.* (2020) 'Reprogramming normal cells into tumour precursors requires ECM stiffness and oncogene-mediated changes of cell mechanical properties', *Nature Materials*, 19(7). Available at: https://doi.org/10.1038/s41563-020-0615-x.

126. Papini, D. *et al.* (2015) ‘TD-60 links RalA GTPase function to the CPC in mitosis’, *Nature Communications*, 6. Available at: https://doi.org/10.1038/ncomms8678.

127. Park, J.B. (2001) ‘Regulation of GTP-binding state in RalA through Ca2+ and calmodulin’, *Experimental and Molecular Medicine*, 33(1). Available at: https://doi.org/10.1038/emm.2001.10.

128. Pawar, A. *et al.* (2016) ‘Ral-Arf6 crosstalk regulates Ral dependent exocyst trafficking and anchorage independent growth signalling.’, *Cellular Signalling*, 28(9), pp. 1225–1236. Available at: https://doi.org/10.1016/j.cellsig.2016.05.023.

129. Peinado, H., Lavotshkin, S. and Lyden, D. (2011) ‘The secreted factors responsible for pre-metastatic niche formation: Old sayings and new thoughts’, *Seminars in Cancer Biology*. Available at: https://doi.org/10.1016/j.semcancer.2011.01.002.

130. Prieto-Dominguez, N., Parnell, C. and Teng, Y. (2019) ‘Drugging the small GTPase pathways in cancer treatment: Promises and challenges’, *Cells*. Available at: https://doi.org/10.3390/cells8030255.

131. Prior, I.A. *et al.* (2001) ‘GTP-dependent segregation of H-ras from lipid rafts is required for biological activity’, *Nature Cell Biology*, 3(4). Available at: https://doi.org/10.1038/35070050.

132. Prior, I.A., Hood, F.E. and Hartley, J.L. (2020) ‘The frequency of ras mutations in cancer’, *Cancer Research*, 80(14). Available at: https://doi.org/10.1158/0008-5472.CAN-19-3682.

133. Punekar, S.R. *et al.* (2022) ‘The current state of the art and future trends in RAS-targeted cancer therapies’, *Nature Reviews Clinical Oncology*. Available at: https://doi.org/10.1038/s41571-022-00671-9.

134. Pylayeva-Gupta, Y., Grabocka, E. and Bar-Sagi, D. (2011) ‘RAS oncogenes: weaving a tumorigenic web.’, *Nature Reviews. Cancer*, 11(11), pp. 761–774. Available at: https://doi.org/10.1038/nrc3106.

135. Qi, X.-J., Wildey, G.M. and Howe, P.H. (2006) ‘Evidence that Ser87 of BimEL is phosphorylated by Akt and regulates BimEL apoptotic function.’, *The Journal of Biological Chemistry*, 281(2), pp. 813–823. Available at: https://doi.org/10.1074/jbc.M505546200.

136. Ran, F.A. *et al.* (2013) ‘Genome engineering using the CRISPR-Cas9 system.’, *Nature Protocols*, 8(11), pp. 2281–2308. Available at: https://doi.org/10.1038/nprot.2013.143.

137. Rankin, E.B. and Giaccia, A.J. (2016) ‘Hypoxic control of metastasis’, *Science*. Available at: https://doi.org/10.1126/science.aaf4405.

138. Ratner, N. and Miller, S.J. (2015) ‘A RASopathy gene commonly mutated in cancer: The neurofibromatosis type 1 tumour suppressor’, *Nature Reviews Cancer*. Available at: https://doi.org/10.1038/nrc3911.

139. Rebhun, J.F., Chen, H. and Quilliam, L.A. (2000) ‘Identification and characterization of a new family of guanine nucleotide exchange factors for the Ras-related GTPase Ral’, *Journal of Biological Chemistry*, 275(18). Available at: https://doi.org/10.1074/jbc.C000085200.

140. Reymond, N., D’Água, B.B. and Ridley, A.J. (2013) ‘Crossing the endothelial barrier during metastasis’, *Nature Reviews Cancer*. Available at: https://doi.org/10.1038/nrc3628.

141. Ribatti, D., Nico, B. and Crivellato, E. (2015) ‘The development of the vascular system: A historical overview’, *Methods in Molecular Biology*, 1214. Available at: https://doi.org/10.1007/978-1-4939-1462-3_1.

142. Richardson, D.S. *et al.* (2022) ‘The RAL Enigma: Distinct Roles of RALA and RALB in Cancer’, *Cells*. MDPI. Available at: https://doi.org/10.3390/cells11101645.

143. Richarson, A.D. *et al.* (2016) ‘Registered report: IDH mutation impairs histone demethylation and results in a block to cell differentiation’, *eLife*, 5(MARCH2016). Available at: https://doi.org/10.7554/eLife.10860.

144. Röhrig, F. and Schulze, A. (2016) ‘The multifaceted roles of fatty acid synthesis in cancer’, *Nature Reviews Cancer*. Available at: https://doi.org/10.1038/nrc.2016.89.

145. Rous, P. (1911) ‘A sarcoma of the fowl transmissible by an agent separable from the tumor cells’, *Journal of Experimental Medicine*, 13(4). Available at: https://doi.org/10.1084/jem.13.4.397.

146. Roy, S. *et al.* (1999) ‘Dominant-negative caveolin inhibits H-Ras function by disrupting cholesterol-rich plasma membrane domains’, *Nature Cell Biology*, 1(2). Available at: https://doi.org/10.1038/10067.

147. Ryan, M.B. and Corcoran, R.B. (2018) ‘Therapeutic strategies to target RAS-mutant cancers’, *Nature Reviews Clinical Oncology*. Available at: https://doi.org/10.1038/s41571-018-0105-0.

148. Sabharwal, S.S. and Schumacker, P.T. (2014) ‘Mitochondrial ROS in cancer: Initiators, amplifiers or an Achilles’ heel?’, *Nature Reviews Cancer*. Available at: https://doi.org/10.1038/nrc3803.

149. Sablina, A.A. *et al.* (2007) ‘The Tumor Suppressor PP2A Aβ Regulates the RalA GTPase’, *Cell*, 129(5), pp. 969–982. Available at: https://doi.org/10.1016/j.cell.2007.03.047.

150. Sakaguchi, A.Y. *et al.* (1983) ‘Human c-Ki-ras2 proto-oncogene on chromosome 12’, *Science*, 219(4588). Available at: https://doi.org/10.1126/science.6823569.

151. Salvatore, C. *et al.* (2018) ‘A RAB35-p85/PI3K axis controls oscillatory apical protrusions required for efficient chemotactic migration’, *Nature Communications*, 9(1). Available at: https://doi.org/10.1038/s41467-018-03571-8.

152. dos Santos, E.O. *et al.* (2016) ‘Aurora kinase targeting in lung cancer reduces KRAS-induced transformation’, *Molecular Cancer*, 15(1). Available at: https://doi.org/10.1186/s12943-016-0494-6.

153. Sceneay, J., Smyth, M.J. and Möller, A. (2013) ‘The pre-metastatic niche: Finding common ground’, *Cancer and Metastasis Reviews*. Available at: https://doi.org/10.1007/s10555-013-9420-1.

154. Schreiber, R.D., Old, L.J. and Smyth, M.J. (2011) ‘Cancer immunoediting: Integrating immunity’s roles in cancer suppression and promotion’, *Science*. Available at: https://doi.org/10.1126/science.1203486.

155. Schwartz, P.B. *et al.* (2023) ‘The circadian clock is disrupted in pancreatic cancer’, *PLoS Genetics*, 19(6 June). Available at: https://doi.org/10.1371/journal.pgen.1010770.

156. Seibold, M. *et al.* (2020) ‘RAL GTPases mediate multiple myeloma cell survival and are activated independently of oncogenic RAS’, *Haematologica*, 105(9). Available at: https://doi.org/10.3324/haematol.2019.223024.

157. Senga, S.S. and Grose, R.P. (2021) ‘Hallmarks of cancer—the new testament’, *Open Biology*. Available at: https://doi.org/10.1098/rsob.200358.

158. Sheffels, E. *et al.* (2018) ‘Oncogenic RAS isoforms show a hierarchical requirement for the guanine nucleotide exchange factor SOS2 to mediate cell transformation.’, *Science Signaling*, 11(546). Available at: https://doi.org/10.1126/scisignal.aar8371.

159. Sheng, C. *et al.* (2018) ‘Knockdown of Ran GTPase expression inhibits the proliferation and migration of breast cancer cells’, *Molecular Medicine Reports*, 18(1). Available at: https://doi.org/10.3892/mmr.2018.8952.

160. Sherwood, L.M., Parris, E.E. and Folkman, J. (1971) ‘Tumor Angiogenesis: Therapeutic Implications’, *New England Journal of Medicine*, 285(21). Available at: https://doi.org/10.1056/nejm197111182852108.

161. Shimizu, K. *et al.* (1983) ‘Isolation and preliminary characterization of the transforming gene of a human neuroblastoma cell line’, *Proceedings of the National Academy of Sciences of the United States of America*, 80(2 I). Available at: https://doi.org/10.1073/pnas.80.2.383.

162. Shipitsin, M. and Feig, L.A. (2004) ‘RalA but Not RalB Enhances Polarized Delivery of Membrane Proteins to the Basolateral Surface of Epithelial Cells’, *Molecular and Cellular Biology*, 24(13). Available at: https://doi.org/10.1128/mcb.24.13.5746-5756.2004.

163. Shirakawa, R. and Horiuchi, H. (2015) ‘Ral GTPases: crucial mediators of exocytosis and tumourigenesis.’, *Journal of Biochemistry*, 157(5), pp. 285–299. Available at: https://doi.org/10.1093/jb/mvv029.

164. Sigoillot, F.D. and King, R.W. (2011) ‘Vigilance and validation: Keys to success in RNAi screening’, *ACS Chemical Biology*, pp. 47–60. Available at: https://doi.org/10.1021/cb100358f.

165. Simanshu, D.K., Nissley, D. V. and McCormick, F. (2017) ‘RAS Proteins and Their Regulators in Human Disease’, *Cell*. Available at: https://doi.org/10.1016/j.cell.2017.06.009.

166. Simicek, M. *et al.* (2013) ‘The deubiquitylase USP33 discriminates between RALB functions in autophagy and innate immune response.’, *Nature Cell Biology*, 15(10), pp. 1220–1230. Available at: https://doi.org/10.1038/ncb2847.

167. Smith, I. *et al.* (2017) ‘Evaluation of RNAi and CRISPR technologies by large-scale gene expression profiling in the Connectivity Map’, *PLoS Biology*, 15(11). Available at: https://doi.org/10.1371/journal.pbio.2003213.

168. Sowalsky, A.G. *et al.* (2010) 'RalA suppresses early stages of Ras-induced squamous cell carcinoma progression', *Oncogene*, 29(1). Available at: https://doi.org/10.1038/onc.2009.307.

169. Srivastava, M. and Raghavan, S.C. (2015) 'DNA double-strand break repair inhibitors as cancer therapeutics', *Chemistry and Biology*. Available at: https://doi.org/10.1016/j.chembiol.2014.11.013.

170. Steeg, P.S. (2006) 'Tumor metastasis: Mechanistic insights and clinical challenges', *Nature Medicine*. Available at: https://doi.org/10.1038/nm1469.

171. Stegner, D., Dütting, S. and Nieswandt, B. (2014) 'Mechanistic explanation for platelet contribution to cancer metastasis', *Thrombosis Research*, 133(SUPPL. 2). Available at: https://doi.org/10.1016/S0049-3848(14)50025-4.

172. Stehelin, D. *et al.* (1976) 'DNA related to the transforming gene(s) of avian sarcoma viruses is present in normal avian DNA', *Nature*, 260(5547). Available at: https://doi.org/10.1038/260170a0.

173. Suire, S., Hawkins, P. and Stephens, L. (2002) 'Activation of phosphoinositide 3-kinase γ by Ras', *Current Biology*, 12(13). Available at: https://doi.org/10.1016/S0960-9822(02)00933-8.

174. Szablewski, L. (2013) 'Expression of glucose transporters in cancers', *Biochimica et Biophysica Acta - Reviews on Cancer*. Available at: https://doi.org/10.1016/j.bbcan.2012.12.004.

175. Tatsuka, M. *et al.* (2005) 'Overexpression of Aurora-A potentiates HRAS-mediated oncogenic transformation and is implicated in oral carcinogenesis.', *Oncogene*, 24(6), pp. 1122–1127. Available at: https://doi.org/10.1038/sj.onc.1208293.

176. Thies, K.A. *et al.* (2021) 'The small G-protein RalA promotes progression and metastasis of triple-negative breast cancer', *Breast Cancer Research*, 23(1). Available at: https://doi.org/10.1186/s13058-021-01438-3.

177. Tsai, S.Q. *et al.* (2015) 'GUIDE-seq enables genome-wide profiling of off-target cleavage by CRISPR-Cas nucleases', *Nature Biotechnology*, 33(2). Available at: https://doi.org/10.1038/nbt.3117.

178. Tzeng, H.T. and Wang, Y.C. (2016) 'Rab-mediated vesicle trafficking in cancer', *Journal of Biomedical Science*, 23(1). Available at: https://doi.org/10.1186/s12929-016-0287-7.

179. Uegaki, M. *et al.* (2019) 'Downregulation of RalGTPase-activating protein promotes invasion of prostatic epithelial cells and progression from intraepithelial neoplasia to cancer during prostate carcinogenesis', *Carcinogenesis*, 40(12). Available at: https://doi.org/10.1093/carcin/bgz082.

180. Umstead, M. *et al.* (2017) 'Aurora kinase A interacts with H-Ras and potentiates Ras-MAPK signaling.', *Oncotarget*, 8(17), pp. 28359–28372. Available at: https://doi.org/10.18632/oncotarget.15049.

181. Vader, G. and Lens, S.M.A. (2008) 'The Aurora kinase family in cell division and cancer', *Biochimica et Biophysica Acta - Reviews on Cancer*. Available at: https://doi.org/10.1016/j.bbcan.2008.07.003.

182. Valastyan, S. and Weinberg, R.A. (2011) 'Tumor metastasis: Molecular insights and evolving paradigms', *Cell*. Available at: https://doi.org/10.1016/j.cell.2011.09.024.

183. Vogelstein, B. *et al.* (2013) 'Cancer genome landscapes', *Science*. Available at: https://doi.org/10.1126/science.1235122.

184. Walsh, A.B. and Bar-Sagi, D. (2001) 'Differential Activation of the Rac Pathway by Ha-Ras and K-Ras', *Journal of Biological Chemistry*, 276(19). Available at: https://doi.org/10.1074/jbc.M010573200.

185. Wang, H. *et al.* (2010) 'Phosphorylation of RalB is important for bladder cancer cell growth and metastasis', *Cancer Research*, 70(21), pp. 8760–8769. Available at: https://doi.org/10.1158/0008-5472.CAN-10-0952.

186. Wang, K. *et al.* (2013) 'The role of RalA in biology and therapy of ovarian cancer', *Oncotarget* [Preprint].

187. Wang, S. *et al.* (2017) 'Rab25 GTPase: Functional roles in cancer', *Oncotarget*. Available at: https://doi.org/10.18632/oncotarget.19571.

188. Wang, X. *et al.* (2017) 'Abstract 3194: A new mechanism of drug resistance in cancer: extracellular ATP-induced resistance through ATP internalization and upregulation of protein phosphorylation in Akt and ERK pathways', *Cancer Research*, 77(13_Supplement). Available at: https://doi.org/10.1158/1538-7445.am2017-3194.

189. Wang, Y. *et al.* (2019) 'ARL3 is downregulated and acts as a prognostic biomarker in glioma', *Journal of Translational Medicine*, 17(1). Available at: https://doi.org/10.1186/s12967-019-1914-3.

190. Warburg, O., Wind, F. and Negelein, E. (1927) ‘The metabolism of tumors in the body’, *Journal of General Physiology*, 8(6). Available at: https://doi.org/10.1085/jgp.8.6.519.

191. Ward, Y. *et al.* (2001) ‘Signal Pathways Which Promote Invasion and Metastasis: Critical and Distinct Contributions of Extracellular Signal-Regulated Kinase and Ral-Specific Guanine Exchange Factor Pathways’, *Molecular and Cellular Biology*, 21(17). Available at: https://doi.org/10.1128/mcb.21.17.5958-5969.2001.

192. Weiss, R.A. (2020) ‘A perspective on the early days of RAS research’, *Cancer and Metastasis Reviews*. Available at: https://doi.org/10.1007/s10555-020-09919-1.

193. Welte, T. *et al.* (2016) ‘Oncogenic mTOR signalling recruits myeloid-derived suppressor cells to promote tumour initiation’, *Nature Cell Biology*, 18(6). Available at: https://doi.org/10.1038/ncb3355.

194. Witsch, E., Sela, M. and Yarden, Y. (2010) ‘Roles for Growth Factors in Cancer Progression’, *Physiology*. Available at: https://doi.org/10.1152/physiol.00045.2009.

195. Wolthuis, R.M.F. *et al.* (1998) ‘Ras-dependent activation of the small GTPase Ral’, *Current Biology*, 8(8). Available at: https://doi.org/10.1016/S0960-9822(98)70183-6.

196. Wu, J.C. *et al.* (2005) ‘Identification of V23RalA-Ser194 as a critical mediator for Aurora-A-induced cellular motility and transformation by small pool expression screening’, *Journal of Biological Chemistry*, 280(10), pp. 9013–9022. Available at: https://doi.org/10.1074/jbc.M411068200.

197. Xu, N. *et al.* (2015) ‘Protein prenylation and human diseases: a balance of protein farnesylation and geranylgeranylation’, *Science China Life Sciences*. Available at: https://doi.org/10.1007/s11427-015-4836-1.

198. Yamauchi, J. *et al.* (2005) ‘Ras activation of a Rac1 exchange factor, Tiam1, mediates neurotrophin-3-induced Schwann cell migration’, *Proceedings of the National Academy of Sciences of the United States of America*, 102(41). Available at: https://doi.org/10.1073/pnas.0507125102.

199. Yan, C. and Theodorescu, D. (2018) ‘RAL gtpases: biology and potential as therapeutic targets in cancer.’, *Pharmacological Reviews*, 70(1), pp. 1–11. Available at: https://doi.org/10.1124/pr.117.014415.

200. Ye, X. and Weinberg, R.A. (2015) ‘Epithelial-Mesenchymal Plasticity: A Central Regulator of Cancer Progression’, *Trends in Cell Biology*. Available at: https://doi.org/10.1016/j.tcb.2015.07.012.

201. Yin, G. *et al.* (2023) ‘Targeting small GTPases: emerging grasps on previously untamable targets, pioneered by KRAS’, *Signal Transduction and Targeted Therapy*. Available at: https://doi.org/10.1038/s41392-023-01441-4.

202. Yoshimachi, S. *et al.* (2021) ‘Ral GTPase–activating protein regulates the malignancy of pancreatic ductal adenocarcinoma’, *Cancer Science*, 112(8). Available at: https://doi.org/10.1111/cas.14970.

203. Yuen, H.F. *et al.* (2016) ‘Ran GTPase promotes cancer progression via Met receptor-mediated downstream signaling’, *Oncotarget*, 7(46). Available at: https://doi.org/10.18632/oncotarget.12420.

204. Zago, G. *et al.* (2018) ‘RalB directly triggers invasion downstream Ras by mobilizing the Wave complex.’, *eLife*, 7. Available at: https://doi.org/10.7554/eLife.40474.

205. Zhou, F.X. *et al.* (2001) ‘Polar residues drive association of polyleucine transmembrane helices’, *Proceedings of the National Academy of Sciences of the United States of America*, 98(5). Available at: https://doi.org/10.1073/pnas.041593698.

206. Zwartkruis, F.J.T. *et al.* (1998) ‘Extracellular signal-regulated activation of Rap1 fails to interfere in Ras effector signalling’, *EMBO Journal*, 17(20). Available at: https://doi.org/10.1093/emboj/17.20.5905.